Lena Wengeler

Testing Regional Authenticity of Foodstuff by Means of Water Stable Isotopes: A Comparison of Methods

Freiburg i.Br., May 2021

CHAIR OF HYDROLOGY

ALBERT- LUDWIGS- UNIVERSITY FREIBURG I.BR

MASTER THESIS

Testing Regional Authenticity of Foodstuff by Means of Water Stable Isotopes: A Comparison of Methods

---

Advisor: DR. NATALIE ORLOWSKI

Co- Advisor: JUN.-PROF. DR. ANDREAS HARTMANN

Research Supervisor: DR. BARBARA HERBSTRITT

Lena Wengeler 4723422

Freiburg i.Br. 15.05.2021

Danksagung

An erster Stelle möchte ich mich herzlich Dr. Natalie Orlowski bedanken, die mir ermöglichte an diesem spannenden Thema zu arbeiten und auch für die vielen guten Diskussionen und Ideen zur Auswertung der Daten.

Einen großen Dank möchte ich außerdem Dr. Barbara Herbstritt aussprechen, die mich bei der Laborarbeit auf so vielfältige Weise unterstützte und ohne deren kreative Ideen diese Arbeit nicht so gut umsetzbar gewesen wäre. Danke, für die geduldigen, und trotz der vielen Fragen freudigen und leidenschaftlichen Erklärungen und Anregungen. „Immer schön kritisch hinterfragen!".

Ich möchte mich auch sehr bei Benjamin Gralher für das Korrekturlesen und besonders für die vielen Ideen und Anregungen bedanken. Ein großes Dankeschön auch an Craig und Mark für die finale Korrektur meiner Thesis und an alle Freunde, die mir Anregungen und Denkanstöße lieferten, oder einfach zwischendurch ein Lächeln ins Gesicht zauberten.

Für die Bereitstellung der Gemüse- und Wasserproben gilt mein Dank den landwirtschaftlichen Betrieben, ohne die diese Arbeit nicht möglich gewesen wäre.

Jun.- Prof Dr. Andreas Hartmann danke ich für die unkomplizierte Übernahme der Zweitkorrektur.

Nicht zuletzt möchte ich herzlich meiner Familie danken, die mich immer unterstützte und ermutigte, meinen eigenen Weg zu gehen und mir besonders in dieser turbulenten letzten Zeit Halt gaben.

Danke!

Contents

List of Figures

List of Tables

List of Figures in the Appendix

List of Tables in the Appendix

Extended Summary

As consumers become more interested in the origin of the food they consume, verifying the geographical origin and detecting food fraud becomes increasingly important. Due to the varying global composition of water stable isotopes in precipitation water, they can be used like a fingerprint to identify the geographical origin of foods. Analytical methods, such as IRMS, have already shown their potential for verifying origin information. However, these methods are often time-consuming and expensive, and therefore, three new approaches for the determination of food origin are analyzed in this thesis. More specifically, this study will seek to determine if isotopically known source water can be detected in local vegetables (cauliflower: CAU, celery root: CEL, kohlrabi: KOH, and potatoes: POT from four farms in south-west Germany) and if these clusters can be distinguished from those found in imported vegetables (Spain, Italy, and the Netherlands), by laser-based analysis (CRDS).

Since every vegetable was analyzed with each of the three methods, the results of the water stable isotopes were expected to be the same. However, Cryogenic Vacuum Distillation (CVD) showed heavier isotopic values for the vegetables with SDs of ±1.7‰ in $\delta^{18}O$ and ±4.6‰ in $\delta^{2}H$. The isotopic values of the continual *in situ* monitoring measurement plotted much closer to the Global Meteoric Water Line (GMWL) with SDs of ±1.5‰ in $\delta^{18}O$ and ±8.7‰ in $\delta^{2}H$. The data of the Direct Vapor Equilibrium-Laser Spectroscopy (DVE-LS) method scattered the furthest with SDs of ±4.4‰ in $\delta^{18}O$ and ±36‰ in $\delta^{2}H$, but the data showed an implausible scattering of CAU and KOH. These strongly deviating values could be attributed to the known influence of volatile organic compounds (VOC), in this case, specifically methanol and methane. Although the local vegetable varieties grew under the same climatic conditions, some of the varieties, especially the POT, have different values and can be distinguished from each other. However, in relation to the scatter of data of the methods, these differences are smaller.

The analyzed approaches were able to achieve faster results than IRMS-based methods. Moreover, the CVD data for all samples and the DVE-LS for CEL and POT samples were able to determine the source water's isotopic composition and are therefore potentially suitable to verify the geographical origin. The direct comparisons of most methods and vegetable varieties of local and imported vegetables often showed significant differences in the isotopic composition. However, the accuracy and distinction of the water stable isotopes of individual vegetables is not sufficient to identify the different areas of geographical origin without any uncertainty.

A great potential to improve the measurement accuracy could be achieved by the subsequent correction of the co-measured organic compounds or by avoiding them with the help of a modified experimental setup and execution.

Keywords: geographical origin authentication; water stable isotopes; isotope ratio; vegetables; isotope ratio infrared spectroscopy (IRIS); CRDS; $\delta^{18}O$; $\delta^{2}H$; authenticity, volatile organic compounds

Zusammenfassung

Mit zunehmendem Interesse der Verbraucher für die Herkunft der von ihnen konsumierten Lebensmittel, wird die Überprüfung der Herkunft und das Aufdecken von Lebensmittelbetrug zunehmend wichtiger. Aufgrund der variierenden globalen Zusammensetzung der stabilen Wasserisotope im Niederschlagswasser können diese wie ein Fingerabdruck verwendet werden, um die Herkunft der Lebensmittel zu identifizieren. Analytische Methoden, wie z.B. IRMS, haben bereits ihr Potential zur Verifizierung von Herkunftsinformationen gezeigt. Allerdings sind diese Methoden oft zeitaufwendig und teuer, weshalb in dieser Arbeit drei neue Ansätze zur Bestimmung der Lebensmittelherkunft getestet werden. Im Einzelnen wird untersucht, ob das isotopisch bekannte Wasser, welches von dem lokalen Gemüse (Blumenkohl: CAU, Knollensellerie: CEL, Kohlrabi: KOH und Kartoffeln: POT von vier Betrieben in Südwestdeutschland) während der Wachstumsphase aufgenommen wurde, wieder gefunden werden kann. Des Weiteren wird untersucht, ob diese Gruppen mittels laserbasierter Analyse (CRDS) von importiertem Gemüse (aus Spanien, Italien und der Niederlande) unterschieden werden können.

Da jedes Gemüse mit allen drei Methoden analysiert wurde, sollten die Ergebnisse der stabilen Wasserisotope gleich sein. Die kryogene Vakuumdestillation (CVD) zeigte jedoch schwerere Isotopenwerte für das Gemüse, insbesondere in $\delta^{18}O$, mit SDs von ±1,7‰ in $\delta^{18}O$ und ±4,6‰ in $\delta^{2}H$. Die Isotopenwerte der kontinuierlichen *in situ* Messung lagen mit SDs von ±1,5‰ in $\delta^{18}O$ und ±8,7‰ in $\delta^{2}H$ deutlich näher an der Global Meteoric Water Line (GMWL). Die Daten der direkten Dampfgleichgewichts-Laser Spektrometrie (DVE-LS) Methode streuten am weitesten mit SDs von ±4,4‰ in $\delta^{18}O$ und ±36‰ in $\delta^{2}H$, wobei die Daten eine unplausible Streuung der CAU und KOH Daten. Diese stark abweichenden Werte könnten auf den bereits bekannten Einfluss flüchtiger organischer Verbindungen (VOC), in diesem Fall vor allem Methanol und Methan, zurückgeführt werden. Obwohl die lokalen Gemüsesorten unter den gleichen klimatischen Bedingungen wuchsen, weisen einige der Sorten, insbesondere POT, unterschiedliche isotopische Werte auf und können voneinander unterschieden werden. In Relation zu den Streuungen der Methoden sind diese Unterschiede jedoch geringer.

Die untersuchten Ansätze konnten schnellere Ergebnisse erzielen als IRMS-basierte Methoden. Darüber hinaus wurde mit der CVD (alle Gemüsesorten) bzw. der DVE-LS Methode (CEL und POT) die isotopische Zusammensetzung des während der Wachstumsphase aufgenommenen Wassers bestimmt. Daher sind diese beiden Methoden potenziell geeignet, die geographische Herkunft zu verifizieren. Die direkten Vergleiche der meisten Methoden und Gemüsesorten von lokalem und importiertem Gemüse konnten signifikante Unterschiede der isotopischen Zusammensetzung zeigen. Die Genauigkeit und Unterscheidung der Wasserisotope einzelner Gemüsesorten ist jedoch nicht ausreichend, um die verschiedenen Herkunftsgebiete zweifelsfrei zu identifizieren.

Ein großes Potential zur Verbesserung der Messgenauigkeit könnte durch die anschließende Korrektur der mitgemessenen organischen Verbindungen oder durch die Vermeidung dieser aufgrund eines abgeänderten Versuchsaufbaus und -durchführung erreicht werden.

1 Introduction

1.1 Motivation

Globalization and global food trade have connected the world, while simultaneously reducing the contacts between producers and consumers. Nowadays, food often travels long distances, passing through different hands and across national borders. As a result, there are many different stakeholders and a lot of opportunities for them to make changes to products for a variety of reasons. Profit in particular is a common driver of these changes (van Ruth et al., 2017; Abbas et al., 2018; Moyer et al., 2017). Changes may include replacing expensive products with cheaper ones, adding cheaper materials (e.g., some fruit juice producers add water or sugar because of the much lower price of these products (Carter and Chesson, 2017)) or indicating a different origin of the food (Esslinger et al., 2014).

Spink and Moyer (2011) specified food fraud as "a collective term used to encompass the deliberate and intentional substitution, addition, tampering, or misrepresentation of food, food ingredients, or food packaging; or false or misleading statements made about a product, for economic gain" (Spink and Moyer, 2011). Danezis et al. (2016) state, that the origin of foodstuffs is the primary authenticity issue in Europe.

There is an increasing awareness and demand for regional products, as consumers are paying more attention to the origin of their food (Kelly et al., 2005). Furthermore, less harmful effects on the climate and animal welfare are reasons for certain customer choices (Drivelos and Georgiou, 2012). Many consumers prefer foodstuff from their own country over those from other countries (Ekelund et al., 2007) and are generally more interested in the origin of the food they buy (Danezis et al., 2016). For instance, some consumers buy products that come from a particular region, for example, because of a particular taste or the way a certain food is cultivated or processed (Camin et al., 2017). Others take into account the rules and regulations of pesticide use prevailing in the country of origin when making their purchase decisions. Consumer confidence in the quality and authenticity of the food being offered in stores is vulnerable when scandals like the horsemeat scandal (Danezis et al., 2016) or the mad cow disease (Montet and Ray, 2017) emerge. Regardless of the exact reasons, consumers often base their purchasing decisions on the information provided by labelling systems on the products they buy (Katerinopoulou et al., 2020). However, consumer preferences are not the only reason why food fraud should be tracked. Health concerns also play a major role. As Moore et al. (2012) mentioned, events like the melamine incident in 2007 and 2008 showed the importance of detecting food fraud in order to prevent hazardous situations. In addition, allergies or religious

practices can be a reasons for a certain dietary choices and the consumers' need for reliance on product claims (Moore et al., 2012).

Food authentication and traceability is important for several stakeholders. Besides consumers, producers and authorities have an interest as well. Food authorities, for example, are interested in this because of risk avoidance and traceability in the event of a crisis (Montet and Ray, 2017). The European Union (EU) has made some efforts to counter food fraud and to make distribution along the food chain safer. In 2002, the EU published general principles and requirements of food law and created the European Food Safety Authority (European Union, 2002). Furthermore, the EU specified three different designations that products, meeting certain conditions, can obtain. These are: Protected Designation of Origin (PDO) (e.g., Mozzarella di Bufala Campana), Protected Geographical Indication (PGI) (e.g., Westfälischer Knochenschinken) and Traditional Specialty Guaranteed (TSG) (e.g., Mozzarella) (Grunert and Aachmann, 2016; Kelly et al., 2005). These products are characterized by a specific cultivation method, traditional practices, animal breeds or a specific cultivation region (Danezis et al., 2016). As these protected products garner a higher price on the market, they are vulnerable to counterfeiting and therefore it is important to protect them (Danezis et al., 2016). Additionally, there are several laws regulating this area, e.g. Food Regulation (EU) No 1169/2011 (European Union, 2011), which requires the labeling of foodstuffs. It is mandatory that, in addition to other foodstuffs such as honey and beef products, the origin of fruits and vegetables must be indicated. However, due to price differences and consumers' willingness to pay more money for certain products, there will always be some participants in the market who seek to illegally circumvent the rules and regulations (Rossier et al., 2016).

Since legal regulation does not fully prevent food fraud (Ballin, 2010), control is very important. Although traceability and testing of origin play an elementary role, control is not yet that easy (Katerinopoulou et al., 2020). There is a need for robust and reproducible methods that can be used by the regulatory authorities (Camin et al., 2017; Danezis et al., 2016). There is still a lack of standardized methods that can be used on a large scale, as well as being inexpensive and easy to apply.

1.2 State of research

Increased research is being conducted on the topic of food fraud and testing for authenticity of origin (Katerinopoulou et al., 2020; Moore et al., 2012). The analysis of water stable isotopes is generally the main method used to test the geographic origin of food (Camin et al., 2017). In hydrology, water stable isotopes ($\delta^{18}O$ and $\delta^{2}H$) are often considered ideal tracers, since they are part of the water molecule and therefore behave naturally (Sprenger et al., 2017).

One of the methods of using water stable isotopes to determine the geographic origin of vegetables is to use these water stable isotopes to determine the origin.

This method is based on the fact that the isotopic composition of precipitation and local groundwater differs by region, thus forming so-called 'isoscapes' (isotopic landscapes) (Vander Zanden and Chesson, 2017). Water stable isotopes are subject to various influences that affect their composition. There are three fractionation processes to which isotopes are subjected because the different isotopologues have different rates of reaction (Clark and Fritz, 2013). These processes are equilibrium, kinetic and nuclear spin (Sulzman, 2007). Equilibrium fractionation occurs when the isotopes of two corresponding reservoirs (e.g. liquid water and a vapor-saturated atmosphere) are in equilibrium in a closed, well-mixed system because they change between the two phases at the same rate (Clark and Fritz, 2013). Due to different strengths of the bonds of the heavier and lighter isotope, these physiochemical fractionations occur. The stronger bonds of the heavier isotopes lead to an enrichment of the heavier isotopes in the denser (e.g., liquid) phase (Clark and Fritz, 2013). This process is strongly temperature-dependent, with stronger isotope effects for lower temperatures (Leibundgut et al., 2009). As water evaporates in an open system and no equilibrium can be established, the evaporating water is transported away and kinetic isotopic effects are encountered (Sulzman, 2007). The isotope effects in such systems are also humidity dependent (Gonfiantini, 1986) and generally greater than in closed systems. An important kinetic fractionation process is '*Rayleigh distillation'* (Lord Rayleigh, 1902). In this process, parts of e.g. a liquid water reservoir are gradually transferred to another phase and then removed directly from the system without further reactions (Leibundgut et al., 2009). These two processes exist because of differences in the atomic masses of the heavier and lighter isotope (Clark and Fritz, 2013). Nuclear spin does not depend on the mass differences, but instead on differences in the nuclear structure, which leads to a different nuclear spin (Sulzman, 2007). Some analytical methods, such as nuclear magnetic resonance (NMR), take advantage of this fact.

The isotopic composition of precipitation varies spatially due to the influence of various factors. On the global scale, these are the *latitude effect* and the *continental effect*. As Dansgaard (1964) described, there is a strong correlation between the $\delta^{18}O$ values and temperature. As a result,

precipitation water of higher latitudes is more depleted in heavy isotopes (Clark and Fritz, 2013). The *continental effect* is evident because the air masses ascending from the sea are being driven to rain out during their passage over land. The heavier isotopes accumulate in the precipitation. In this way, the isotopic composition in the remaining water vapor changes and the isotopic compositions in both vapor and precipitation become lighter the further inland the precipitation falls (Clark and Fritz, 2013; McGuire and McDonnell, 2007).

On the regional scale, the *altitude, amount,* and *seasonal effects* are of greater importance. With increasing altitude, the isotopic composition generally becomes lighter due to orographic precipitation (Sulzman, 2007). The amount effect is clearly visible in regions with significant differences in the amount of precipitation. Regions which are influenced by monsoon show depleted water stable isotope ($\delta^{18}O$ and $\delta^{2}H$) values in times with a lot of rainfall, compared to those with less rainfall. Regions with distinct seasonal differences in temperature also show these differences in the isotopic composition of precipitation (seasonal effect) (Clark and Fritz, 2013). Craig (1961a) discovered the linear relationship between $\delta^{18}O$ and $\delta^{2}H$ in global precipitation and specified it in a formula (see chapter 2.1.1). In hydrology, for example, these differences are used to determine the season and rate of groundwater recharge (Koeniger et al., 2016; Leibundgut et al., 2009). However, the distinction and delimitation of these effects is not simple, as they occur in combination.

One idea for the determination of the origin of food is to try to find these differences in the isotopic composition of the precipitate in the vegetables, because they take up the water around them (e.g. irrigation or precipitation water) (Vander Zanden and Chesson, 2017). The high water content of the vegetable samples is thus advantageous for this approach. Wershaw et al. (1966), Dawson and Ehleringer (1991) and others state that the water uptake of plants does not change the isotopic composition and therefore does not differ from the soil water. In addition to water, plants also absorb the minerals from the surrounding soil. The composition of macro- , micronutrients and rare earths elements (REE) differs between the various regions, which is also taken advantage of when studying the origin of food in some cases (Danezis et al., 2016).

The detection of altered or mislabeled products is quite complicated. Moore et al. (2012) examined food fraud occurring between the years 1980 and 2010. Their research showed that the most commonly used methods for determining the geographical origin of foods were High-Pressure Liquid Chromatography (HPLC), Infrared Spectroscopy (IR), Gas Chromatography (GC) and Isotope Ratio Mass Spectrometry (IRMS). In recent years, more and more research has been done in this field. Katerinopoulou et al. (2020) examined 205 documents on geographical origin authentication published between 2015 and 2019. They indicated that the most commonly used methods for analysis in them were IRMS, IR and Inductively Coupled Plasma Mass Spectrometry (ICP-MS). The most frequently analyzed products in this survey were plant-crops and herbs (e.g. potatoes, tomatoes,

rice, flour, oranges) , oils (mostly olive oil), seafood, wine and beverages, honey, meat, mushrooms, milk and dairy products in this survey (Katerinopoulou et al., 2020). Further studies were carried out on honey (Magdas et al., 2021), walnuts (Segelke et al., 2020), apples (Oerter et al., 2017) and tomatoes (Bontempo et al., 2020).

The Isotope Ratio Mass Spectrometry (IRMS) method is an established method to determine isotope ratios of $^{13}C/^{12}C$, $^{15}N/^{14}N$, $^{18}O/^{16}O$, $^{2}H/^{1}H$, and $^{34}S/^{32}S$ (Katerinopoulou et al., 2020). In spite of the many advantages of this method, like precise measurements, however, it also has some disadvantages, such as labor intensity, high cost and the site-bound structure (West et al., 2010).

A more recent method for the determination of water stable isotope compositions is the Isotope-Ratio Infrared Spectroscopy (IRIS). IRIS has increasingly been used over recent years because of several advantages, including lower costs, ease of handling, a fast sample throughput and the fact that samples do not have to be converted to their elemental constituents, over e.g. IRMS (Carter and Chesson, 2017; Brand et al., 2009). Brand et al. (2009) showed that the results of IRMS and IRIS for pure waters are comparable and Wavelength-Scanned Cavity Ring-Down Spectroscopy (WS-CRDS) is one way to measure via IRIS. To perform the measurements with CRDS, the sample water must be extracted beforehand The development of cost-effective extraction methods, such as the Cryogenic Vacuum Distillation (hereinafter referred to as ‘CVD’) and the modification by Koeniger et al. (2011) of the standard protocol of West et al. (2006), make this analytical method even more interesting. The CVD is a frequently used extraction method of plant and soil water (Orlowski et al., 2016a). As Millar et al. (2018) described, during the extraction with the CVD method the entire volatile emissions of the sample are collected in another vial cooled with the aid of liquid nitrogen. It is important that all the water in the sample is extracted in order to avoid isotope effects due to Rayleigh distillation (Orlowski et al., 2013). A minimal amount of residual water in the sample is acceptable (>98% needs to be extracted) (West et al., 2006). Sprenger et al. (2015) stated that the high extraction temperatures extract a mixture of the water pools held at different tensions. While the measurement of CVD-derived samples via CRDS or IRMS yields the isotopic composition of the extracted water, the Direct Water Vapor Equilibration Laser Spectrometry (DVE-LS) method uses a different approach. Here, the isotopic composition is measured directly and continuously in the vapor phase corresponding with the matrix-bound liquid water phase of interest. The sample is placed in a closed system and the water in the sample creates an equilibrium with the dry air added to the system (Wassenaar et al., 2008), which reduces the risk of partial extraction. The third method investigated has the potential of reducing the processing time significantly. This is the method of Continual *In Situ* Monitoring (hereinafter referred to as '*in situ*') developed by Volkmann and Weiler (2014). Here, a porous probe is inserted into the solid matrix of the water-containing sample to be analyzed and, similar to the DVE-LS method, the isotopic composition of a corresponding vapor phase is measured in quasi-real-time.

Unlike IRMS, which is mostly unaffected by the presence of several organic compounds (e.g., methane, methanol and/or ethanol), these parameters can influence the examination with laser spectrometers (CRDS) due to similar absorption spectra (Brand et al., 2009; Hendry et al., 2011; West et al., 2010; Martín-Gómez et al., 2015).

1.3 Research questions

Until now, only a few studies have been performed with IRIS, specifically with WS-CRDS for the authentication of the geographic origin of foodstuffs (Chesson et al., 2010; Oerter et al., 2017). The aim of this work is to find out which of the three analytical methods studied, using WS-CRDS to analyze the water stable isotopic composition of water stable isotopes, works best for the four vegetables. The methods investigated are intended to contribute to the previously stated problems and to improve the testing of the geographic origins of foodstuffs. The possible interference of organic parameters, which might affect the spectral analysis are considered with special attention in this thesis.

This thesis has five objectives: The water stable isotopic composition of the vegetables will be compared with rainfall and irrigation water. For all vegetables, comparisons will be made between the different methods of analysis. Water stable isotopes of vegetables from four local farms in South-Western Germany will be compared with each other. The influence of co-recorded parameters indicating the presence of several organic compounds (e.g., methanol and/or methane) will be studied. Finally, the differences between local and imported vegetables will be studied. This leads to the following research questions:

1. How does precipitation/irrigation water relate to vegetables' water stable isotopic composition?
2. How do water stable isotope results ($\delta^{18}O$ and $\delta^{2}H$) of cryogenic vacuum distillation, continual in situ monitoring and direct water equilibrium laser spectrometry method compare to each other?
3. Are there differences in the water stable isotopes ($\delta^{18}O$ and $\delta^{2}H$) of the individual vegetable varieties between the local farms from the same region?
4. What influence do organic parameters (e.g., methane, methanol, and ethanol) have on the isotopic composition of $\delta^{18}O$ and $\delta^{2}H$ measured via IRIS?
5. Is the geographical difference between local and supermarket vegetables measurable by the water stable isotopes ($\delta^{18}O$ and $\delta^{2}H$)?

2 Materials and Methods

2.1 Experimental Setup and Test Parameter

2.1.1 Water Stable Isotopes Measurement

Isotopes are atoms of the same chemical element and with the same atomic number but have a different number of neutrons in the nucleus, and therefore different atomic masses. There are two different kinds of isotopes, stable and unstable isotopes. Radioactive (unstable) isotopes, such as Tritium (^{3}H), will not play a role in this thesis. Molecules with different isotopic composition are called isotopologues. Hydrogen can be present as the stable protium (^{1}H) or as the stable deuterium (^{2}H). Oxygen appears as the stable ^{16}O, ^{17}O and ^{18}O. In this work, however, only the isotopologues consisting of protium (^{1}H), deuterium (^{2}H), ^{16}O and ^{18}O are considered.

The study of isotopic composition does not proceed by directly observing the absolute isotopic ratios of the samples and standards, but rather by analyzing the differences between heavier and lighter isotopes. Therefore, the quotient of the less abundant isotope to the more abundant isotope is calculated and expressed as the isotope ratio (R). The content of the isotopes is given as the deviation of the ratio of two isotopes of the same element from an international standard (in this thesis: VSMOW 2). In this way, instead of the absolute ratios, dimensionless δ- values are obtained for a given pair of isotopes:

$$\delta = \frac{R_{sample} - R_{standard}}{R_{standard}} * 1000\ [‰] \qquad (1)$$

Where R_{sample} is the isotopic ratio of the measured sample and $R_{standard}$ is the ratio of the Vienna Standard Mean Ocean Water (VSMOW2) for the identical isotopes. All measurements are expressed relative to the VSMOW2, even if VSMOW is mentioned in this work for simplicity. The results are expressed in the so-called delta notation, e.g., δ^{18}O and δ^{2}H for the ratios of ^{18}O/^{16}O and ^{2}H/^{1}H, respectively, and reported in per mil (‰). Negative δ- values represent a depletion of heavier isotopes, relative to VSMOW, while positive δ- values indicate an enrichment of heavier isotopes (Sulzman, 2007).

The fractionation effects described in the introduction (chapter 1.2) cause the isotope values for δ^{18}O and δ^{2}H in meteoric water to correlate strongly with each other. Craig (1961a) established an equation for this link, known as the Global Meteoric Water Line (GMWL) and a more recent equation was introduced by Rozanski et al. (1993):

$$\delta^2 H = 8.13 * \delta^{18} O + 10.8 \quad (2)$$

In addition to the GMWL, there is the Local Meteoric Water Line (LMWL). It reflects the context of the local precipitation and consists of at least one year of local precipitation (McGuire and McDonnell, 2007). The LMWL ($\delta^2 H = 8.03 * \delta^{18} O + 10.5$) for the precipitation in the area where the regional vegetables were produced almost overlaps with that of the GMWL. In this thesis regional differences of the local vegetables are compared with imported vegetables (from the Netherlands, Italy, and Spain). However, the geographic origin of the imported vegetables is not known more precisely than their national origins, therefore the plots display only the GMWL. The deuterium excess (d-ex $= \delta^2 H - 8.13 * \delta^{18} O$) can be used as an indicator of the influence of evaporation when studying the isotope composition of surface and groundwater (Leibundgut et al., 2009). This is to be considered in this work, to recognize possible fractionation by evaporation with the execution of the different methods.

2.1.2 Farms

Vegetables from four farms (K, M, Q, R), located in the surroundings of Freiburg i.Br. in the southwest of Germany, were compared with each other. Additionally, the same kind of vegetables from a supermarket ('S') were compared to see regional differences on a large scale more clearly. These farms were chosen because they agreed to provide water samples of their irrigation water and were located not too far from the isotope laboratory in Freiburg, making it possible to obtain fresh vegetables and analyze them as soon as possible. Farms Q and K farm organically, while the other two use conventional farming methods. The locations of the participating farms can be found in Figure 1.

A well water sample ("irrigation water") was collected from each farm on 11/23/2020 and analyzed using the same CRDS instrument (L2130-*i*, Picarro Inc., USA) in the same manner as the water extracted from CVD. Farm K irrigates vegetables from two different wells due to physical distance. However, due to the small difference in isotopic values, an average of these wells is used to represent the irrigation water from farm K for all comparisons in this study.

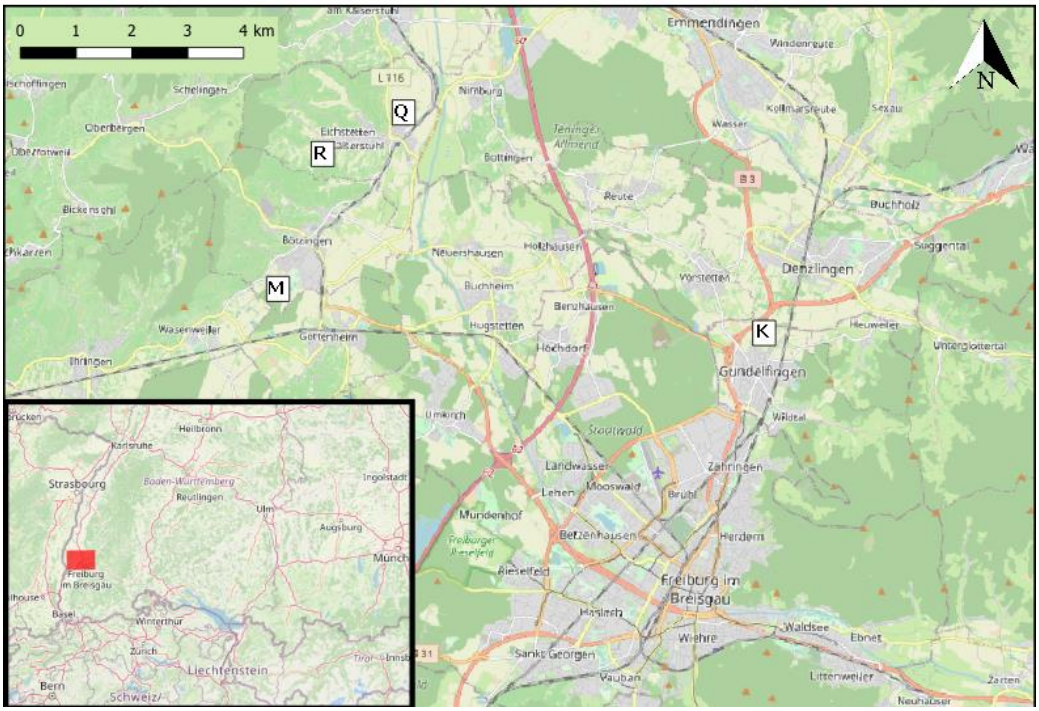

Figure 1: Map of local farms (M, R, Q and K) in South-West Germany, from which the vegetables studied originate.

2.1.3 Meteorology

The hourly amount of precipitation covering the duration of the growing phases of the vegetables used for this study were downloaded from the Albert- Ludwigs University of Freiburg ("http://weather.uni-freiburg.de/"). The respective climate station that recorded them is located in the city of Freiburg on the roof of the chemistry building (Albertstraße 21, Freiburg i.Br., Germany). The isotopic values ($\delta^{18}O$ and $\delta^{2}H$) were measured in the precipitation collected as bulk samples per precipitation event on the roof of the Rektorat (Fahnenbergplatz 1, Freiburg i.Br., Germany), which is only about 220 m away from the climate (precipitation) station. The annual precipitation in that area is about 934 mm (DWD 2021, station ID: 1443; Freiburg). A low amount of precipitation in the summer of 2020 made it necessary to irrigate the plants. However, no information was available regarding the amount and timing of irrigation.

To determine the water stable isotope composition in precipitation, to which every vegetable was exposed, the isotopic compositions in precipitation (bulk samples per event) were averaged, based on the different length of growth phases. To calculate the isotopic composition weighting of precipitation was conducted. Therefore, the growing phases of the different vegetable varieties were defined, and the respective precipitation amounts, and stable isotopic values of precipitation were averaged for the respective time periods.

2.1.4 Vegetables

The analyzed vegetables were cauliflower (CAU: *Brassica oleracea* var. *botrytis* L.), celery root (CEL: *Apium graveolens* var. *rapaceum*), kohlrabi (KOH: *Brassica oleracea* var. *gongylodes*) and potatoes (POT: *Solanum tuberosum*). These vegetables were chosen because of the season when the field campaign was executed, and because of their size, so that all measurements could be carried out on the same sample of vegetable. The vegetable samples had to be of a minimum size in order to both accommodate the relatively large probe of the *in situ* measurements and on the other hand, for comparative reasons, to allow all three methods to be carried out on the same piece of vegetable. Considerations of performing five replicates on one sample of vegetable were quickly discarded, as the samples of vegetable, apart from the celery root, were not large enough.

Therefore, five samples from each farm were chosen for every kind of vegetable. Since the laboratory testing was late in the year (late November and December), most of the vegetables (CEL, KOH and POT) had already been harvested and stored in refrigerated rooms. Only the cauliflower could still be harvested from the fields on farms Q and K. Farm M's cauliflower was taken from the refrigerated storage. Unfortunately, farm R had not grown cauliflower, so samples of this vegetable could only be analyzed from the three remaining farms and from the supermarket. All vegetables were grown outdoors and irrigated (except POT) when needed.

Unfortunately, the samples of vegetables examined from the supermarket could not all be obtained from the same country. The celery roots and potatoes were from the Netherlands, the cauliflowers from Spain and the kohlrabi from Italy. These were the vegetables originating from the most distant countries, found in 6 different supermarkets at the time of the study. The exact place of cultivation could not be obtained from the label.

2.1.5 Isotope Calibration Standards

Commonly, at least three working standards referenced to SMOW, or rather the VSMOW-SLAP scale (Craig, 1961b), are included in isotope measurements of unknown water samples for accuracy assessment.

The samples were normalized with a two-point calibration using the lighter (“FSM”: $\delta^{18}O$: - 16.61‰; $\delta^{2}H$: -125.84‰) and heavier (“North Sea”; $\delta^{18}O$: -0.33‰; $\delta^{2}H$: -2.46‰) in-house laboratory standards. The additional medium standard (“WEK”; $\delta^{18}O$: -9.5; $\delta^{2}H$: -65.99‰) was measured for validation purposes. Using laboratory standards instead of the international standards that can be obtained from the international atomic energy agency (IAEA) is more affordable. Therefore, these standards can be used in greater volumes. The laboratory standards had been calibrated

previously against the international reference standard Vienna Standard Mean Ocean Water 2 (VSMOW2). The accuracy of the isotope measurements had been confirmed repeatedly in inter-laboratory comparisons organized by the IAEA.

The standards were analyzed like the samples following the principle of identical treatment (Carter and Chesson, 2017; Brand et al., 2014; Werner and Brand, 2001). They were prepared and measured with the same measurement protocols for each method and are used to calibrate the data. Hence, the way the standards were prepared and measured varied for each method.

The liquid standards for the DVE-LS method were placed into the same Al-laminated bags. In order to measure duplicates, the three standards were filled into the bags once before the beginning of the measurements of the samples and once after the completion of these measurements and heat sealed. The reason for preparing multiple sets of standards (DVE-LS method) was to detect potential instrument drift over time and to calculate achievable analytical precision. The calibration was then performed using the mean values of both sets for each respective standard.

The standards for the *in situ* method had to be measured with the same probe and under comparable conditions as the samples. For this purpose, sand was dried for 40 h in a drying oven at 104°C. The sand was then mixed with 10 % by weight for each of the isotopically known standards ('FSM', 'WEK', and 'North Sea') and placed into air- and evaporation- tight glass jars. The pore space vapor of these standards was measured with the same type of probe, permanently with airtight installation in the lid of the jar (for the description, see chapter 2.1.5).

For the calibration of the CVD method, different standards were used than for the other two methods. The values for $\delta^{18}O$ ($\delta^{2}H$) were for the light, medium and heavy standard -14.86‰ (-107.96‰, -9.47‰ (-66.07‰), and -0.3‰ (1.53‰), respectively. These standards were placed in the same vials as the samples and measured with the CRDS (L2130-*i* and L2140-*i*, Picarro Inc., USA) at the beginning, in between and at the end of the vegetable tissue water measurements. The respective mean value of these measurements was then used for the calibration and validation of each method.

The precision, usually expressed as the standard deviation, is calculated from replicate analyses of the co-measured standards.

2.1.6 Analysis with CRDS

CRDS, one technique to measure via IRIS, measures the stable isotopes in vapor form. In this thesis, this is done either directly (DVE-LS and *in situ* method) or the liquid samples are injected to the vaporizing chamber with the attached autosampler, where the liquid water sample is converted into water vapor and then measured by the CRDS.

CRDS measures the different absorption spectra of different isotopologues. A pulsed laser beam is fed into the cavity. When a certain high-intensity threshold value is reached, the laser beam is switched off again, causing the observed intensity to gradually decline, i.e., the so-called Ring-Down. This way, the molecules and their concentration can be determined by their known wavelength and the resulting absorption peak (Picarro Inc., 2020).

In this work, three different CRDS devices were used. The device L2120-*i* (Picarro Inc., USA) was used for the *in situ* and DVE-LS vapor measurements, whereas for liquid samples the devices L2130-*i* and L2140-*i* (Picarro Inc., USA) were used to determine the isotopic composition of the plant tissue water obtained during the CVD.

Table 1: Explanation of the spectral parameters that are recorded by the analyzing instrument and react sensitively to volatile organic compounds (VOCs) used to examine spectral interference. Source: Johnson et al. (2017).

Instrument	Parameter name	Parameter definition	Diagnostic meaning
L2120-i	organic_res	RMS residuals of the least squares fit (organics)	Indicates how well the observed absorption spectrum can be fitted to the spectrum of pure water; poor fit may indicate organic interference
L2120-i	organic_shift	Change in constant term of fitted organic baseline	Indicates whether the y-intercept of the baseline underlying the absorption spectrum has been distorted relative to original factory calibration
L2120-i	organic_slope	Change in linear term of fitted organic baseline	Indicates whether the slope of the baseline underlying the absorption spectrum has been distorted relative to original factory calibration
L2120-i	organic_MeO-Hampl	Absorption of MeOH peak	Indicates whether methanol (MeOH) is present in the sample, and if present then in what concentration
L2120-i	organic_CH4_conc	CH4 mole fraction with no calibration	Indicates whether methane (CH4) is present in the sample, and if present then in what concentration

The Picarro's instruments also measure spectral parameters that are recorded by the analyzer and react sensitively to volatile organic compounds (VOCs) in addition to isotope values. These values

are not used to calibrate the isotopic values reported by the devices, but rather allow the user to identify the more conspicuous values (personal correspondence with Picarro Inc.). These parameters are not calibrated and are therefore considered as unitless proportions in this work. The unitless parameters studied were ‘organic_res’, ‘organic_shift’, ‘organic_slope’, ‘organic_MeOHampl’ (for MeOH), ‘organic_CH4_conc’ (for CH4) and ‘organic_base’ (for EtOH) from the raw data output files (‘Datalog_Private’). The explanation of all parameters (except for ‘organic_base’) can be found in Table 1. The meaning of ‘organic_base’ is taken from Martín-Gómez et al. (2015).

2.1.7 Measurement Campaign

All three methods were executed in the laboratory of the Chair of Hydrology of the Albert- Ludwigs- University of Freiburg. The experiments took place in November and December 2020. Because all three methods were each carried out on the same sample of vegetable, time was of the essence, as evaporation and accompanying isotope effects had to be avoided. The experimental set-up was chosen in such a way that all measurements were performed on each vegetable sample, on all varieties in the same way with the same measurement protocol, thus following the principle of identical treatment (Werner and Brand, 2001). The *in situ* method was always performed first. After the sampling time of the *in situ* measurement (for method description see chapter 2.2.2), samples for the other two methods were collected. For this purpose, samples were taken from adjacent spots on the same vegetable pieces. This was necessary because pre-tests (data not presented) showed that there were isotopic differences depending on the analyzed part for some vegetables. The stem of the CAU was examined. CEL and KOH were always sampled at the same height (centered) through the vegetable sample and POT centered through the longest side.

The collected samples were then placed in the sampling bags (for the Direct Equilibrium Method) and vials (for the Cryogenic Extraction Method) provided for each method. In case of the Cryogenic Extraction Method, they were stored in a fridge and in case of the DVE-LS method stored in the temperature regulated laboratory, where the analysis took place the next day.

2.2 Continual *in situ* Monitoring

Volkmann and Weiler (2014) developed probes to continuously and uninterruptedly study water stable isotopes of soil pore water. They thus created a fast and more cost-effective method that eliminates the need for destructive soil sampling and subsequent laboratory workload and allows for repeated, minimally- invasive water stable isotope analyses on the same location. In my thesis these probes are used for the analysis of tissue water of the vegetables to obtain instant results of the water stable isotopes, while also shortening the time of the measurement process.

2.2.1 Working Principle and Material

The method referred to as the '*in situ*' method uses the diffusion dilution sampling (DDS) method (Volkmann and Weiler, 2014). Dry air is delivered into the tip of the probe and it absorbs the water vapor corresponding with the liquid phase surrounding the probe which consists of a hydrophobic microporous tube (Fischer Plastics GmbH). The resulting moist air is then carried to the L2120- *I* analyzer where it is analyzed for $\delta^{18}O$ and $\delta^{2}H$.

The CRDS analyzer takes in air at a steady flow of about 30 - 35 $mL*min^{-1}$ through the sample line. Preliminary tests showed that the best setting for the throughflow into the microporous tube was found to be approximately 27 $mL*min^{-1}$ and 5 $mL*min^{-1}$ for the dilution. These settings were maintained for all measurements. They result in vapor mixing ratios of about 15000 ppmv to 20000 ppmv which is within the analyzers optimum measurement range. Reducing the vapor concentration below saturation by adding dry air for dilution, reduces the risk of potential condensation in the sample line and unwanted isotope effects (Volkmann et al., 2016). The flow rate of the throughflow and the dilution were each regulated by a programmable digital mass flow controller (dilution: Mass Flow Controller GFC Analyt (0-50 $mL*min^{-1}$); throughflow: Analyt-MTC (0-200 $mL*min^{-1}$), Messtechnik GMBH, Müllheim, Germany).

The core of the probe was 10 mm in external in diameter and was 50 mm long. During analysis, it was important that the probe was entirely surrounded by the sample matrix in order to avoid exchange with ambient air. For this purpose, a hole with a diameter of 11 mm had been drilled into the sample of the vegetable to be examined. The resulting higher risk of exchange with ambient air when drilling a slightly wider hole was eliminated by adding a silicone cone to the shaft of the probe (Figure 2).

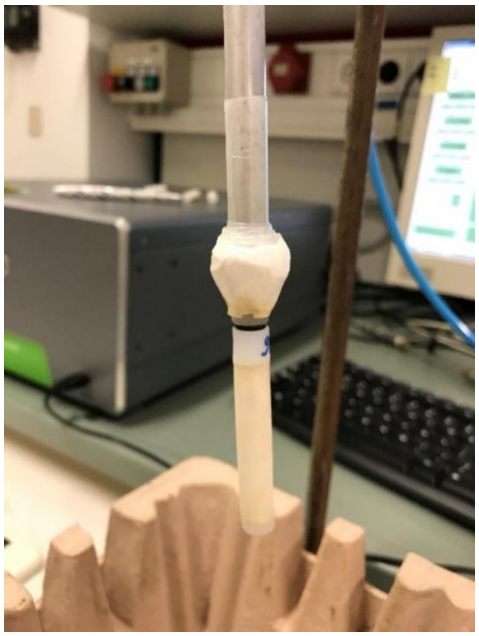

Figure 2: *In situ* probe with silicon cone for sealing purposes.

Figure 3: Measuring structure of the *in situ* probe, as well as a bag for the DVE-LS method and the exetainer vials for the CVD.

2.2.2 Sample Preparation and Execution

The *in situ* method was the first to be carried out on each sample of vegetable. After drilling the hole for the probe, the top of the vegetable sample, where the sensor entered, was cut at a 90-degree angle to the hole for the sensor, so that the contact surface of the silicone cone was flat and undisturbed. The probe was then inserted vertically and held in place with a clamp (Figure 3). Each measurement lasted for 7 minutes. After vapor concentration and stable isotope readings had stabilized, a 90 second average of the isotope data was calculated and used for further analysis. Afterwards, the probe was pulled out. The microporous tube probe was disconnected and replaced by another dry one. A flushing phase of 3 minutes followed using dry air. Then the measurement cycle was repeated with a new sample of vegetable. To minimize errors due to evaporation, the borehole was additionally covered with transparent film during the measurements. Of the three methods applied, the *in situ* method is the least time-consuming and needs the least preparation.

2.3 Direct Vapor Equilibration- Laser Spectroscopy Method

The direct water vapor equilibrium method, in the following description also referred to as 'DVE-LS' was first described by Wassenaar et al. (2008) and later modified by Hendry et al. (2015). It became feasible with the invention of laser-based analyzers and was developed for stable isotope analysis of matrix-bound water contained in sediment or geologic cores. In the meantime, this method has been used extensively for rapid analyses of high-resolution depth profiles of soil and rock water stable isotopes. The data obtained from these analyses were then used for the investigation of subsurface water flow and solute transport processes and subsequent assessments of groundwater recharge and vulnerability, for example. Lately, Millar et al. (2018) tested this method on plant samples.

2.3.1 Concept and Material

DVE-LS is based on the principle that in an isotherm and closed system, an isotopic equilibrium of the liquid water isotopes contained in the vegetables and the corresponding water vapor in the available headspace is established.

An advantage of this method is that it avoids laborious and time-consuming water extraction steps, for example CVD, prior to the actual isotope analysis. Instead, the sample is placed in an air and vapor impermeable Al-laminated 500 mL bag (CB400-311siZ, WEBER Packaging, Güglingen, Germany) and left standing until equilibria are set. The isotopic composition is measured by extracting the headspace vapor and analyzing it with the same CRDS (Picarro L2120-*i*, Picarro Inc., USA) as for the *in situ* method. A hollow needle attached to the CRDS via a 1/8'' Teflon (PFA) tube was inserted into the bag through the previously added silicone drop on the bag. The silicone serves as a seal while the needle is in the bag and to seal the bag once the needle is pulled out.

By means of continuous flow headspace sampling, the isotope ratios of hydrogen and oxygen are measured. This method enables a fast sample throughput and instantaneous results of the isotopic composition. There is no active laboratory work required during the equilibration phase, but the hollow needle needs to be switched manually in between the bags for consecutive measurements.

2.3.2 Sample Preparation and Execution

After the *in situ* measurement of a vegetable sample was completed, that sample was cut into smaller samples for the other two remaining methods. Care was taken to ensure that the samples for the

DVE-LS method were taken at a sufficient distance from the drilled hole of the *in situ* measurement so that the isotope values were not influenced by the previous measurement. Furthermore, the samples were always taken from the same area of the vegetable (ie. in the center of the vegetable). In this way, the variations observed in the pre-tests with certain types of vegetables should not influence the results undesirably. For example, because the stem of the CAU is very thin, the distance of the samples taken for the other two methods to the hole of the *in situ* measurement and the outer wall of the stem was less than it was for the KOH and CEL samples. About 20 g of the vegetable samples were cut into 0.5 cm cubes to increase the surface area and placed in a bag. Preliminary tests showed that it was worse to crush the vegetable samples. The samples treated in this way in preliminary tests showed very high values for methane and methanol. It was assumed that the increasing of the surface area in this way accelerated the build-up of spectrally interfering volatile organic compounds.

Sampling bags for the DVE-LS method were heat- sealed after squeezing out the remaining air and inflating them up with dry air. Care was taken to reduce the time the vegetable samples were in contact with the atmospheric air to minimize errors due to evaporation. Afterwards, all bags (samples and standards) were stored for about 18 hours in the air- conditioned laboratory (21°C), in which they were subsequently analyzed. Care was taken to ensure that samples of all vegetables were equilibrated for the same duration of time in order to comply with the principle of identical treatment.

Subsequent to the equilibration phase, the liquid water standards were measured before and after the samples. The actual measurement is quite simple and not labor-intensive. However, the sampling bags must be exchanged manually between measurements. After each measurement phase (240 s), the needle must be withdrawn from the sample being tested. The time of the flushing phase (120 s) must be waited for. In that phase, unsaturated ambient air is sampled in order to remove vapor- saturated air of the previous sample from the analyzer. After that phase, the needle must be manually inserted into the new bag. During the measurement, the bag volume decreases due to the gas flow demand of the Picarro L2120-*i* of approximately 32 ml*min $^{-1}$, but the pressure remains constant due to the bags‘ flexibility. As with the *in situ* measurement, the CRDS measures continuously, hence a 90-second mean value of the plateau of vapor and isotopic values that sets in is calculated and used for interpretation. The temperature in the laboratory varied between 19.6°C and 21.1°C for all days of measurements. Possible resulting measurement inaccuracies are considered minimal and therefore not considered in this work.

2.4 Cryogenic Vacuum Distillation

2.4.1 Concept and Sample Preparation

The cryogenic vacuum distillation ('CVD') is a very commonly used method for the quantitative extraction of soil and plant water (Millar et al., 2018; Araguás-Araguás et al., 1995; Orlowski et al., 2016b). It is based on the principle that a sample is heated to evaporate the contained liquid water, which is then collected it in a cold trap. The experimental setup used in this study is based on the vacuum extraction technique modified by Koeniger et al. (2011).

Laboratory tests were previously conducted to determine the volume of sample tissue that resulted from the extraction of a sufficient amount of water while keeping extraction time minimal. All vegetable samples were cut into ~ 5 mm strips and placed into 12 mm glass Exetainer® vials (Labco Ltd, Lampeter, UK). These vials were weighed and stored in a refrigerator to minimize potential evaporation prior to extraction.

As Koeniger et al. (2011) described, a glass vial (referred to in the following as 'extraction vial') was filled with the sample and a second, empty glass vial (referred to in the following as 'collection vial') was connected to the first via a 1mm stainless steel capillary tubing of about 8 cm in length. The samples were cut into thin strips and approximately 1.3 g was placed into each vial. To avoid evaporation, the vegetable samples had to be processed quickly and sealed airtight. Both glass vials were sealed by a rubber septum (IVA Analysetechnik GmbH & Co. KG, Meerbusch, Germany) through which the connecting steel capillary was pierced.

2.4.2 Extraction

The next step was to immerse the extraction vial in liquid nitrogen to prevent loss of water vapor from being removed from the system during subsequent evacuation (Koeniger et al., 2011). With a hollow needle and a connected vacuum pump (Edwards), a vacuum of approximately 0.03 mbar was generated in the collection vial and therefore in the extraction vial. Koeniger et al. (2011) used this threshold in their study and the pump in the isotopic laboratory of the university was able to reach this threshold in less than a minute. Then the evacuation needle was removed from the rubber septum again.

Unlike Koeniger et al. (2011) described, the extraction vial in this setup was subsequently inserted into a block of aluminum which allowed for up to ten vials to be processed simultaneously. The block was placed on a heating plate, which was heated to approximately 120°C. The bottom part of the collection vial was simultaneously hung into a Dewar flask filled with liquid nitrogen (~ -196°C)

(Koeniger et al., 2011). To avoid incomplete water extraction due to different thicknesses of the tissue samples, all samples were extracted for 60 minutes. This relatively long extraction time was used for this experimental setup because the number of the replicates was limited. Therefore, it was important to ensure that the tissue water from all samples was extracted as thoroughly as possible. Preliminary tests showed that in most cases the time necessary for complete extraction was shorter. However, the applied setup did not allow for monitoring the vacuum and thus the vapor pressure inside the vials once the extraction was initiated. For this reason, the extraction time was planned with such a large buffer. It was always possible to extract 10 vegetable samples at a time.

The vials were disconnected from the connecting steel capillary afterwards and left standing at ambient temperature until the tissue water fully thawed. The extracted water samples were not filtered or treated further. The vials were subsequently weighted, and the collected water pipetted into a 2 ml vials (12 x 32 mm clear glass screw-top vial with a 9 mm thread and PTFE/Silicone septa caps, Klaus Ziemer GmbH, Langerwehe, Germany).

2.4.3 Analysis

The extracted water was then analyzed with L2130-*i* or L2140-*i* for the isotope composition ($\delta^{18}O$ and $\delta^{2}H$). Water extracted from the local vegetable CAU and CEL and irrigation water was measured with the L2140-*i* and water extracted from local KOH and POT, as well as all supermarket vegetables, was measured with the L2130-*i*. Each sample was measured six times. The first three measurements were discarded due to a possible memory effect and the mean value from the last three measurements was used for further consideration.

To ensure that all cell water was extracted, the extraction vials were weighed before and immediately after extraction, and again after drying in the drying oven at 104°C for about 20 h. To check the efficiency of the cryogenic vacuum distillation, the formula described by Fischer et al. (2019) was applied:

$$E_{eff} = \frac{W_I - W_E}{W_I - W_D} \quad (1)$$

where W_I represents the weight before the extraction, W_E describes the weight after the extraction and W_D is the weight after oven- drying until no weight difference could be measured anymore. Samples with resulting E_{eff} values of more than ± 0.03 were discarded.

2.5 Data Processing

All data processing and statistical analyses of the isotopic data were carried out using the RStudio software (version 1.1.453, RStudio Inc, 2020).

All isotope data were referenced to the international standard VSMOW2. Subsequently, they were checked for consistency and plausibility. The vapor humidity in the laboratory was also constantly monitored during the situ and DVE-LS measurements. The visual inspection of the data was followed by a cluster analysis to identify and remove possible outliers. Therefore, in the cluster analysis, the vegetable varieties were examined in separate analyses for each method. The approach of a hierarchical, agglomerative procedure was used to perform the cluster analysis (Almeida et al., 2007). This involves a step-by-step examination to determine which of the clusters are closest to each other. The linkage- method ("single linkage") was used. The minimum of all possible distances (Euclidean distance) between the data points of the two compared clusters was checked and the data points with the smallest distance were placed in the same clusters accordingly. The formula for the Euclidean distance (d) is as following:

$$d_{(x,y)} = \sqrt{\sum_i (x_i - y_i)^2} \tag{2}$$

x and *y* represent the two compared vectors. Several cluster analyses of the data were performed to identify possible offsets in the data. For this purpose, the $\delta^{18}O$ and $\delta^{2}H$ values and additional spectral parameters that were recorded by the analyzer and reacted sensitively to VOCs were analyzed individually with a cluster size (k) of k = 2 for each vegetable.

Clusters that contained only one data point were labeled. The labeled data were then visually examined again, at which point six data points were removed from the dataset. Due to the comparability and the following statistical analysis, only samples for which values were available for all three methods will be considered in the following. The values labeled by the cluster analysis were also examined with respect to the spectral parameters.

2.6 Statistical Data Analysis

The data were tested for normal distribution using histograms, quantile-quantile plots, and the Shapiro-Wilk normality test.

The comparison of the respective vegetable varieties between the farms, the examination of the differences between local and imported vegetables and the comparison of the methods was performed, using the Kruskal-Wallis test (kruskal.test() in R). The Kruskal-Wallis test is suitable for

non-parametric, independent data and is a rank-based test (Dormann, 2020). The test was conducted with the function stat_compare_means() of the R package ‘ggpubr’ (Kassambara, 2020). Attempts to transform my data to a normal distribution failed.

2.6.1 Comparison of the Methods

Bland- Altman plots (Bland and Altman, 1995) were additionally used due to the better comparison of the methods than with regressions and correlations (Grouven et al., 2007). Instead of comparing the average differences of the methods, the differences of the methods (A-B) were plotted against the mean values ((A+B)/2) of these methods (Bland and Altman, 1995). The dashed line indicates the overall mean difference (bias) in values obtained from the two compared methods (Altman and Bland, 1983). When the bias is approximately zero, it means that the methods do not differ from each other. The dashed-dotted lines represent the limits of agreement (LOA). They are calculated using the standard deviations (-1.96 SD and 1.96 SD). Between these LOA lie approximately 95% of the values (Altman and Bland, 1983). One problem with the comparison of several methods is the unknown true value. Plotting the mean values of the two methods compared for the Bland-Altman method is assumed to come closest to this true value (Grouven et al., 2007).

The maximum accepted bias (MAB) is chosen to check the quality of the method comparisons. This is, as Martín-Gómez et al. (2015) used, 0.8‰ and 6‰ for $\delta^{18}O$ and $\delta^{2}H$, respectively. Compared to other studies (Orlowski et al., 2016b) these values are chosen very widely, however, in this work different methods are compared with each other and not with a reference value. These values are shown as the grey areas in the Bland- Altman plots. Spearman's ρ is the most used correlation coefficient for non-normally distributed data (Dormann, 2020) and is calculated for each plot. By ranking the data, possible outliers do not strongly influence the data (Dormann, 2020). The significance level (α) is set at 0.05.

2.6.2 Examining the Influence of Spectral Parameters

In addition to the $\delta^{18}O$ and $\delta^{2}H$ values, the Picarro L2120-*i* additionally records the previously described parameters that react sensitively to spectral interference. This allows for conclusions regarding possible organic contamination of the samples and therefore any influence on the measured isotopic values. To determine the correlating and influencing parameters, General Linear Models (GLMs) were used. Since the δ - values and some organic parameters are negative values and cannot be examined with the GLM, they were previously shifted into the positive range by adding the minimal value. Based on a visual examination and a previously performed cluster analyses for each

method, a preselection of (non-) correlated factors was determined. Nevertheless, all parameters were reduced with the 'backwards stepwise model selection' (Dormann, 2020), regarding the minimization of the AIC (Akaike information criterion), so that in the end only the significant parameters remained in the model. Based on the GLMs, the influence of the organic parameters on the $\delta^{18}O$ and $\delta^{2}H$ values is investigated.

2.6.3 Testing regional authenticity

As Oerter et al. (2017) stated, the analysis of the recovery of the source water is tested using the intersection of the regression lines of $\delta^{18}O$ and $\delta^{2}H$ with the GMWL. Kruskal- Wallis tests are performed between the local and imported vegetables to detect significant differences.

3 Results

3.1 Analysis of Isotopic Composition of Precipitation and Irrigation Water

In the following chapter, the relationship between precipitation and irrigation water and the isotopic composition of the vegetable samples will be analyzed. For this purpose, the amounts and isotopic composition of the precipitation were considered (Figure 4). In this figure, the respective average growth phases of the vegetable varieties on all farms are presented.

Differences in irrigation water of the farms (Figure 4 and Figure 5: dark red dots) were almost indistinguishable. The $\delta^{18}O$ values for the farms K, R, Q and M were -8.3‰, -8.22‰, -8.22‰, - 8.14‰. The $\delta^{2}H$ values for the same farms were -58.4‰, -58.3‰, -59.0‰, -58.8‰.

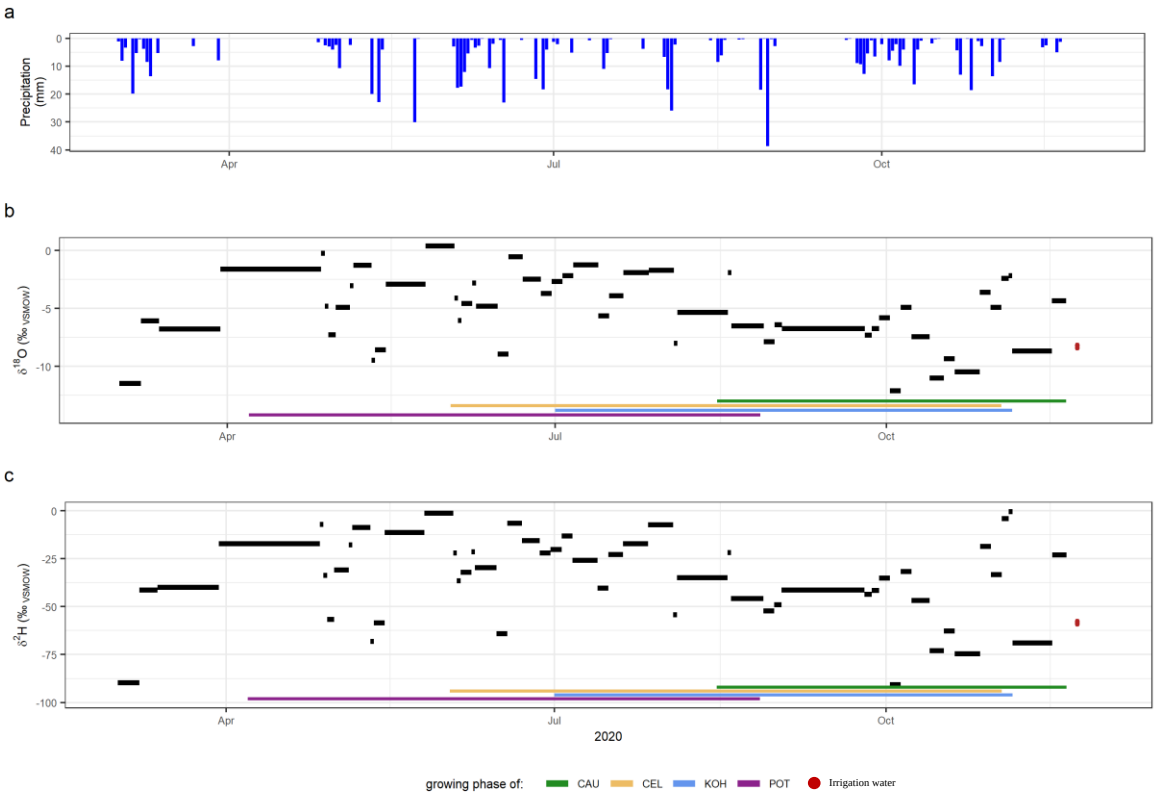

Figure 4: Daily values of precipitation amount in mm (a), The values for $\delta^{18}O$ (‰$_{VSMOW}$) and $\delta^{2}H$ (‰$_{VSMOW}$) of these precipitation events are shown in b and c, respectively. Since these are bulk samples, the black bars indicate the time over which the samples were collected. In addition, the growth phases of the vegetable samples (CAU, CEL, KOH and POT) are shown in b and c. The dark red dots mark the isotopic values of the irrigation water and the time it was sampled.

Weighting of the stable isotope values of the precipitation showed that the POT were growing in a timespan with the heaviest isotope values in precipitation and CAU samples were growing in the phase with the lightest isotopic composition (Figure 5). CEL and KOH data differed only negligibly, with CEL data being slightly more depleted in heavy isotopes. The mean $\delta^{18}O$ values of the precipitation were -7.5 ± 2.9‰, -6.3 ± 2.9‰, -6.7 ± 3.0‰ and -5.3 ± 2.7‰ for the vegetables CAU, CEL, KOH and POT, respectively. The $\delta^{2}H$ values for the same vegetables were -49.3 ± 23.5‰; - 41.9 ± 20.4‰; -44.4 ± 22.7‰ and -35.3 ± 18.1‰, respectively. These values and their SD are plotted in Figure 5. Numerical values of these data can be found in Table A. 1.

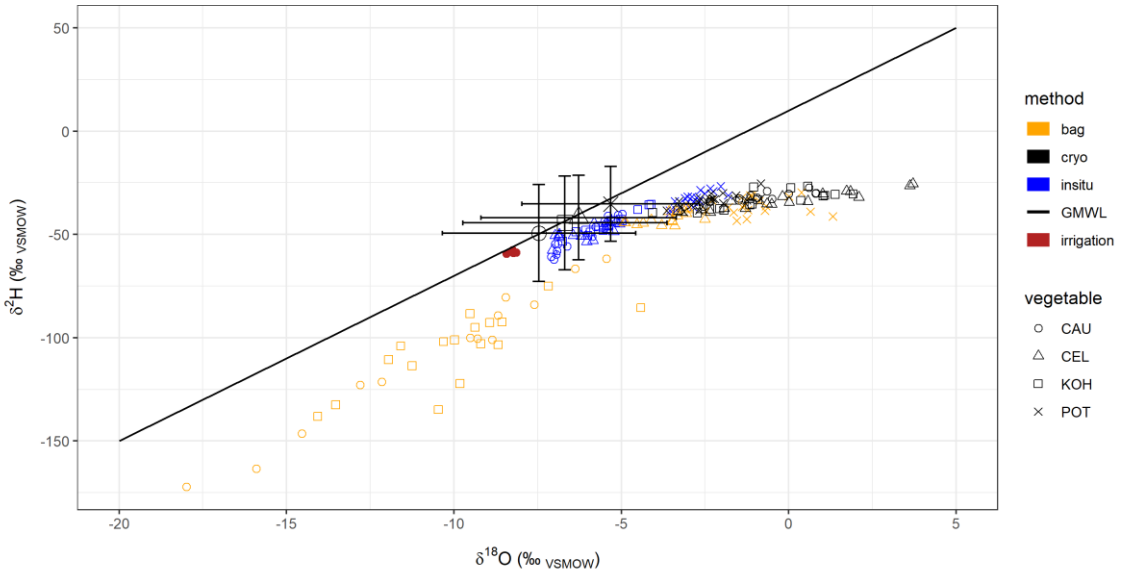

Figure 5: Dual isotope plot of local data with the mean isotopic composition of the precipitation (larger black symbols) during the respective growth phase of each vegetable and their standard deviation. The colors indicate the three methods and the shapes the four different vegetables. The black line represents the GMWL.

3.2 Measurement accuracy of the methods

Repeated measurements of the calibration standards resulted in an analytical precision for the CVD method of ± 0.1‰ of the $\delta^{18}O$ values and ± 0.9‰ of the $\delta^{2}H$ values. The $\delta^{18}O$ values are all within the manufacturer's stated precision of ± 0.16‰ for $\delta^{18}O$. The precision of the $\delta^{2}H$ values is slightly worse than the manufacturer's stated precision of ± 0.6 for $\delta^{2}H$. The values for the *in situ* method are very similar. The analytical accuracy for $\delta^{18}O$ is slightly worse than the CVD (± 0.2‰ $\delta^{18}O$),

but the δ^2H values coincide (± 0.9‰). For the δ^{18}O and δ^2H values of the DVE-LS, the precision was ± 0.3‰ and ± 1‰, respectively.

For the DVE-LS and *in situ* methods, 94 samples were available for each method. Since the extraction of two samples was incomplete for the CVD, these samples were discarded, and the data set consists of 92 measurements per method. The final data set, after removing the data points with the previously described criteria, consisted of a total of 86 samples of vegetables per method.

3.3 Comparison of the Methods

In the following section, the differences between the methods and the differences of these between the local farms are presented, as well as the influence of the volatile organic compounds on the results of δ^{18}O and δ^2H.

3.3.1 Isotopic Results for All Types of Vegetables by Farms and Methods

The direct visual comparison of the methods (Figure 6) shows the isotope values of the vegetables depending on which method was used for each individual farm. All data plots below the Global Meteoric Water Line (GMWL).

Although the DVE-LS data were more scattered, the DVE-LS and *in situ* measurements had similar tendencies, because POT and CAU data (δ^{18}O and δ^2H) tended to have heavier and lighter values, respectively, in the results from both methods (Figure 6). The POT data, analyzed with the CVD, were more centered compared to the results for the other vegetables using this method, and for farm R they had lighter δ^{18}O values. The comparison of the CVD and *in situ* data showed that the results of the CVD measurements had more depleted δ^{18}O values and slightly heavier δ^2H values. Furthermore, the values of the CVD method plotted closer to the GMWL. The CAU and KOH isotope values of the DVE-LS scattered over a wide range for all farms. The CEL and POT isotope data of the DVE-LS method each formed clusters, with the POT data being heavier in δ^{18}O and δ^2H than the CEL data, except in the case of the supermarket vegetables. Data from the supermarket vegetables plot between the CEL data. These were more scattered than the data for the vegetables from other farms.

Measured with the DVE-LS method, CEL and POT were individually forming separate clusters, which was in contrast with the isotopic values of the CAU and KOH data, which were more scattered (SD: δ^{18}O: ± 3.8‰ and ± 2.3‰; δ^2H: ± 35.1‰ and ± 17.9‰, respectively). All values can be found in Table 2. Figure A. 17 shows that the local CAU, measured with the DVE-LS method have

a greater slope (9.1) than the GMWL (8). The other three vegetables showed reduced slopes of the regression lines (CEL: 2.6, KOH: 6.1 and POT: 0.14).

Isotope data of the analyzed vegetables via the CVD method did not show a clear grouping or such large ranges of scatter of the vegetable varieties compared to data obtained using the DVE-LS method. CEL, measured with the CVD, had the heaviest $\delta^{18}O$ values and was the most scattered (SD ±2‰). The $\delta^{2}H$ values scatter between -39.4‰ and -25.6‰ (mean -33.3 ± 4.1‰). The $\delta^{2}H$ values of CAU, KOH and POT differ only slightly from each other. The differences in the $\delta^{18}O$ were more distinct. KOH scatters in $\delta^{18}O$ between -4.1‰ and 2.1‰ (mean - 0.7‰ ± 1.8‰) and in $\delta^{2}H$ -39.6‰ and -25.5‰ (mean -33.1‰ ± 4.7‰). POT was more distinctly different from the other local vegetables in $\delta^{18}O$ (between -3.6‰ and - 0.8‰; mean -2.3‰ ±0.8‰). In $\delta^{2}H$, the differences from the other vegetables were less evident. They range in $\delta^{2}H$ between -39.0‰ and -25.4 ‰ (mean -33.7‰ ± 3.2‰). The isotope values of the CVD plot also all below the GMWL (Figure 6). This was also evident from the regression lines of $\delta^{18}O$ and $\delta^{2}H$, which in Figure 11 all show lower slopes than the slope of the GMWL. For CAU, CEL, KOH and POT these were 2.6, 1.4, 1.4 and 3.1, respectively. The isotopic data of all four types of vegetables correlate significantly with each other. The strength of the correlations was very similar for all vegetable varieties (ρ = 0.63, 0.59, 0.66 and 0.6 for CAU, CEL, KOH and POT, respectively).

Table 2: Minimum (min), maximum (max), mean ± standard deviation for $\delta^{18}O$ and $\delta^{2}H$ for every vegetable measured with each method.

Vegetable_ method	min $\delta^{18}O$	max $\delta^{18}O$	Mean $\delta^{18}O$	min $\delta^{2}H$	max $\delta^{2}H$	Mean $\delta^{2}H$
CAU_DVE	-17,99	-5,44	-10,59±3,8	-172,19	-61,8	-108,41±35,08
CAU_CVD	-2,54	0,82	-0,87±1,18	-36,49	-27,32	-31,81±2,49
CAU_ insitu	-7,09	-4,98	-6,24±0,81	-62,07	-40,04	-51,4±8,1
CEL_ DVE	-4,91	-2,5	-3,63±0,67	-45,78	-37,23	-41,9±2,95
CEL_ CVD	-3,21	3,71	-0,06±2,06	-39,36	-25,55	-33,43±4,17
CEL_ insitu	-7,06	-5,05	-6,01±0,69	-57,59	-43,61	-49,13±3,73
KOH_ DVE	-14,07	-4,42	-9,93±2,27	-138,07	-74,98	-105,5±17,91
KOH_ CVD	-4,07	1,92	-0,84±1,76	-39,6	-26,71	-33,74±4,42
KOH_ insitu	-6,75	-4,11	-5,41±0,72	-53,33	-35,47	-45,02±4,96
POT_ DVE	-2,47	1,32	-0,98±0,97	-43,27	-29,64	-36,29±4,02
POT_ CVD	-3,65	-0,83	-2,33±0,79	-38,97	-25,35	-33,66±3,29
POT_ insitu	-3,56	-1,81	-2,82±0,49	-39,89	-26,66	-32,96±3,69

The isotope results of the *in situ* measurements were on average lighter than those of the CVD measurements. With this method, the mean values ($\delta^{18}O$ and $\delta^{2}H$) of CAU, CEL and KOH were in relative agreement. POT data were more enriched in heavy isotopes than the other vegetables (Figure 5) and formed a distinct group. The CAU data scattered the most among all the vegetables

studied with the *in situ* method and had therefore also the largest SD (±0.8‰ for $\delta^{18}O$ and ±8.1‰ for $\delta^{2}H$). As with the DVE-LS, the CAU values measured via *in situ* method had a greater slope of the regression line ($\delta^{2}H$ and $\delta^{18}O$) (9.6) than the GMWL, while the other three types of vegetables had lower slopes (Figure A. 16; CEL: 3.9; KOH: 6.7 and POT: 6.1). The isotopic values of CAU and those of KOH indicated a strong, significant correlation (ρ = 0.95 and 0.94, respectively). CEL and POT also correlated significantly with each other, but their correlations were slightly lower at ρ = 0.71 and 0.81, respectively.

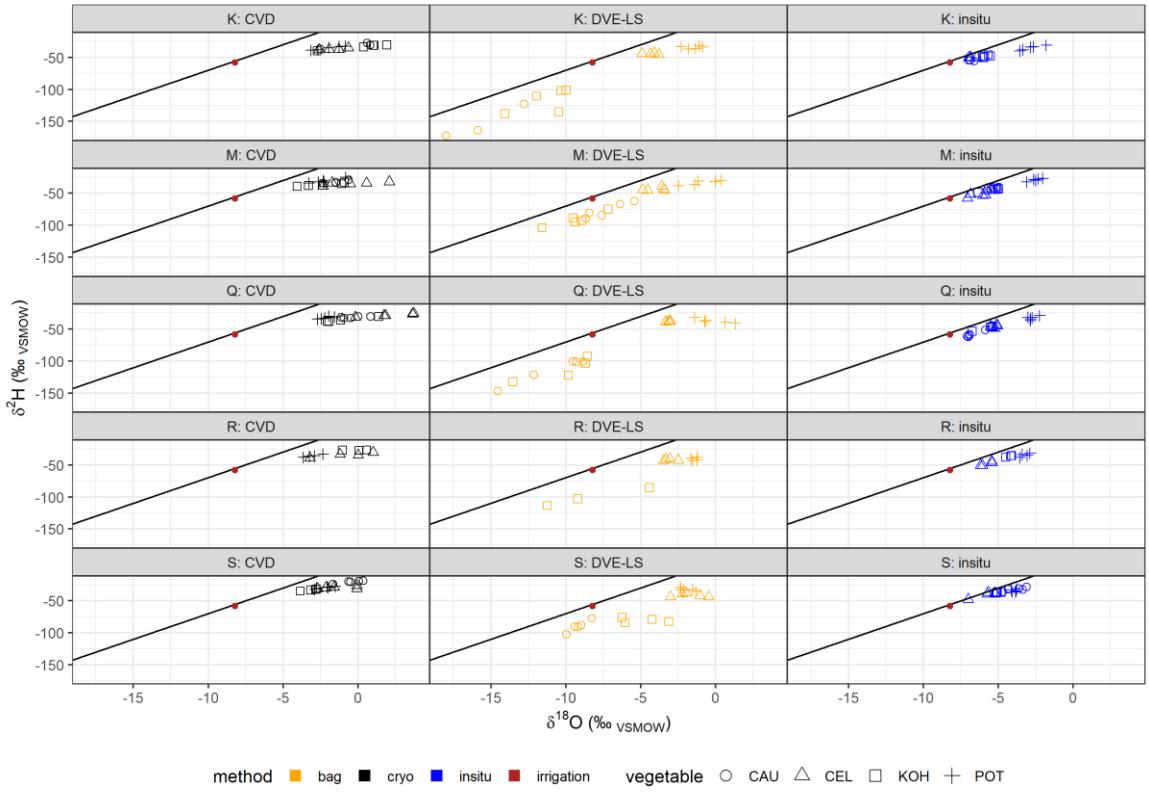

Figure 6: Dual isotope plots ($\delta^{18}O$ and $\delta^{2}H$) of all measurements. The single letters (K, M, Q and R) indicate the different farms and 'S' represents the supermarket vegetables. The colors indicate the three different methods (DVE-LS = direct vapor equilibrium, CVD = cryogenic vacuum distillation, *in situ* = continuous *in situ* monitoring), and the shapes represent the vegetables (CAU = cauliflower, CEL = celery root, KOH = kohlrabi and POT = potatoes), the red dots indicate the irrigation water, and the lines are the GMWL.

The water content ranges on average from about 80 % (POT) to 93 % (CAU) for all the vegetables studied. CEL and KOH were in between with 90 % and 91%, respectively.

3.3.2 Differences between the Methods

Figure 7 shows the results of the Kruskal- Wallis tests, which showed significant differences for each type of local vegetable, except POT, with all methods for the δ^2H values. The δ^{18}O data showed significant differences for all comparisons (Figure A. 6). The different farms did not show a consistent pattern and their results can be found in the appendix (Figure A. 1 - Figure A. 5). Figure A. 2 shows that the comparison of the methods worked best for POT, as no differences were found between the methods (δ^2H) and only minimal significant differences in central tendencies between DVE-LS and *in situ* in δ^{18}O data. Data from the other vegetables showed significant differences between the methods for both δ^{18}O and δ^2H.

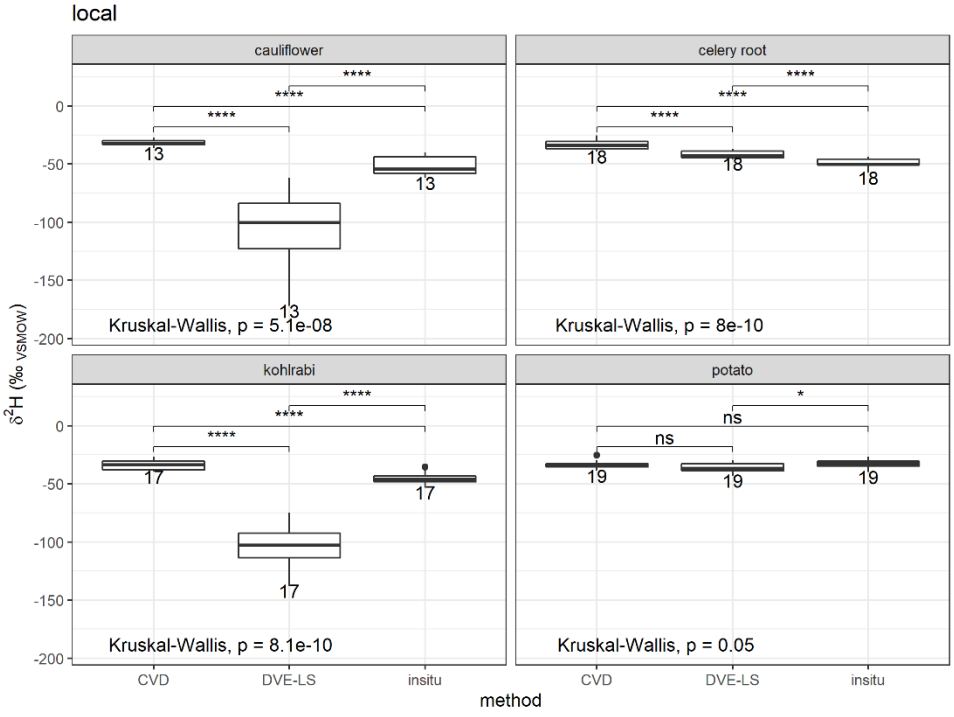

Figure 7: Boxplots of all local vegetable samples, plotted by the different methods and type of vegetable for δ^2H values. The number indicates the number of observations (n) and the lines and associated symbols indicate the results of the Kruskal-Wallis test. The respective comparisons are indicated by the p-value ('ns': $p > a$; '*': $p \leq 0.05$; '**': $p \leq 0.05$; '***': $p \leq 0.01$).

All comparisons of the methods (Figure 8; Figure A. 11; Figure A. 12; Figure A. 13) show clear differences. The bias should be zero, as this indicates that there were no differences between the methods studied. Figure 8 (A) shows a negative bias (-0.5‰). This indicates that the *in situ* method yields on average more negative values than the CVD method does for the POT samples. The bias of the corresponding δ^2H values (B) was in the positive range with 0.7 ‰. The bias of the

comparison of *in situ* and DVE-LS method was also in the negative and positive range, respectively (δ^{18}O: -1.8‰; δ^{2}H: 3.3‰). The other comparison (DVE-LS vs. CVD method) showed that the biases of δ^{18}O and δ^{2}H were positive (1.4‰) and negative (-2.6‰), respectively.

For most comparisons of POT samples, the bias is within the MAB. Only Figure 8 C and E (the comparison of δ^{18}O of *in situ* vs. DVE-LS and DVE-LS vs. CVD) resulted in biases outside the accepted range. The δ^{2}H of the same method comparisons were within the MAB. For some comparisons, there is a significant trend in the data (A and C), with larger differences being associated with lower mean values.

The comparison of the methods for the POT samples worked best. No other vegetable could achieve biases for a method comparison that were within the maximum accepted bias (MAB).

All plots (except A) of the CAU data in Figure A. 11 indicate a significant trend or error in the CAU data that was proportionally related to the size of the measurement. It was evident that smaller differences between the two methods were associated with larger mean values. Plot C and D point in the opposite direction than the rest of the plots (except A), but this was due to the positive values of the y-axis.

The comparison of the biases of the CEL data (Figure A. 12) showed that the *in situ* and DVE-LS data (C and D) had biases closest to zero (-2.4‰ and -7.2‰ for δ^{18}O and δ^{2}H, respectively), which means they compared best for CEL, but the values were still outside the MAB. The biases in comparing the DVE-LS and CVD data (E and F) were slightly larger with -3.6‰ for δ^{18}O and -8.5‰ for δ^{2}H. The comparison of *in situ* and CVD data (A and B) performed the worst when analyzing the CEL data. The bias of δ^{18}O was -5.6‰ and the bias of δ^{2}H was -15.7‰.

Comparison of method pairs of CEL data indicated a significant trend or error in the data only for the comparison of DVE-LS and CVD (δ^{18}O and δ^{2}H) and *in situ* and CVD (δ^{18}O), which was in the opposite direction (Figure A. 12; A; E; F). Comparison of the *in situ* and DVE-LS method showed, especially for the δ^{18}O data, that the data points were well distributed around the mean difference (bias) (Figure A. 12; C).

The pattern was similar for KOH data (Figure A. 13). The trends were all in the same direction as for CAU data (Figure A. 11). However, the trends for KOH data were statistically significant for plots A, C, D and F. Here, the comparison showed that the differences in δ^{18}O of the *in situ* and CVD data (A) and *in situ* and DVE-LS data (C) comparisons had very similar differences (biases), with -4.57‰ and 4.53‰, only in the opposite direction since the data of the DVE-LS method were lighter than those of the *in situ*. The δ^{2}H values showed statistically significant differences for the same method comparison (B: -11.3‰ and D: 60.5‰). The worst biases were obtained by comparing

the KOH data from the DVE-LS and CVD methods (E and F) with biases for $\delta^{18}O$ and $\delta^{2}H$ of - 9.1‰ and -71.8‰, respectively).

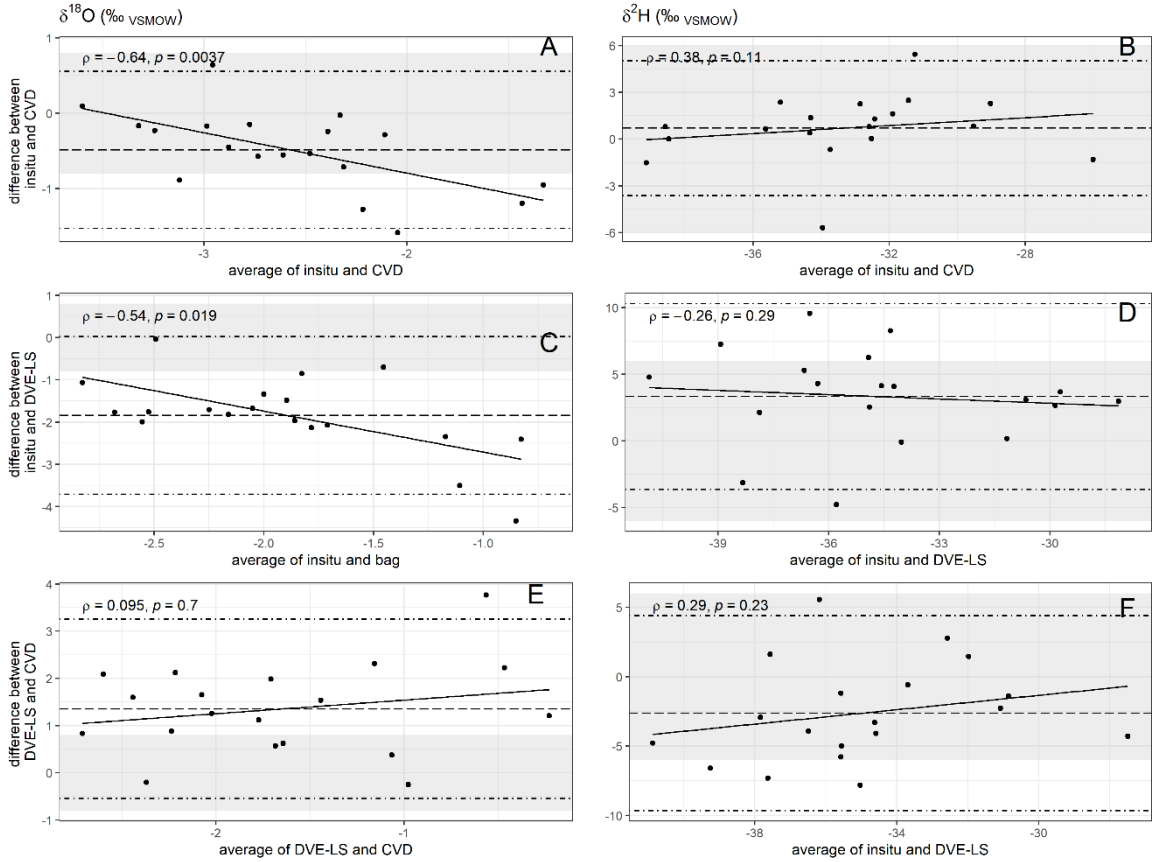

Figure 8: Bland- Altman plots of the POT data. A and B plot the difference between the *in situ* and CVD for $\delta^{18}O$ and $\delta^{2}H$ in [‰], respectively. The other plots show the difference between the *in situ* and CVD (C and D) and between the DVE-LS and CVD (E and F) for $\delta^{18}O$ and $\delta^{2}H$, respectively. The dashed line indicates the bias, and the two dotted lines indicate the upper and lower 95% limits of agreement (LOA) (=bias ±1.96 ×SD) of the respective data. The gray area indicates the maximum accepted bias of the data. All calibrated values are given in per mil (‰ VSMOW).

For the POT data, the bias of $\delta^{18}O$ ($\delta^{2}H$) from the comparison of *in situ* and CVD data was closest to zero at -0.5 ‰ (0.7‰). The biases of *in situ* and DVE-LS data and DVE-LS and CVD data was -1.8‰ (3.3‰) and 1.4% (-2.6‰), respectively. The trends for POT data, although not very strong, were statistically significant for A (ρ = -0.64; p = 0.0037) and C (ρ = - 0.54; p = 0.019). The other, very low correlations were statistically insignificant.

To ensure that approximately 95% of the values fell between the limits of agreement, a wide range was sometimes selected. This shows how much the methods differ. The narrower the range, the more similar the examined values were to each other. The range of the limits of agreement (LOA) suggest, that the comparison of *in situ* and CVD (Figure 8, Figure A. 11, Figure A. 13) worked best

for the CAU, KOH and POT samples and the comparison of *in situ* and DVE-LS data (Figure A. 12) worked the best for the CEL samples.

3.4 Comparison of the Vegetables from the Local Farms

The following section compares the similarities and differences in the isotopic compositions found in the vegetable samples from the different local farms.

As previously described, the isotopic values by vegetable type and location of origin depended on the method used to analyze the samples. The extent to which the isotopic composition of the vegetable samples varied by the local farm will be investigated in this chapter.

By examining Figure 9, Figure A. 8 and Figure A. 9, it was evident that there was no consistent pattern between farms of each vegetable variety. To investigate to what extent the isotopic composition of each vegetable differs by farms, additional Kruskal- Wallis tests were performed excluding the supermarket vegetables. Examination of the global p-values showed that there were the fewest significant differences ($p > a = 0.05$) in the results from the CVD method.

The Kruskal- Wallis tests of the CVD data (Figure 9) showed significant differences of CAU $\delta^{18}O$ values between farms M and Q. In $\delta^{2}H$ such significant differences in the CAU data could not be found. If we take the scatter of the local CEL $\delta^{18}O$ values into consideration, it can be assumed that only the isotopic values of the CEL of the farms K and Q differ significantly. This could be confirmed by the Kruskal-Wallis test. For the other two vegetables, the Kruskal-Wallis test could not find significant differences between the farms for $\delta^{18}O$. More significant differences in $\delta^{2}H$ values were found for CEL (K vs. Q, M vs. Q, Q vs. R). For the vegetable samples KOH and POT ($\delta^{2}H$) three farms each were found, which differ significantly from each other (KOH: K+R and M+R; POT: K+M and M+R). The data of the separate farms for each method can be found in Table A. 5.

The analysis with the *in situ* method showed that for $\delta^{18}O$ only the POT data results were indistinguishable by farm and for $\delta^{2}H$ there were significant differences for all investigated vegetables by farm (Figure A. 8). CAU data ($\delta^{18}O$) showed significant differences for all farms, except for the comparison of farms K and Q. CEL data showed significant differences in $\delta^{18}O$ between K and Q, K and R, and M and Q. Only K and M, M and R and Q and R did not show significant differences in $\delta^{18}O$.

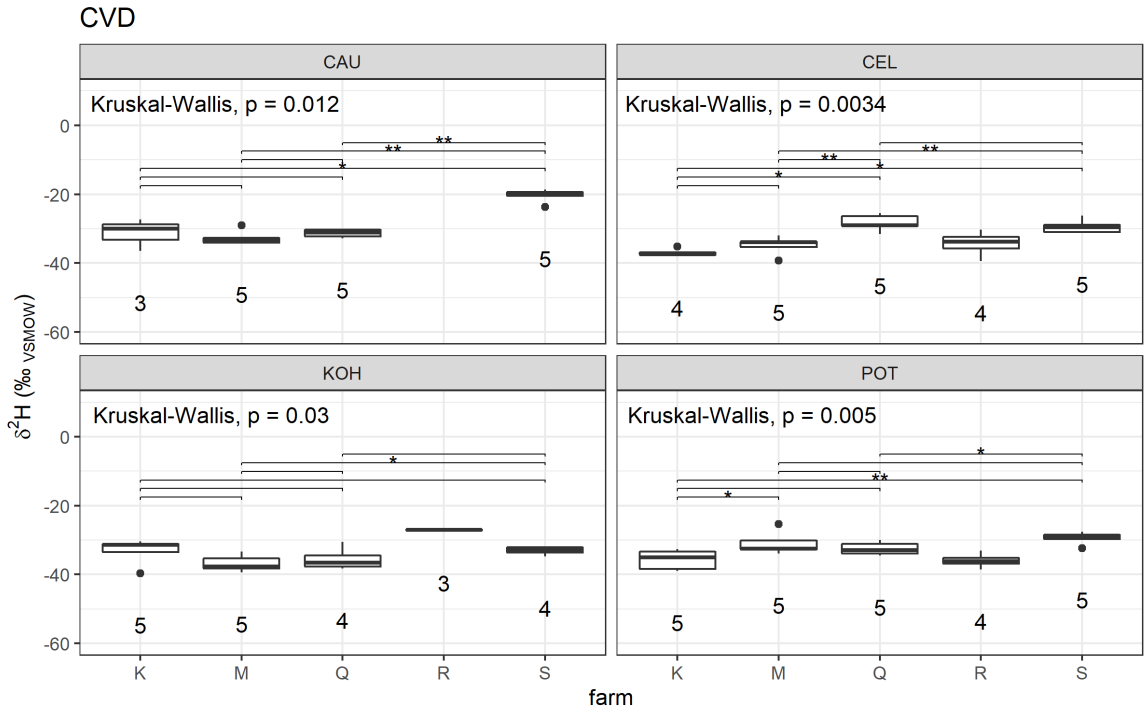

Figure 9: Boxplots of all vegetable samples of each farm and supermarket (δ^2H) for the CVD method, plotted by the different kinds of vegetables. The number indicates the number of observations (*n*) and the lines and associated symbols indicate the results of the individual Kruskal-Wallis test. The respective comparisons are indicated by the p-value ('ns': p > a; '*': p ≤ 0.05; '**': p ≤0.05; '***': p ≤ 0.01). In addition, the total result of the Kruskal- Wallis test for each vegetable variety (δ^2H) is given.

For KOH, only K vs. R and M vs. R differ significantly from each other (Figure A. 8). Only the POT from farms Q vs. R differed significantly from each other. In δ^2H, the CAU comparison looked the same. The δ^2H of the CEL differed only significantly between farms K and Q. The KOH from farms K vs. R and M vs. R differed significantly from each other. The POT data from farms M vs. R and K vs. M were significantly different. Data from the rest of the vegetables were not significantly different from each other.

There were more significant differences in the DVE-LS data, especially in δ^{18}O (Figure A. 9). There POT was the only vegetable without significant differences in δ^{18}O. In δ^2H, all vegetables except KOH show significant differences. More precisely, in δ^{18}O the CAU of farms K vs. M and M vs. Q differ significantly. The same pattern was seen for δ^2H of CAU. However, for farm K only 3 samples of CAU were available, as opposed to the 5 samples from each of the other farms. The scatter ranges of CEL were smaller for the individual farms. Farms K and R provided 4 samples each and M and Q provided 5 each. Significant differences in δ^{18}O existed between farms K and Q, K and R, M and Q and M and R. In δ^2H there were significant differences between K and Q, M and Q and Q and R. The KOH showed no significant difference by local farms in the δ^{18}O. In the δ^2H, only the

comparison of farms K and M showed small, yet significant differences. The POT data showed no significant differences in $\delta^{18}O$ and in $\delta^{2}H$ between farms M and Q and M and R.

3.5 Influence of Organic Parameters

Due to the interference of organic contamination with the laser absorption spectrum and the resulting possible influence on the isotopic values of the measurements, the organic parameters measured by the CRDS were examined in the following and the influence on the isotopic results was highlighted.

The results of the *in situ* measurements showed that the parameters 'organic_res', 'organic_shift_p', 'organic_base', 'organic_slope_p', and 'organic_CH4_conc' (see explanation in Table 1) did not seem to have an influence on the isotopic composition of $\delta^{18}O$ and $\delta^{2}H$ (Figure 10). These parameters scattered a little more for the samples analyzed than for the pure water standards (Figure A. 10) but did not show a discernable pattern. This was supported by the results of the GLMs for the first three parameters, in which no significant correlation could be found. The variability of the CAU isotope data was influenced by 'organic_slope_p' values according to the GLM results (Table 3). 'organic_CH4_conc' values significantly influenced the KOH data (*in situ* method) (Table A. 3). The observed linear relationship showed that the parameter 'organic_MeOHampl' influenced the CAU data (Figure 10). These values were only a little more scattered than those of the standards and the applied GLM indicated a significant influence of this parameter on the *in situ* CAU data (Table 3).

The results of the DVE-LS method showed a different pattern (Figure 10). Except for 'organic_shift_p' and 'organic_base', for which the applied GLMs (Table A. 2 - Table A. 4) could not find any significant correlation either, all spectral parameters showed a visual influence on the isotopic compositions. This was also supported by the GLM, which additionally showed an effect of this parameter on the variability of POT data. 'organic_CH4_conc_p' and 'organic_slope_p' affected the POT values, and the latter additionally explains some of the variance in the CAU data. The spectral parameters were not available to the same extent for the measurements of the cryogenically extracted water samples and can therefore not be described here.

The results of the GLMs were able to show the correlation between the spectral parameters and the isotope values of the DVE-LS method (Figure 10). This was shown by the comparison of the model coefficient of determination (R^2), which was quite good (>0.98) for all vegetables (except $\delta^{18}O$ CEL). R^2 values of CAU and KOH data (DVE-LS method) showed that the spectral parameters correlated with the variance of the data. This agreed with the strong scattering of the isotopic values

of these vegetable varieties found earlier (Figure 5). The correlations of the spectral parameters on the isotope data of the other two vegetable varieties using the DVE-LS method (CEL and POT) were lower (δ^{18}O: 0.461 and 0.799; δ^{2}H: 0.725 and 0.998).

The isotope data of the co- measured standards were less scattered (Figure 10), but differences between the data from the DVE-LS and the *in situ* method could be seen. These differences will be further investigated in Figure A. 10.

The spectral parameters were uncalibrated and, moreover, plotted against the uncalibrated isotopic values δ^{18}O and δ^{2}H of the standards, therefore Figure 10 and Figure A. 10 show the comparison of the spectral parameters of the respective methods rather than the absolute values. The ranges of the parameter 'organic_res', 'organic_shift_p' and 'organic_slope_p ' of the standards (Figure A. 10) were very similar to each other, with the DVE-LS data varying a little more. More obvious differences were shown by the parameters 'organic_MeOHampl' and 'organic_CH4_conc_p'.

Table 3: Results of the GLM for the δ^{18}O and δ^{2}H values of CAU (*in situ* and DVE-LS method) for the dependent variables (δ^{18}O and δ^{2}H) and the parameter analyzed in Figure 10, reduced if dependent and not significant. '_p' indicates which parameters were shifted to the positive range and the coefficient of determination for linear regressions (R^2).

	δ^{18}O_p (*in situ*)		**δ^{2}H_p (*in situ*)**		**δ^{18}O_p (DVE-LS)**		**δ^{2}H_p (DVE-LS)**	
Coeffcient	*Estimates*	*P-Value*	*Estimates*	*P-Value*	*Estimates*	*P-Value*	*Estimates*	*P-Value*
(Intercept)	0.01	0.912	0.01	**0.030**	66.42	**0.013**	278.13	**<0.001**
organic_CH4_conc_p	-39.43	0.127	-3.92	**0.006**				
organic_MeOHampl	5.05	**<0.001**	0.65	**<0.001**	-714.31	**<0.001**	-5920.24	**<0.001**
organic_slope_p	0.00	**0.002**	0.00	**<0.001**	-0.31	**0.037**	-0.78	0.051
organic_res	0.01	0.120			-2.74	**0.044**	-10.81	**0.005**
organic_shift_p					-63504.10	0.174	-3272.02	0.121
organic_base					-0.01	0.116		
Observations	14		14		14		14	
R^2 Nagelkerke	0.937		0.983		1.000		1.000	

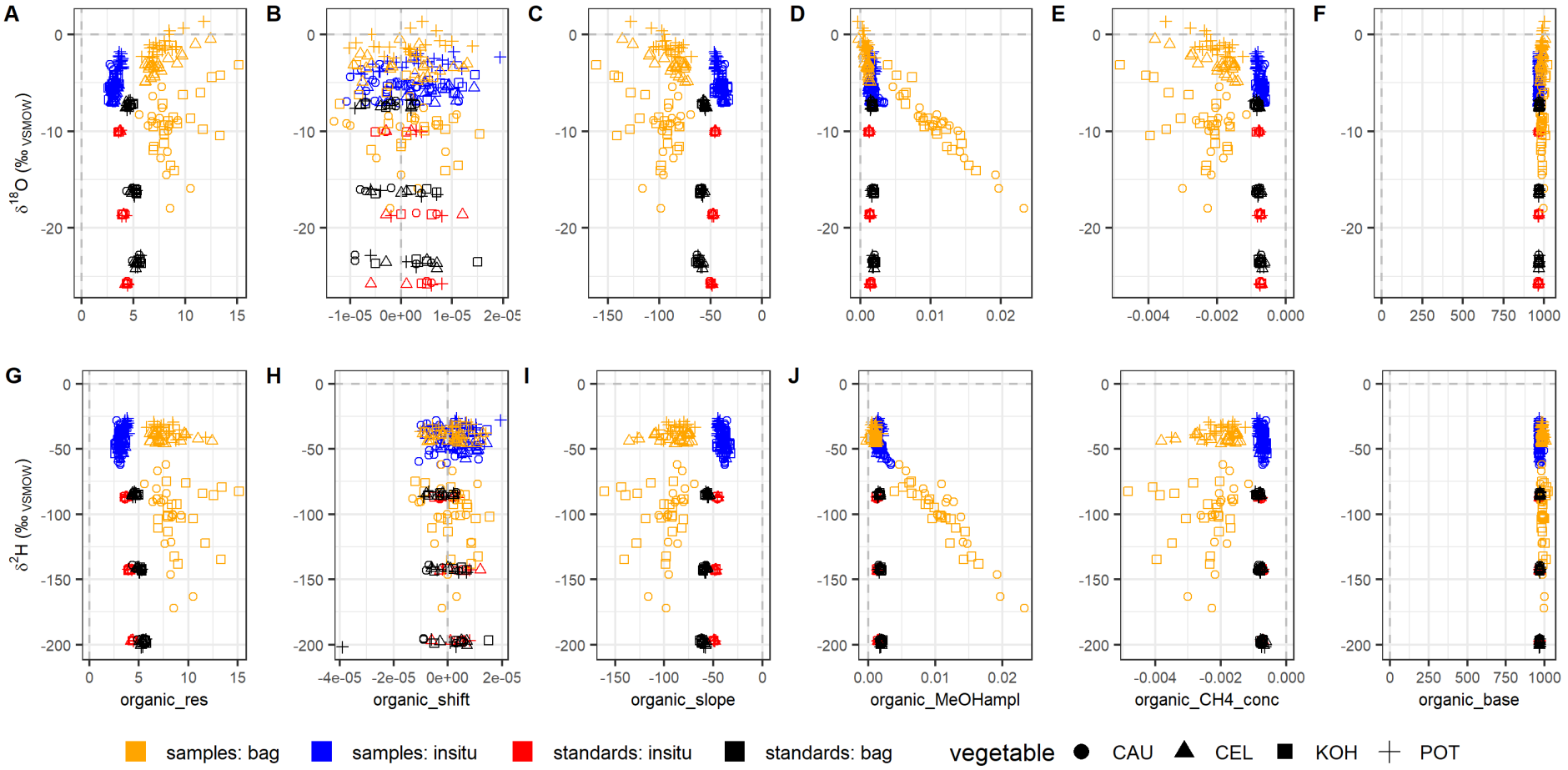

Figure 10: Selected spectral parameters, which were additionally measured with the L2120- *i*, analyzer by the *in situ* and DVE-LS method (all data: local and S). These are the values of the samples (blue: *in situ*; orange: DVE-LS) and the values of the standards (black: DVE-LS; red: *in situ*). *A* to *E* plot the parameters against $\delta^{18}O$ and *F* to *J* against $\delta^{2}H$. Dashed lines indicate the zero positions on each axis.

3.6 Determination of the Regional Influence

This chapter examines the extent to which the methods can recover the source water from the local vegetables and how the water stable isotopes of the local and imported vegetables differ from each other.

Visual inspection of the data showed that the differences in the water stable isotopic composition between vegetables from different regions (countries) appeared to be greater than the differences between the different local farm samples. The extension of the regression lines ($\delta^{18}O$ and $\delta^{2}H$) of the vegetable pieces measured by CVD are very close to the isotopic values of the source water (Figure 11). The regression lines of CAU and KOH intersect the GMWL above the weighted isotopic composition of the precipitation. The regression line closely reflects the isotopic composition in precipitation water from CEL. The regression line from the POT data intersects the GMWL between the mean precipitation water during the period of growth (Table A. 1) of the POT and the irrigation water. The DVE-LS method obtained similar results for CEL and POT, only in reverse (Figure A. 17). The CAU and KOH data, on the other hand, did not come close to reflecting the source water. The *in situ* method could not find the source water for any vegetable (Figure A. 16). The CEL data came closest to the irrigation water.

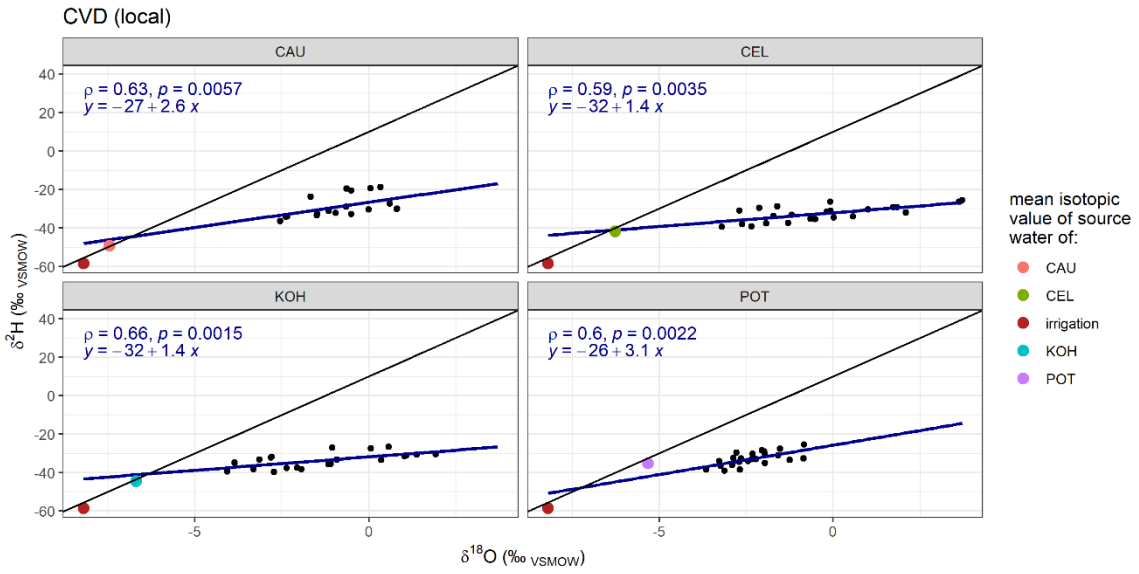

Figure 11: Regression lines for each local vegetable analyzed with the CVD with formula, the correlation coefficient (spearman's ρ), and the significance level (p).

The *in situ* and DVE-LS methods showed that all imported vegetables, except for the POT data, had heavier $\delta^{18}O$ and $\delta^{2}H$ values than their local counterpart. The examination of the isotopic values of the CAU data (analyzed with the DVE-LS method, Figure 12) showed that the $\delta^{18}O$ and $\delta^{2}H$

values of the CAU samples from farm M were the heaviest on average (δ^{18}O: -7.3‰; δ^{2}H: -76.4‰) followed by the imported CAU (δ^{18}O: -9.2‰; δ^{2}H: -89.7‰). The imported CEL (DVE-LS method) had the heaviest δ^{18}O isotope values on average (-1.7‰). The imported KOH had the heaviest δ^{18}O and δ^{2}H values (mean: -4.9‰ δ^{18}O and -80.4‰ δ^{2}H). The POT (DVE-LS method) had the lightest δ^{18}O and heaviest ^{2}H values.

The δ^{2}H values of the supermarket CAU samples (analyzed with the CVD method, Figure 12) were on average heavier (-20.4‰) than those of the local farms (K: -31.3‰; M: -32.6‰; Q: -31.3‰). In δ^{18}O, data from the imported CAU (- 0.5‰) did not differ too much from the local CAU data. Only data for CAU from farm M (-1.7‰) deviated more from the other values (K: - 0.4‰, Q: - 0.4‰). The imported CEL (CVD method) showed on average heavier δ^{2}H values (-29.4‰). Only the CEL data of farm Q were on average slightly heavier (-28.4‰). In δ^{18}O, however, a different pattern emerges. The imported CEL data (apart from those of farm K) were the lightest (S: - 1.3‰, K: - 1.6‰, M: - 0.4‰, Q: 2.14‰, R: -0.8‰). The imported KOH data analyzed with the CVD method (-3.2 ‰) showed in comparison (K: 0.3‰; M: -2.4‰; Q: -1.2‰; R: 0.24‰) on average the lightest δ^{18}O values. In the δ^{2}H, the imported KOH data had the heaviest isotopic values apart from the farm R (S: -33.0, R: -27.0 ‰). The imported POT had on average the heaviest δ^{2}H value (-29.5 ‰), but in δ^{18}O they plotted in the middle range between the other farms.

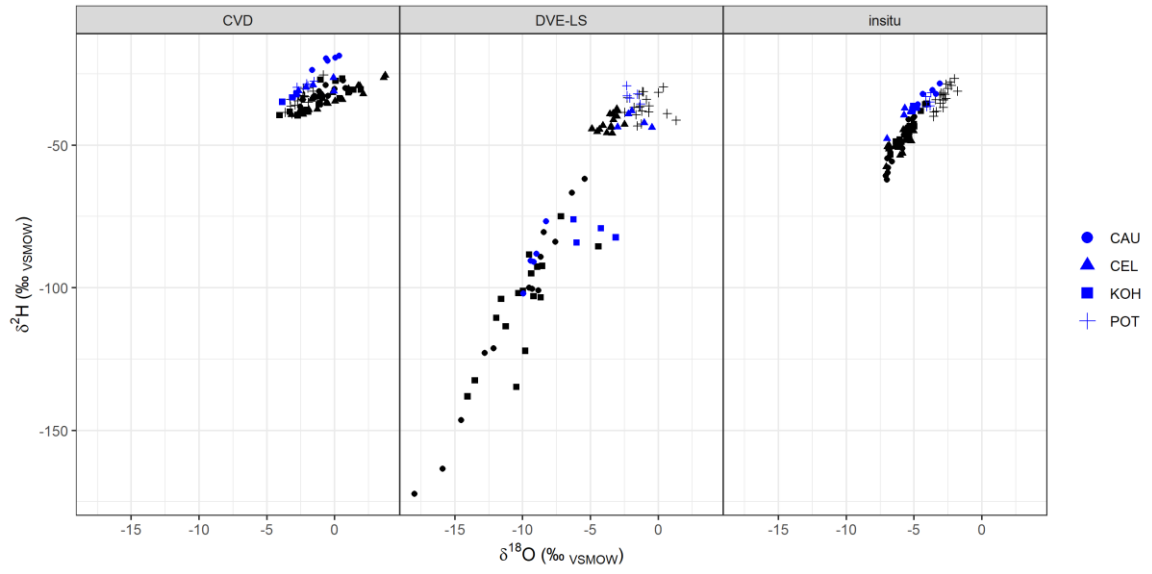

Figure 12: Dual isotope plot separated according to the three methods (DVE-LS; CVD; *in situ*). The blue points mark the results of the vegetables from the supermarket. The black values represent the vegetables from all other farms and the shapes indicate the type of vegetable.

The results of the *in situ* method (Figure 12) showed that the vegetables from the supermarket (except for POT data: mean: -3.9‰) had the heaviest δ^2H values on average (CAU: -31.8‰, CEL: -40.1‰, KOH: -37.2‰). In δ^{18}O, CAU had the heaviest average value with -3.8‰. The supermarket samples of CEL and KOH ranged in the middle compared to the local farms. The imported POT showed the lightest mean δ^{18}O values (-3.9‰). All isotopic values of the imported vegetables can be found in Table A. 6.

Figure 13 shows that the d-ex values were significantly lower for all kinds of local vegetables than their imported (supermarket) counterparts (except *in situ*: CAU and POT; DVE-LS: CEL and KOH). The DVE-LS method showed significant lower d-ex values for CEL and KOH, while the other methods showed the opposite for the same vegetables.

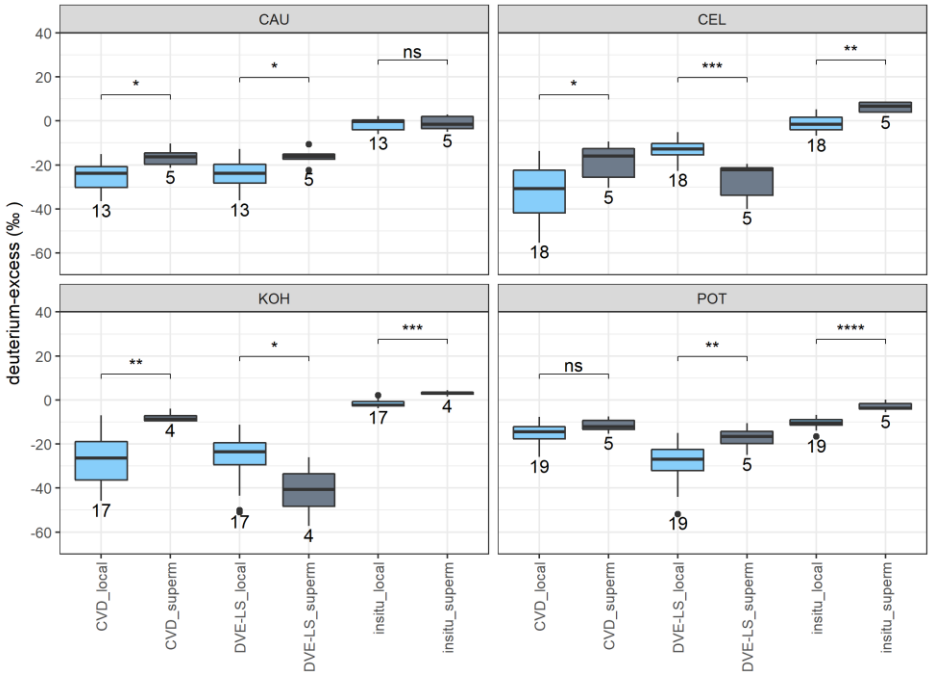

Figure 13: Boxplots of the deuterium- excess (‰) of all local ('_local') and imported ('_superm') kind of vegetable samples (CAU, CEL, KOH and POT) for each method (CVD, DVE-LS and in situ). The number indicates the number of observations (n) and the lines and associated symbols indicate the results of the individual Kruskal-Wallis test. The respective comparisons are indicated by the p-value ('ns': $p > a$; '*': $p \leq 0.05$; '**': $p \leq 0.05$; '***': $p \leq 0.01$).

4 Discussion

4.1 Applicability of the Methods: Methodological Advantages and Limitations

The aim of this thesis was to find a faster, less labor intensive, cheaper and more flexible method to reliably analyze the place of origin of foodstuffs by means of water stable isotopes. The time required for analysis was very compelling especially for the *in situ* (< 10 min) and the DVE-LS method (< 15 min + equilibration time). The CVD method required comparatively more time (60 min) but up to ten samples could be extracted simultaneously and the post-extraction isotope analysis was automated and thus performed unattended. The CVD protocol does not depend on the method of isotope analysis (e.g., CRDS vs. IRMS) so this method's potential overall gain in time compared to more traditional methods comes exclusively from the use of laser-based analysis which allows for higher sample throughput.

There is a lack of comparable studies with vegetables, as the extraction methods studied in this work were mainly performed on soil and plants (Millar et al., 2018; Orlowski et al., 2018). Therefore, the applied methods were compared with studies on plant and soil samples.

Each vegetable was examined with all three methods which mostly showed significant differences (e.g., Figure 7, Figure A. 6). Therefore, the null hypothesis was rejected, that all methods would yield the same results of water stable isotopes. In relation to the other methods, when compared on a per farm and vegetable variety basis, the results of CVD were more enriched in heavy isotopes and differ significantly from the other methods (except POT) (Figure A. 6, Figure 7). This was contrary to the findings of Millar et al. (2018) where CVD yielded the most depleted heavy isotopes. Presumably, evaporation would have caused similar slopes of less than 8 as well as sharper trend lines originating from precipitation or irrigation water and pointing towards the upper right in dual isotope space for all vegetables investigated. Possible differences between the methods and the resulting different slopes of the respective vegetable varieties could be due to the different procedures applied. The DVE-LS method analyzed all stable isotopes that have evaporated into the gas phase during the 18 hours of equilibrium time and then the CRDS analyzed them directly in vapor form. In contrast, the CVD method sees the water is first extracted at very high temperatures and collected in another vial. This is then opened to pipette the liquid phase into the smaller tube for analysis with the CRDS. Since the time from thawing of the samples to transferring them was not very long, it is conceivable that the lighter isotopes evaporated more quickly, and that more heavier isotopes

remained in the transferred water and therefore resulted in the comparatively heavier isotopic values found with the CVD method. This is also shown by the lower slopes of the regression lines of $\delta^{18}O$ and $\delta^{2}H$ of all vegetables measured with the CVD method, since, as Orlowski et al. (2016b) showed, the $\delta^{2}H$ are less affected by evaporation. A suggestion for future investigations of the CVD method is to cryogenically extract the standards as well. In this thesis, the standards were only analyzed with the CRDS, but not extracted beforehand. As Orlowski et al. (2016a) showed, the CVD method presents some problems because they did not recover the isotopic composition of the added spiked water in the extracted water. They stated that the methods they studied underwent a phase change (e.g., CVD) had greater deviations of the recovered water from the spiked water than methods without such phase transitions (e.g., mechanical squeezing). To what extent this applies to food samples is unknown, but as Orlowski et al. (2018) were able to show, different laboratories found significant differences in the extraction of soil water when applying the CVD, so the applicability of that method needs to be further investigated.

Compared to CVD, *in situ* results plot closer to the GMWL (Figure 6) and were on average more depleted in heavy isotopes. The correlations of $\delta^{18}O$ and $\delta^{2}H$ were also significant and much stronger ($\rho = 0.71 – 0.95$) than with the CVD. These comparatively lighter values are assumed to result from the fact that the *in situ* method samples more of the lighter isotopes. The dry air supplied to the probes only remains in them for a very short time before it is diluted and supplied to the CRDS. Therefore, the lighter values are presumably more likely to be sampled. Although these differences should be avoided by identical treatment of the standards and the subsequent calibration, it is conceivable that other substances in the vegetables behave differently than pure water and therefore these lighter values are obtained.

One problem with standards, and this affects all methods, is that there are no standards for positive values. As Figure 10 shows, some values are outside the range covered by the standards. The VSMOW is the heaviest water standard with 0.0‰ for both $\delta^{18}O$ and $\delta^{2}H$, respectively. Therefore, extrapolations were made for the calibration of the vegetable samples. As a result, inaccuracies may have occurred if the assumption of linear extrapolation is not correct. Using vegetable standards instead of water standards is a consideration for future research to obtain more accurate values. In this way, the principle of identical treatment would be followed more closely.

The analysis of the statistical differences was problematic due to the studied groups being very small (n = 3 to 5) (e.g., Figure A. 2 and Figure A. 5). As a result of the small sample number, the boxplots contain only three to five data points. Therefore, the significance levels should be regarded with caution, as these differences may be random due to the small sample numbers. Visually, the boxplots scatter to varying degrees. The magnitude of the p- value, and thus the level of significance depends, among other things, on the sample size. The tests are more likely to show significant

differences the smaller the standard deviation and the larger the sample size (Dormann, 2020; Dahiru, 2008). All local vegetables combined resulted in group sizes of 13 to 19 individuals. However, the analysis showed significant differences for all comparisons (Figure A. 6). The stronger significance levels in this figure show that these are due to the larger sample size.

In the study of Chesson et al. (2010) some samples could be analyzed without prior preparation, but they also noted that other samples, especially those containing sugar, clogged the syringe of the employed analyzing device. This was the case in some preliminary experiments to my study, when extracting the vegetable's water by squeezing failed because there were too many other substances in the juice, which clogged the syringe of the Picarro's autosampler and there were brownish residues found on the septum of the vaporizer chamber, indicating severe contamination of the samples. That happened even though the squeezed vegetable juices had been centrifuged and filtered (45µm). Therefore, the CVD method was chosen, although it was more time consuming than squeezing, for example, but resulted in less contamination of the extraction water.

For all samples extracted by the CVD method, a water content of ≥98% was extracted. West et al. (2006) and Araguás-Araguás et al. (1995) claimed, that a minimal residue (<2%) of water in the samples of stems of plants, has no measurable influence on the fractionation of the examined isotopes. There were some samples where a little more tissue water was lost due to extraction, but this amount of water was negligible (< 0.04 g) and within the measurement accuracy. Therefore, it was assumed in this work that there was no significant evaporation due to Rayleigh distillation. However, the three methods show very different isotopic vales for the same vegetable samples analyzed, which could be due to the fact that they analyzed different water pools in the plants. As a result of the extraction of almost all water from each sample with the CVD method, the entire water pool was extracted and analyzed (Millar et al., 2018). The samples placed in the bags (for the DVE-LS method) were previously cut into small pieces. That destroyed some cell walls, and their water evaporated more quickly into the added dry air. As Millar et al. (2018) suggested, the main share of the sampled water stable isotopes with the DVE-LS probably originated from the mobile water. Furthermore, they suggested that the duration of equilibration could have an influence. Besides the mobile water, cell water diffuses through the cell walls and was additionally analyzed. The same was conceivable for the *in situ* method, because again some cell walls were destroyed by drilling the hole. However, it was likely that primarily the mobile water from xylem and phloem, and some more strongly bound cell water was analyzed. It is open to question how much different water pools studied affect the results, assuming that they are all fed by the same water (precipitation/irrigation) and, therefore, should not differ too much from each other.

It is known that the δ-values and the air temperature correlate significantly (Mimmo et al., 2015). Since the laboratory was temperature regulated, the observed minimal differences in air temperature were not considered in the analysis of the data in this thesis due to time constraints.

Differences between the methods can already be found in the measurement precision. The best measurement precisions (standard deviations of the co-measured calibration standards) were achieved by the CVD method with ± 0.16 ‰ for $\delta^{18}O$ and ± 0.6‰ for $\delta^{2}H$. Comparable results were achieved with *in situ* method (± 0.2 ‰ and ± 0.9 ‰) and the DVE-LS method performed the worst, comparatively (± 0.3 ‰ and ± 1 ‰). In addition, there were differences in the SD ('noise') measured by continuous flow (DVE-LS and *in situ* method) of the 90-second averages of each vegetable sample. The SDs of the DVE-LS method always showed larger values for the samples than for the corresponding standards. An example were the SDs of the DVE-LS $\delta^{2}H$, which deviated up to ±7.22 ‰. These values were well outside the reported instrument precisions of ±0.16 ‰ for $\delta^{18}O$ and ±0.6 ‰ for $\delta^{2}H$. This shows the comparatively poorer precision of the DVE-LS method compared to the *in situ* measurements, whose SDs were only minimally larger than the instrument accuracies.

More research needs to be done on the best equilibration time (DVE-LS method) so that isotopic equilibrium is achieved, and the influence of organic interference is minimized (cf. Sprenger et al. (2015)). It is conceivable that the influence on the isotopic values of CAU and KOH in particular would be exacerbated by a longer equilibration time. Since the lighter isotopes evaporate faster than heavier ones, longer equilibration times could lead to data more enriched in heavy isotopes for the DVE-LS method. It is assumed that this will have to be done separately for the individual foods under investigation, since the four vegetables studied in this work already show strong differences in organic interference (Figure 10). It was assumed, that no evaporitic enrichment occurred during the equilibration time of the DVE-LS happened due to impermeable bags. Sprenger et al. (2015) tested the diffusion-tightness of the bags with soil samples and could show that they were almost impermeable, as they only lost < 0.15% soil pore water within 30 days. They list other literature, which give various values for the duration of the equilibrium phase (15 h to 7 days). Gralher et al. (2021) tested the diffusion-tightness of several types of bags over a period of 28 days. Their results showed that the bags used for this work achieved the best results and recommend equilibration periods of not less than 2 days (Gralher et al., 2021). Since in this thesis the duration of the equilibration phase was only ~ 18 hours, it can be assumed that no water was lost from the bags and that no fractionation occurred. The equilibration time of the DVE-LS samples was chosen to be relatively short in this setup, to minimize errors due to organic contamination. Stockinger et al. (2020) analyzed tomato and strawberry samples with the DVE-LS methods and recommend equilibrium times of less than 24 hours because with increasing time the influence of VOCs increases strongly and also the R^2 of the relationship of $\delta^{18}O$ and $\delta^{2}H$ declines progressively. Assuming that lighter

water stable isotopes evaporate faster, it was surprising that the CEL and POT samples, which performed better than CAU and KOH within the DVE-LS method, have heavier $\delta^{18}O$ values than they were found to have with the CVD method, which analyzed the entire water pool. However, the extent to which the proportion of analyzed mobile pore water to cell water changes in these vegetables, as a result of different equilibration times, while at the same time, the influence of organic contaminations is kept low, needs to be investigated in more detail in future studies. Furthermore, research on how to correct for the issue of interference of VOCs needs to be investigated.

The used amount of vegetable sample of about 20 g for the DVE-LS method was sufficient compared to the 2 mL of minimum sample water content suggested by Gralher et al. (2021) because the vegetables in this study had a gravimetric water content between 80 - 93% and therefore a water amount of at least 16 g was added to the bags. In order to analyze the entire water in the sample and not only the outermost water layers (Gralher et al., 2021) despite the relatively short equilibration time, the samples examined from the respective vegetable sample were cut into small pieces to increase the surface area. Although the time spent cutting the pieces was kept to a minimum, it is conceivable that minor fractionation processes occurred during the cutting. Preliminary tests to fill the (POT) sample into the bags and to crush them from the outside before inflating the bag with dry air, showed a very large influence of the organic parameters. Some vegetables (e.g., POT) showed a visual change in their surface after they were removed from the bags (after measurement). This resembled a re-closure of the pores. However, especially for the POT data, it presumably did not have a negative effect on the equilibration (Figure A. 2), as there was little or no significant difference in the water stable isotopes between the methods. It is assumed that this will have to be done separately for the individual foods under investigation, since the four vegetables studied in this work already showed strong differences in organic interference (Figure 10).

The *in situ* method was limited to analyses of solid samples with a minimum size. The other two methods can be performed with all aggregate states provided that samples contain enough water (2 mL for DVE-LS, ~0.1 mL for CVD). The minimum size of foods excludes the use of the *in situ* method for their examination, in many cases. The amount of sample required differs for each method. For the DVE-LS and CVD, only small sample quantities are necessary. The *in situ* method, on the other hand, requires whole vegetables because it employs a relatively large sensor and the analysis of only one portion of a vegetable may be influenced by fractionation processes due to evaporation. The size of the sensor, however, cannot be changed arbitrarily as it needs to be balanced with the employed analyzers gas flow demand, at least in DDS mode.

Comparisons must be made between the investigated extraction methods used (and analyzed with CRDS) and established methods, such as IRMS, so that the results can be compared with previously known values. The Bland-Altman plots illustrate the difficulties of finding the 'true value' (West et

al., 2010) when two previously unknown methods are combined (Figure 8; Figure A. 11; Figure A. 12; Figure A. 13), which makes it impossible to draw conclusions about results obtained with the IRMS in other studies and to classify the values obtained with these methods. As Chesson et al. (2010) pointed out, the comparison of foods (in their case beverages) worked well between IRMS and IRIS for some (e.g., milk and soda), while others (e.g., beer) showed large differences between the two methods. They suspect that in this case ethanol or methanol contaminations were the reason for the differences between IRIS and IRMS data. Due to the organic impurities (see chapter 4.4), it is reasonable to assume that the values obtained in this work (with IRIS) would be quite different from those obtained with IRMS, especially for the DVE-LS method. However, this requires further research.

4.2 Investigating the Origin of Foodstuffs

The samples of CEL and POT were from the Netherlands, while CAU and KOH were from Spain and Italy, respectively. The exact provenance of the samples was unfortunately unknown, but it was assumed for all samples that the distance to the coast was shorter than that of the local vegetables, and therefore the isotopic composition in precipitation was expected to be more enriched in heavy isotopes. Furthermore, it was likely that the air temperatures in Italy and Spain were higher, which would also cause more enriched water stable isotopes in precipitation and soil water due to an increased evaporation, primarily due to the latitude effect. Significant differences were found for some vegetables with the different methods between local and imported (supermarket) vegetables. The $\delta^{18}O$ and $\delta^{2}H$ values indicated varying significances for several method comparisons of the different vegetables (Figure A. 14 and Figure A. 15). Therefore, instead of examining the individual water stable isotopes, the d-ex was considered instead (Figure 13).

As shown in, for example, Figure A. 8 and Figure A. 9, the results of the POT data were the most enriched in heavy isotopes. A possible explanation for this could be that these crops were not irrigated and therefore exposed to the isotopically heavier weighted precipitation (Figure 5). However, general differences between POT and other crops could also be responsible.

D-ex reacts sensitively to evaporation (Pfahl and Sodemann, 2014). Since evaporation in particular influences the isotopic composition of the precipitation water and thus ultimately the composition of the vegetable water, it was reasonable to assume that this second-order isotope parameter would be helpful in investigating regional differences.

By analyzing $\delta^{18}O$ values separately, 6 comparisons showed significant differences (Figure A. 14) within the case of $\delta^{2}H$, 7 significant differences were found (Figure A. 15). Some of these differences did not coincide with each other. On the other hand, the study of the d-ex values found 10 of

a total of 12 comparisons between local and imported vegetables to be significantly different (Figure 13). Apart from the comparison of local and imported CAU (*in situ*) and POT (CVD), all comparisons show significant differences, with the DVE-LS method being the only method finding significantly lower d-ex values for CEL and KOH (Figure 13). This result was questionable because the other two methods indicate significantly heavier isotopes in the imported vegetables.

Various approaches are used to analyze and evaluate the data, with multivariate methods being the most common. These are divided into supervised (e.g. linear regression k-nearest neighbors (K-NN), linear discriminant analysis (LDA)) and unsupervised methods (e.g. hierarchial cluster analysis (HCA) and principal component a nalysis (PCA)) (Creydt and Fischer, 2018). Which method should be applied depends on the research question and on the distribution of the data. Since the number of samples was limited in this work and not normally distributed, methods like the PCA could not be carried out. A higher number of samples would probably allow these analyses.

However, the exclusive use of water stable isotopes for the determination of the origin of food is probably not sufficient. The comparisons of local and imported vegetables showed significant differences, but the groups were not completely separable due to overlapping areas. Furthermore, differing annual weather patterns and therefore varying isotopic compositions of precipitation and different isotopic compositions during cultivation phases (Figure 5) influence the isotopic composition certain vegetables are exposed to. Instead, the compositions of elements like Al, Ba, Co, Cu and Fe to name a few (Segelke et al., 2020) are unaffected by the harvest year and should be considered. There have been several studies on the subject that additionally investigate the multi- element composition of food samples, for example $^{13}C/^{12}C$, $^{15}N/^{14}N$, $^{34}S/^{32}S$ and rare elements with promising results (Mimmo et al., 2015; Drivelos and Georgiou, 2012; Segelke et al., 2020; Magdas et al., 2021; Aceto et al., 2018). Since some analyses of certain elements use additional methods (additionally to IRMS) anyway, it is conceivable that CRDS could measure the water stable isotopes and other methods (e.g., ICP-MS) measure the additional elements. Further research is needed to investigate whether the combination of CRDS and additional methods to study specific elements can improve forecast accuracy and work around the variations resulting from different annual weather fluctuations.

4.3 Variety Specific Differences

It was expected that due to the spatial proximity of the local farms to each other, that no differences in the isotopic composition of the respective vegetable varieties would be detected. Because of this spatial proximity, the assumption is made that there are no differences in water stable isotopes in irrigation and precipitation water, and that the effects described in the introduction (e.g., altitude, amount) have the same impact on all local vegetables. However, it became apparent that this

assumption was not true for most of the vegetables investigated. Whether significant differences existed depended on the analytical method applied. The differences in isotopic composition of each vegetable variety between local farms were mostly very small. It was conceivable that these differences could result because of different harvesting time and thus different storage times (and storage conditions). Additionally, the growth phases of the vegetables varied between farms by some weeks, exposing them to minimally different isotopic composition in the precipitation. In the absence of data on irrigation amounts, it was conceivable that the irrigation of the fields on the different farms differed in timing and amount. The differences were much larger between the respective methods.

Orlowski et al. (2016b) and others showed, that δ^2H was less influenced by fractionation effects than δ^{18}O. This may explain, why the regression lines of most vegetables (see Figure A. 16 to Figure A. 17) showed a lower slope for all vegetables (except CAU: *in situ* and DVE-LS) than the slope of the GMWL. Bong et al. (2008) showed, that heavier δ^{18}O isotopes result from evapotranspiration and plot below the GMWL. Waters influenced by evaporation usually show slopes (δ^2H - δ^{18}O regression line) between three and six (Bong et al., 2008). These expected values could only be found in a few cases. The slopes of the regression lines in this thesis ranged from 0.14 to 9.6, depending strongly on the method and vegetable considered. Similar trends in the slopes of regression lines were found for CAU and KOH (*in situ*: Figure A. 16 and DVE-LS: Figure A. 17), whereby these values are significantly steeper than the slope of the GMWL. The slopes of the CVD data (Figure 11) were generally lower than those of the other two methods. The fact that the slopes were different for different kinds of vegetables suggests that in this case something variety- specific and different than evaporation was occurring. Future research should therefore examine vegetable varieties individually.

The data also showed that variations between vegetable varieties were greater than within a vegetable variety. Bong et al. (2008) state, that even if crops were grown in the same climate, different varieties of vegetables (and fruits) can show different variations in the composition of water stable isotopes. This was also evident from the results of this study. The differences of the isotopic composition (δ^{18}O and δ^2H) between CEL and POT were particularly large. While the potatoes grew in the soil and were therefore less exposed to evaporation, the other plants studied grew above (CAU and KOH) and half in (CEL) the ground. Changes in isotopic composition, for example in leaves (Cernusak et al., 2016), occur due to transpiration. Thus, the water taken up by the roots in the plants was altered. Cernusak et al. (2016) further state that water altered in leaves due to transpiration was transported to other parts of the plant. The fact that a change in isotopic composition (compared to the source water) had occurred was shown by the water stable isotope data of the vegetables collected for this work, as they all plot below the GMWL (Figure 6).

Cauliflower and kohlrabi both come from the same plant family (Brassica oleracea). Since their results of the DVE-LS method scatter a lot and they were strongly influenced by methanol and methane, it can be assumed that vegetables from this family were not well suited for straight-forward investigation with this method. However, this needs to be verified separately for other vegetables. Also, the results of the *in situ* method, although lower, were affected by this, as the GLMs showed.

Some preliminary experiments (data not shown) have suggested that the isotopic signature differed depending on the part of the crop studied. For example, some differences were found in carrots with lighter isotopic values at the bottom, corresponding to the growth direction, compared to the part close to the leaves. An isotopic gradient in leaves was also presented by Cernusak et al. (2016) for some plant species with heavier $\delta^{18}O$ and $\delta^{2}H$ values towards the outer end of the leaves. Further research should clarify how great the differences were in the variation of water stable isotopes within each vegetable sample for every type of vegetable, the impacts on testing of origin of these crops and as a result, the need for a standardized measurement protocol regarding the identical treatment.

Studies of Cristea et al. (2020) showed that the regional influence is not the only determinant of $\delta^{18}O$ and $\delta^{2}H$ values, but also the cultivation location. In a comparison of field vs. greenhouse, more enriched values were found in the greenhouse vegetables. Information on where and how the vegetables were grown must therefore be indicated more precisely on the label.

Another factor creating uncertainty in the study of the determination of the origin of food was the degree of ripeness of the food. Bong et al. (2008) found significant differences between ripe and unripe tomato samples. For the studied vegetables in this thesis, it was probably less important because they were harvested when they were ripe.

Two of the local farms farmed organically and two conventionally. As was the case for Cristea et al. (2017), no clear differences in $\delta^{18}O$ and $\delta^{2}H$ values were found in this work between organic or conventional cultivation of the crops. Instead, $\delta^{15}N$ values should be considered for this purpose.

4.4 Influence of the Co-Extracted Compounds

VOCs have similar electromagnetic absorption spectra in the near-infrared range und can therefore influence the results of $\delta^{18}O$ and $\delta^{2}H$ measured by CRDS. In the study by Millar et al. (2018), the CVD and DVE-LS method showed very similar results for the head, stem and root crown of spring wheat. The leaves samples, however, showed a high influence of methanol and ethanol. In this thesis I was able to show that some methods extracted more VOCs from the vegetable samples and therefore their results were more strongly influenced by them. Specifically, the DVE-LS method

was strongly influenced by methanol and methane of CAU and KOH samples. This significant influence of VOCs on the isotopic values of the DVE-LS method is contrary to the results of Millar et al. (2018), who showed that the DVE-LS of their samples were the least influenced by VOCs. The influence due to the VOCs shown in (Figure 10) could possibly be minimized by purifying the samples with activated charcoal. However, that would mean extra sample processing workload. As West et al. (2010) were able to show, this was not necessarily effective for all samples and must therefore be tested for each vegetable variety separately. Another approach is the subsequent correction of the isotopic values, as applied by Martín-Gómez et al. (2015) and Schultz et al. (2011), for example. Martín-Gómez et al. (2015) showed, that their post- processing worked well for concentrations of up to 8% of methanol and 0.4% of ethanol. Because the organic parameters, measured with the CRDS, are unitless it is not possible in this work to assess whether they are within these ranges. Chang et al. (2016) successfully tested solid-phase extraction. However, all these methods have in common that they are only applicable for liquid samples, and therefore can only be considered for the CVD method.

As described earlier, the evaluation of the data by PCA is often used. However, it was not possible to use PCA in this case because the data were not normally distributed. Instead, the influence of organic parameters was investigated by GLMs. These showed that the influence of some organic substances strongly depends on the studied vegetable variety and applied method. Methane and methanol had the greatest influence, with the DVE-LS method being the most affected. This again shows the importance of taking a closer look at the substances that interfere spectrally in the future.

The analytical technique most commonly used to date to investigate the origin of food (IRMS) is almost unaffected by the organic contaminants that were often present only in small amounts (Millar et al., 2018; Brand et al., 2009). Therefore, further studies should investigate the influence of organic parameters on isotopic composition (via CRDS) and abnormal results of foods could then perhaps be excluded from the investigation via CRDS and investigated via IRMS instead.

4.5 Influence of Precipitation and Irrigation Water

The isotopic composition ($\delta^{18}O$ and $\delta^{2}H$) in precipitation varies due to the effects described in the introduction (e.g., altitude and amount effect). In addition, these compositions also vary at the same location throughout the year (seasonal effect). Since no comparisons were made with measurements of sophisticated IRMS analyses in this study, the CRDS results can only be compared to precipitation and irrigation values. The water stable isotopic values varied a lot over the course of the growing phases of all vegetables in this study, with $\delta^{18}O$ values ranging from -12.09‰ to -0.53‰ and the $\delta^{2}H$ values from -90.62‰ to -0.26‰. All vegetables were grown in the open field and were therefore exposed to precipitation. The weighting of rainwater for each growth phase of each kind

of vegetable showed that the isotopic composition of rainwater differed between varieties. Thus, on average, CAU were exposed to the lightest and POT to the heaviest isotopic values ($\delta^{18}O$ and $\delta^{2}H$) in precipitation and KOH and CEL in between (Figure 5, Table A. 1). However, the data showed that these differences were not necessarily reflected in the vegetable varieties. The assumption also lies in other plant-specific differences.

Oerter et al. (2017) calculated the source water from the intersection of the respective regression lines ($\delta^{18}O$ and $\delta^{2}H$) with the GMWL. This intercept is to indicate what values the vegetable samples would have without the influence of evaporation (Oerter et al., 2017). Since exact values of the amount of applied irrigation water are not available, the exact source water cannot be determined in this work. Therefore, for simplicity, the source water is expected to range between the precipitation water of the respective growing season and the irrigation water. As Figure 11 shows, with this approach, the CVD could best recover the source water for all vegetables, with CAU and KOH yielding slightly too heavy values. Although the POT were not irrigated, the regression line intersects the GMWL lower than the precipitation water from the growth phase of the POT. POT root deeper (90cm) than the other kinds of vegetables and is planted first in the year. Based on this, it is conceivable that the POT take up older precipitation water with a different isotopic composition. However, quantitative estimates of this effect via modeling soil water fluxes are not possible as they would require detailed information about, for example, soil physical parameters or irrigation timing and amount in addition to rainfall characteristics. The DVE-LS was also able to provide conclusions about the isotopic composition of the source water for CEL and POT (Figure A. 17). Even better for the POT, since these were not irrigated. However, the DVE-LS method is unsuitable for CAU and KOH, unless the data are cleaned with respect to the organics. The isotopic composition of the source water of the vegetable pieces could not be recovered with the *in situ* method (Figure A. 16). The intercepts of the regression lines and the GMWL did not correspond to the isotopic values of the vegetables.

However, this thesis examined average growing phases, as the farms had slightly different planting and harvesting times. Furthermore, the isotopic composition of precipitation varies annually, for example, depending on the amount of precipitation and air temperature (Moyer et al., 2017). From this it can be seen that testing of geographical origin of foods, based exclusively on the composition of water stable isotopes of the precipitation, could be problematic. The examination of further, additional isotopes (see above) is therefore recommended.

5 Conclusion and Outlook

In the presented study, three analytical methods, which measured via laser- spectrometry (CRDS), were tested. The study was conducted in order to analyze the water stable isotopes (δ^{18}O and δ^{2}H) in four kinds of vegetables to determine the applicability of these methods to test the geographical origin of the vegetables. The approaches chosen did obtain data faster than IRMS-based methods and provided, to the author's knowledge, for the first time, detailed and comprehensive experiences with these new methods (DVE-LS and *in situ*) in testing vegetable samples.

The CVD method was especially successful in recovering the source water from the vegetable samples. In the case of the CEL and POT samples, the DVE-LS method was also successful in this way, although the source water is not fully known due to a lack of information on irrigation volumes. It could be shown that most δ18O and δ2H values differed significantly between the local and imported vegetables. However, the growing location (local vs. imported) could not be clearly distinguished from each other because some values were overlapping, and the accuracy of the water isotopes of individual vegetable pieces is not sufficient to clearly identify the different areas of origin beyond a doubt.

The assumption that all methods produced the same results because the same sample of vegetable was examined had to be rejected. The comparison of the POT samples worked best for all methods, but larger differences were found between the CAU and KOH, which can be attributed to the higher presence of volatile organic compounds (VOCs), especially methanol and methane when measured with the DVE-LS method. In the future, correction procedures must be conducted to reduce the influence of VOCs. This influence of vegetable varieties on measurement results indicates that it is important to test all vegetable varieties separately and probably differently.

The comparison of three new methods yielded different results, which makes finding the true value impossible. It is not possible to compare the results generated in this thesis with previous results obtained by IRMS, since the provenance of the vegetables is different, and the methods are different. Therefore, future studies should directly compare these methods.

Each kind of vegetable was exposed to a slightly different isotopic composition of precipitation water, due to different cropping stages and durations, and these results also support the heavier isotopic values of the POT. Future research should investigate how much the influence of annual variance in isotopic composition in precipitation affects each vegetable species. The CVD method could approximately recover the source water for all local vegetables and the DVE-LS method for CEL and POT. The *in situ* method, on the other hand, could not recover it.

References

Abbas, O., Zadravec, M., Baeten, V., Mikuš, T., Lešić, T., Vulić, A., Prpić, J., Jemeršić, L., Pleadin, J., 2018. Analytical methods used for the authentication of food of animal origin. Food chemistry 246, 6–17.

Aceto, M., Bonello, F., Musso, D., Tsolakis, C., Cassino, C., Osella, D., 2018. Wine Traceability with Rare Earth Elements. Beverages 4 (1), 23.

Almeida, J., Barbosa, L., Pais, A., Formosinho, S.J., 2007. Improving hierarchical cluster analysis: A new method with outlier detection and automatic clustering. Chemometrics and Intelligent Laboratory Systems 87 (2), 208–217.

Altman, D.G., Bland, J.M., 1983. Measurement in Medicine: The Analysis of Method Comparison Studies. The Statistician 32 (3), 307.

Araguás-Araguás, L., Rozanski, K., Gonfiantini, R., Louvat, D., 1995. Isotope effects accompanying vacuum extraction of soil water for stable isotope analyses. Journal of Hydrology 168 (1-4), 159–171.

Ballin, N.Z., 2010. Authentication of meat and meat products. Meat science 86 (3), 577–587.

Bland, J.M., Altman, D.G., 1995. Comparing methods of measurement: why plotting difference against standard method is misleading. The Lancet 346 (8982), 1085–1087.

Bong, Y.-S., Lee, K.-S., Shin, W.-J., Ryu, J.-S., 2008. Comparison of the oxygen and hydrogen isotopes in the juices of fast-growing vegetables and slow-growing fruits. Rapid communications in mass spectrometry: RCM 22 (18), 2809–2812.

Bontempo, L., van Leeuwen, K.A., Paolini, M., Holst Laursen, K., Micheloni, C., Prenzler, P.D., Ryan, D., Camin, F., 2020. Bulk and compound-specific stable isotope ratio analysis for authenticity testing of organically grown tomatoes. Food chemistry 318, 126426.

Brand, W.A., Coplen, T.B., Vogl, J., Rosner, M., Prohaska, T., 2014. Assessment of international reference materials for isotope-ratio analysis (IUPAC Technical Report). Pure and Applied Chemistry 86 (3), 425–467.

Brand, W.A., Geilmann, H., Crosson, E.R., Rella, C.W., 2009. Cavity ring-down spectroscopy versus high-temperature conversion isotope ratio mass spectrometry; a case study on delta(2)H and delta(18)O of pure water samples and alcohol/water mixtures. Rapid communications in mass spectrometry: RCM 23 (12), 1879–1884.

Camin, F., Boner, M., Bontempo, L., Fauhl-Hassek, C., Kelly, S.D., Riedl, J., Rossmann, A., 2017. Stable isotope techniques for verifying the declared geographical origin of food in legal cases. Trends in Food Science & Technology 61, 176–187.

Carter, J.F., Chesson, L.A. (Eds.), 2017. Food forensics. Stable isotopes as a guide to authenticity and origin. CRC Press Taylor & Francis Group, Boca Raton.

Cernusak, L.A., Barbour, M.M., Arndt, S.K., Cheesman, A.W., English, N.B., Feild, T.S., Helliker, B.R., Holloway-Phillips, M.M., Holtum, J.A.M., Kahmen, A., McInerney, F.A., Munksgaard, N.C., Simonin, K.A., Song, X., Stuart-Williams, H., West, J.B., Farquhar, G.D., 2016. Stable isotopes in leaf water of terrestrial plants. Plant, cell & environment 39 (5), 1087–1102.

Chang, E., Wolf, A., Gerlein-Safdi, C., Caylor, K.K., 2016. Improved removal of volatile organic compounds for laser-based spectroscopy of water isotopes. Rapid communications in mass spectrometry: RCM 30 (6), 784–790.

Chesson, L.A., Bowen, G.J., Ehleringer, J.R., 2010. Analysis of the hydrogen and oxygen stable isotope ratios of beverage waters without prior water extraction using isotope ratio infrared spectroscopy. Rapid communications in mass spectrometry: RCM 24 (21), 3205–3213.

Clark, I.D., Fritz, P., 2013. Environmental Isotopes in Hydrogeology. Chapman and Hall/CRC, Boca Raton.

Craig, H., 1961a. Isotopic Variations in Meteoric Waters. Science (New York, N.Y.) 133 (3465), 1702–1703.

Craig, H., 1961b. Standard for Reporting Concentrations of Deuterium and Oxygen-18 in Natural Waters. Science (New York, N.Y.) 133 (3467), 1833–1834.

Creydt, M., Fischer, M., 2018. Omics approaches for food authentication. Electrophoresis 39 (13), 1569–1581.

Cristea, G., Feher, I., Magdas, D.A., Voica, C., Puscas, R., 2017. Characterization of Vegetables by Stable Isotopic and Elemental Signatures. Analytical Letters 50 (17), 2677–2690.

Cristea, G., Feher, I., Voica, C., Radu, S., Magdas, D.A., 2020. Isotopic and elemental profiling alongside with chemometric methods for vegetable differentiation. Isotopes in environmental and health studies 56 (1), 69–82.

Dahiru, T., 2008. P – VALUE, A TRUE TEST OF STATISTICAL SIGNIFICANCE? A CAUTIONARY NOTE. Annals of Ibadan Postgraduate Medicine 6 (1), 21–26.

Danezis, G.P., Tsagkaris, A.S., Brusic, V., Georgiou, C.A., 2016. Food authentication: state of the art and prospects. Current Opinion in Food Science 10, 22–31.

Dansgaard, W., 1964. Stable isotopes in precipitation. Tellus 16 (4), 436–468.

Dawson, T.E., Ehleringer, J.R., 1991. Streamside trees that do not use stream water. Nature 350 (6316), 335–337.

Dormann, C., 2020. Environmental Data Analysis. An Introduction with Examples in R. Springer International Publishing; Imprint: Springer, Cham.

Drivelos, S.A., Georgiou, C.A., 2012. Multi-element and multi-isotope-ratio analysis to determine the geographical origin of foods in the European Union. TrAC Trends in Analytical Chemistry 40, 38–51.

DWD, 2021. Deutscher Wetterdienst. online: https://www.dwd.de/DE/leistungen/klimadatendeutschland/mittelwerte/nieder_8110_fest_html.html?view=nasPublication&nn=16102

Ekelund, L., Fernqvist, F., Tjärnemo, H., 2007. Consumer preferences for domestic and organically labelled vegetables in Sweden. Acta Agriculturae Scandinavica, Section C — Food Economics 4 (4), 229–236.

Esslinger, S., Riedl, J., Fauhl-Hassek, C., 2014. Potential and limitations of non-targeted fingerprinting for authentication of food in official control. Food Research International 60, 189–204.

European Union, 2002. Regulation (EC) No 178/2002 of the European Parliament and of the Council of 28 Januar 2002 laying down the general principles and requirements of food law, establishing the European Food Safety Authority and laying down procedures in matters of food safety.

European Union, 2011. Regulation (EU) No 1169/2011 of the European Parliament and of the Council of 25 October 2011 on the provision of food information to consumers, amending Regulations (EC) No 1924/2006 and (EC) No 1925/2006 of the European Parliament and of the Council, and repealing Commission Directive 87/250/EEC, Council Directive 90/496/EEC, Commission Directive 1999/10/EC, Directive 2000/13/EC of the European Parliament and of the Council, Commission Directives 2002/67/EC and 2008/5/EC and Commission Regulation (EC) No 608/2004 Text with EEA relevance. European Union.

Fischer, B.M.C., Frentress, J., Manzoni, S., Cousins, S.A.O., Hugelius, G., Greger, M., Smittenberg, R.H., Lyon, S.W., 2019. Mojito, Anyone? An Exploration of Low-Tech Plant Water Extraction Methods for Isotopic Analysis Using Locally-Sourced Materials. Front. Earth Sci. 7, 2881.

Gonfiantini, R.: Environmental isotopes in lake studies. In: Fritz, P. and Fontes, J.C. (eds.): Handbook of environmental isotope geochemistry, vol. 2, 113-168, doi:10.1016/B978-0-444-42225-5.50008-5, 1986

Gralher, B., Herbstritt. B, Weiler, M., 2021. Technical note: Controversial aspects of the direct vapor equilibration method for stable isotope analysis ($\delta^{18}O$, $\delta^{2}H$) of matrix-bound water: Unifying protocols through empirical and mathematical scrutiny. Accepted for discussion in Hydrol. Earth. Syst. Sci. Discuss., preprint no. hess-2021-255.

Grouven, U., Bender, R., Ziegler, A., Lange, S., 2007. Vergleich von Messmethoden. Deutsche medizinische Wochenschrift (1946) 132 Suppl 1, e69-73.

Grunert, K.G., Aachmann, K., 2016. Consumer reactions to the use of EU quality labels on food products: A review of the literature. Food Control 59, 178–187.

Hendry, M.J., Richman, B., Wassenaar, L.I., 2011. Correcting for methane interferences on δ2H and δ18O measurements in pore water using H2Oliquid-H2Ovapor equilibration laser spectroscopy. Analytical chemistry 83 (14), 5789–5796.

Hendry, M.J., Schmeling, E., Wassenaar, L.I., Barbour, S.L., Pratt, D., 2015. Determining the stable isotope composition of pore water from saturated and unsaturated zone core: improvements to the direct vapour equilibration laser spectrometry method. Hydrol. Earth Syst. Sci. 19 (11), 4427–4440.

Johnson, J.E., Hamann, L., Dettman, D.L., Kim-Hak, D., Leavitt, S.W., Monson, R.K., Papuga, S.A., 2017. Performance of induction module cavity ring-down spectroscopy (IM-CRDS) for measuring δ18 O and δ2 H values of soil, stem, and leaf waters. Rapid communications in mass spectrometry: RCM 31 (6), 547–560.

Kassambara, A., 2020. ggpubr: 'ggplot2' Based Publication Ready Plots. R package version 0.4.0. https://CRAN.R-project.org/package=ggpubr

Katerinopoulou, K., Kontogeorgos, A., Salmas, C.E., Patakas, A., Ladavos, A., 2020. Geographical Origin Authentication of Agri-Food Products: A Review. Foods (Basel, Switzerland) 9 (4).

Kelly, S., Heaton, K., Hoogewerff, J., 2005. Tracing the geographical origin of food: The application of multi-element and multi-isotope analysis. Trends in Food Science & Technology 16 (12), 555–567.

Koeniger, P., Gaj, M., Beyer, M., Himmelsbach, T., 2016. Review on soil water isotope-based groundwater recharge estimations. Hydrol. Process. 30 (16), 2817–2834.

Koeniger, P., Marshall, J.D., Link, T., Mulch, A., 2011. An inexpensive, fast, and reliable method for vacuum extraction of soil and plant water for stable isotope analyses by mass spectrometry. Rapid communications in mass spectrometry: RCM 25 (20), 3041–3048.

Leibundgut, C., Maloszewski, P., Külls, C., 2009. Tracers in hydrology. Wiley-Blackwell, Chichester.

Magdas, D.A., Guyon, F., Puscas, R., Vigouroux, A., Gaillard, L., Dehelean, A., Feher, I., Cristea, G., 2021. Applications of emerging stable isotopes and elemental markers for geographical and varietal recognition of Romanian and French honeys. Food chemistry 334, 127599.

Martín-Gómez, P., Barbeta, A., Voltas, J., Peñuelas, J., Dennis, K., Palacio, S., Dawson, T.E., Ferrio, J.P., 2015. Isotope-ratio infrared spectroscopy: a reliable tool for the investigation of plant-water sources? The New phytologist 207 (3), 914–927.

McGuire, K., McDonnell, J., 2007. Stable isotope tracers in watershed hydrology. In: R. Michener, K. Lajtha (Editors), Stable Isotopes in Ecology and Environmental Science. John Wiley & Sons, New York, NY.

Millar, C., Pratt, D., Schneider, D.J., McDonnell, J.J., 2018. A comparison of extraction systems for plant water stable isotope analysis. Rapid communications in mass spectrometry: RCM 32 (13), 1031–1044.

Mimmo, T., Camin, F., Bontempo, L., Capici, C., Tagliavini, M., Cesco, S., Scampicchio, M., 2015. Traceability of different apple varieties by multivariate analysis of isotope ratio mass spectrometry data. Rapid communications in mass spectrometry: RCM 29 (21), 1984–1990.

Montet, D., Ray, R.C., 2017. Food Traceability and Authenticity. CRC Press, Boca Raton, FL: CRC Press, 2017. | Series: Food biology series | “A science publishers book.”.

Moore, J.C., Spink, J., Lipp, M., 2012. Development and application of a database of food ingredient fraud and economically motivated adulteration from 1980 to 2010. Journal of food science 77 (4), R118-26.

Moyer, D.C., DeVries, J.W., Spink, J., 2017. The economics of a food fraud incident – Case studies and examples including Melamine in Wheat Gluten. Food Control 71, 358–364.

Oerter, E., Malone, M., Putman, A., Drits-Esser, D., Stark, L., Bowen, G., 2017. Every apple has a voice: using stable isotopes to teach about food sourcing and the water cycle. Hydrol. Earth Syst. Sci. 21 (7), 3799–3810.

Orlowski, N., Breuer, L., Angeli, N., Boeckx, P., Brumbt, C., Cook, C.S., Dubbert, M., Dyckmans, J., Gallagher, B., Gralher, B., Herbstritt, B., Hervé-Fernández, P., Hissler, C., Koeniger, P., Legout, A., Macdonald, C.J., Oyarzún, C., Redelstein, R., Seidler, C., Siegwolf, R., Stumpp, C., Thomsen, S., Weiler, M., Werner, C., McDonnell, J.J., 2018. Inter-laboratory comparison of cryogenic water extraction systems for stable isotope analysis of soil water. Hydrol. Earth Syst. Sci. 22 (7), 3619–3637.

Orlowski, N., Breuer, L., McDonnell, J.J., 2016a. Critical issues with cryogenic extraction of soil water for stable isotope analysis. Ecohydrol. 9 (1), 1–5.

Orlowski, N., Frede, H.-G., Brüggemann, N., Breuer, L., 2013. Validation and application of a cryogenic vacuum extraction system for soil and plant water extraction for isotope analysis. J. Sens. Sens. Syst. 2 (2), 179–193.

Orlowski, N., Pratt, D.L., McDonnell, J.J., 2016b. Intercomparison of soil pore water extraction methods for stable isotope analysis. Hydrol. Process. 30 (19), 3434–3449.

Pfahl, S., Sodemann, H., 2014. What controls deuterium excess in global precipitation? Clim. Past 10 (2), 771–781.

Picarro Inc., 2020. Continuous Monitoring for Real Time Insights. Cavity Ring-Down Spectroscopy (CRDS). https://www.picarro.com/company/technology/crds. Accessed April 20, 2021.

R Core Team (2020). R: A language and environment for statistical computing. R Foundation for Statistical Computing, Vienna, Austria. URL https://www.R-project.org/.

Rossier, J.S., Maury, V., Pfammatter, E., 2016. Locally Grown, Natural Ingredients? The Isotope Ratio Can Reveal a Lot! Chimia 70 (5), 345–348.

Rozanski, K., Araguás-Araguás, L., Gonfiantini, R., 1993. Isotopic Patterns in Modern Global Precipitation. In: P.K. Swart, K.C. Lohmann, J. Mckenzie, S. Savin (Editors), Climate Change in Continental Isotopic Records. American Geophysical Union, Washington, D. C., pp. 1–36.

Schultz, N.M., Griffis, T.J., Lee, X., Baker, J.M., 2011. Identification and correction of spectral contamination in 2H/1H and 18O/16O measured in leaf, stem, and soil water. Rapid communications in mass spectrometry: RCM 25 (21), 3360–3368.

Segelke, T., Wuthenau, K. von, Kuschnereit, A., Müller, M.-S., Fischer, M., 2020. Origin Determination of Walnuts (Juglans regia L.) on a Worldwide and Regional Level by Inductively Coupled Plasma Mass Spectrometry and Chemometrics. Foods (Basel, Switzerland) 9 (11).

Spink, J., Moyer, D.C., 2011. Defining the public health threat of food fraud. Journal of food science 76 (9), R157-63.

Sprenger, M., Herbstritt, B., Weiler, M., 2015. Established methods and new opportunities for pore water stable isotope analysis. Hydrol. Process. 29 (25), 5174–5192.

Sprenger, M., Tetzlaff, D., Soulsby, C., 2017. Soil water stable isotopes reveal evaporation dynamics at the soil–plant–atmosphere interface of the critical zone. Hydrol. Earth Syst. Sci. 21 (7), 3839–3858.

Stockinger, M., Santos Pires, S., Stumpp, C., 2020. Analysis of plant water stable isotopes using the water-vapor equilibrium method.

Sulzman, E.W., 2007. Stable isotope chemistry and measurement: a primer. In: R. Michener, K. Lajtha (Editors), Stable Isotopes in Ecology and Environmental Science. Blackwell Publishing Ltd, Oxford, UK.

van Ruth, S.M., Huisman, W., Luning, P.A., 2017. Food fraud vulnerability and its key factors. Trends in Food Science & Technology 67, 70–75.

Vander Zanden, H.B., Chesson, L.A., 2017. Data Analysis Interpretation. Forensic Applications and Examples. In: J.F. Carter, L.A. Chesson (Editors), Food forensics. Stable isotopes as a guide to authenticity and origin. CRC Press Taylor & Francis Group, Boca Raton.

Volkmann, T.H.M., Kühnhammer, K., Herbstritt, B., Gessler, A., Weiler, M., 2016. A method for in situ monitoring of the isotope composition of tree xylem water using laser spectroscopy. Plant, cell & environment 39 (9), 2055–2063.

Volkmann, T.H.M., Weiler, M., 2014. Continual in situ monitoring of pore water stable isotopes in the subsurface. Hydrol. Earth Syst. Sci. 18 (5), 1819–1833.

Wassenaar, L.I., Hendry, M.J., Chostner, V.L., Lis, G.P., 2008. High resolution pore water delta2H and delta18O measurements by H2O(liquid)-H2O(vapor) equilibration laser spectroscopy. Environmental science & technology 42 (24), 9262–9267.

Werner, R.A., Brand, W.A., 2001. Referencing strategies and techniques in stable isotope ratio analysis. Rapid communications in mass spectrometry: RCM 15 (7), 501–519.

Wershaw R.L., Friedman I., Heller S.J. 1966. Hydrogen isotope fractionation of water passing through trees. In Advances in Organic Geochemistry. Eds. Hobson F. Speers M. Pergamon, New York, pp 55–67.

West, A.G., Goldsmith, G.R., Brooks, P.D., Dawson, T.E., 2010. Discrepancies between isotope ratio infrared spectroscopy and isotope ratio mass spectrometry for the stable isotope analysis of plant and soil waters. Rapid communications in mass spectrometry: RCM 24 (14), 1948–1954.

West, A.G., Patrickson, S.J., Ehleringer, J.R., 2006. Water extraction times for plant and soil materials used in stable isotope analysis. Rapid communications in mass spectrometry: RCM 20 (8), 1317–1321.

Abbreviations

CAU ..... Cauliflower
CEL ..... Celery Root
CRDS ..... Cavity Ring-Down Spectroscopy
CVD ..... Cryogenic Vacuum Distillation
d ..... Euclidean distance
d-ex ..... deuterium excess
DVE-LS ..... Direct Water Vapor Equilibrium- Laser Spectroscopy
EU ..... European Union
FSM ..... Light Standard
GC ..... Gas Chromatography
GLM ..... Generalized Linear Model
HPLC ..... High-Pressure Liquid Chromatography
ICP-MS ..... Inductively Coupled Plasma Mass Spectrometry
in situ ..... Continual *in situ* Monitoring
IR ..... Infrared Spectroscopy
IRIS ..... Isotope-Ratio Infrared Spectroscopy
IRMS ..... Isotope Ratio Mass Spectrometry
k ..... *Cluster size*
K ..... Farm K
KOH ..... Kohlrabi
LMWL ..... Local Meteoric Water Line
M ..... Farm M
MAB ..... Maximum Accepted Bias
NMR ..... Nuclear Magnetic Resonance
North Sea ..... Heavy Standard
PCA ..... Principal Component Analysis
PDO ..... Protected Designation of Origin
PGI ..... Protected Geographical Indication
POT ..... Potatoes
Q ..... Farm Q
R ..... Farm R
R_sample ..... isotopic ratio of the sample
R_standard ..... isotopic ratio of the standard
REE ..... Rare Earth Elements
S ..... Supermarket
SD ..... Standard Deviation
TSG ..... Traditional Specialty Guaranteed
VOC ..... Volatile Organic Compounds
VSMOW ..... Vienna Standard Mean Ocean Water
VSMOW2 ..... Vienna Standard Mean Ocean Water 2
WEK ..... Medium Standard
WS-CRDS ..... Wavelength-Scanned Cavity Ring-Down Spectroscopy
δ ..... Delta notation

Appendix

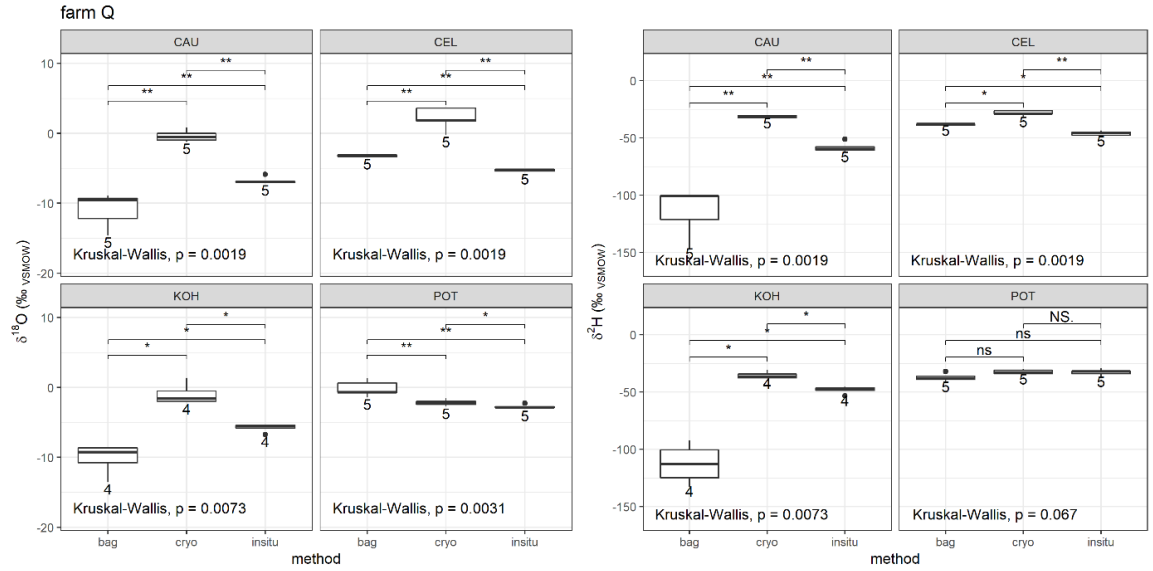

Figure A. 1: Boxplots of all measured vegetable samples (left: $\delta^{18}O$ and right: $\delta^{2}H$) from farm Q, plotted by the different methods and type of vegetable. The number indicates the number of observations (*n*) and the lines and associated symbols indicate the results of the Kruskal-Wallis test. The respective comparisons are indicated by the p-value ('ns': $p > a$; '*': $p \leq 0.05$; '**': $p \leq 0.05$; '***': $p \leq 0.01$).

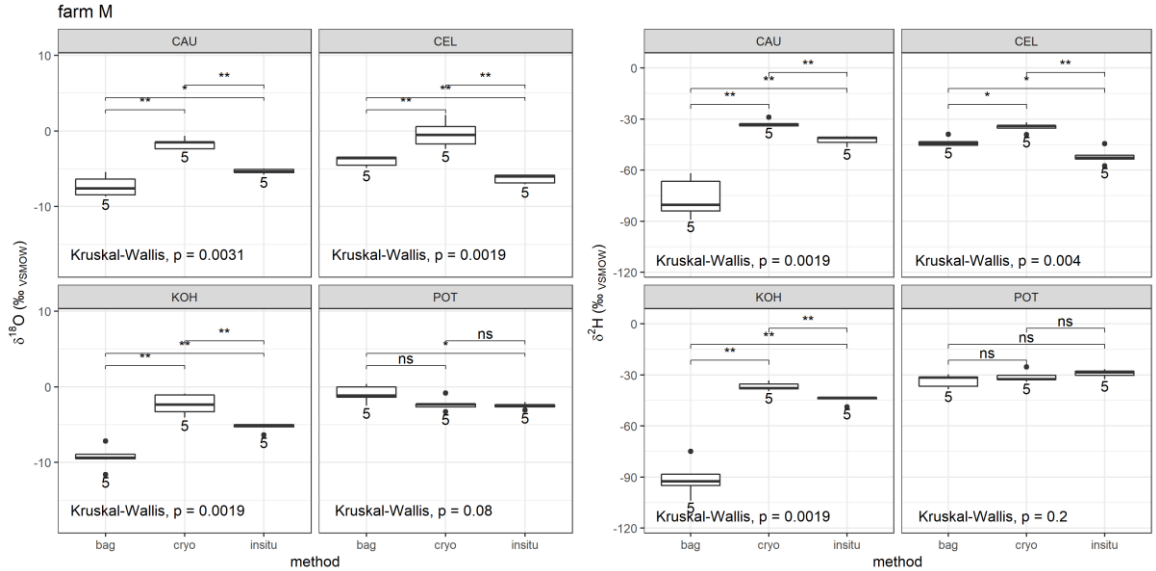

Figure A. 2: Boxplots of isotope data from all measured vegetable samples from farm M, plotted by the different methods and kind of vegetable (left: $\delta^{18}O$ and right: $\delta^{2}H$). The number indicates the number of observations (n) and the lines and associated symbols indicate the results of the Kruskal-Wallis test. The respective comparisons are indicated by the p-value ('ns': $p > a$; '*': $p \leq 0.05$; '**': $p \leq 0.05$; '***': $p \leq 0.01$).

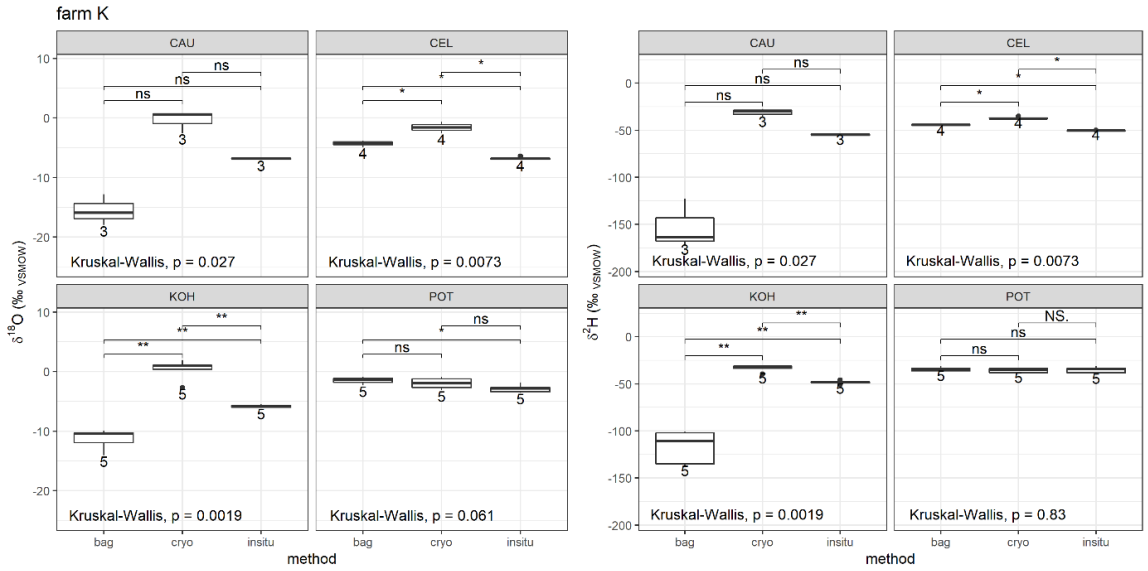

Figure A. 3: Boxplots of isotope data from all measured vegetable samples from farm K, plotted by the different methods and type of vegetable (left: $\delta^{18}O$ and right: $\delta^{2}H$). The number indicates the number of observations (n) and the lines and associated symbols indicate the results of the Kruskal-Wallis test. The respective comparisons are indicated by the p-value ('ns': p > a; '*': p ≤ 0.05; '**': p ≤ 0.05; '***': p ≤ 0.01).

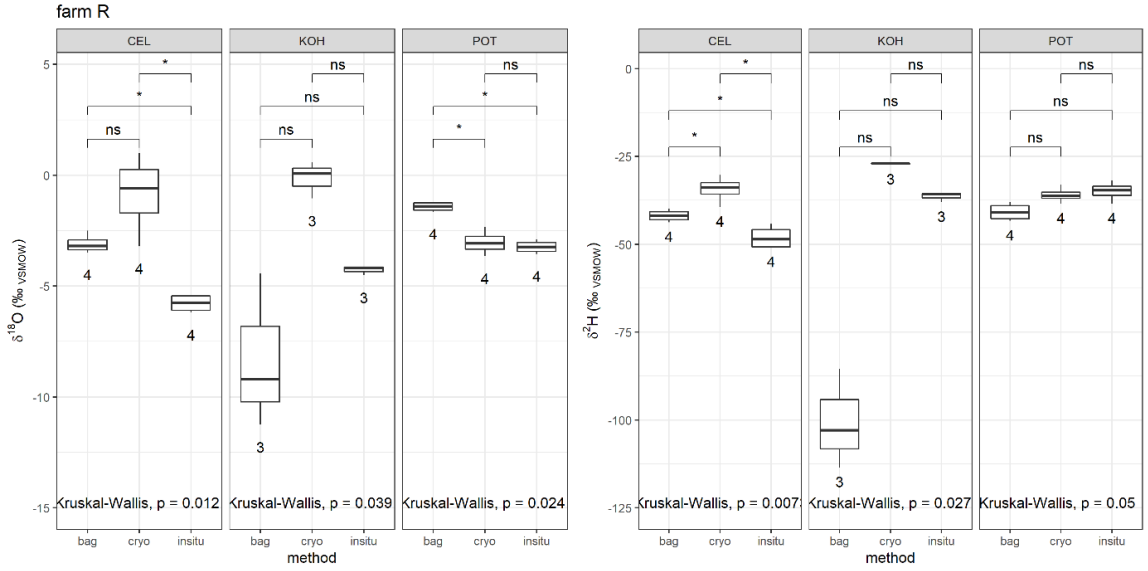

Figure A. 4: Boxplots of isotope data from all measured vegetable samples from farm R, plotted by the different methods and type of vegetable (left: $\delta^{18}O$ and right: $\delta^{2}H$). The number indicates the number of observations (n) and the lines and associated symbols indicate the results of the Kruskal-Wallis test. The respective comparisons are indicated by the p-value ('ns': p > a; '*': p ≤ 0.05; '**': p ≤ 0.05; '***': p ≤ 0.01).

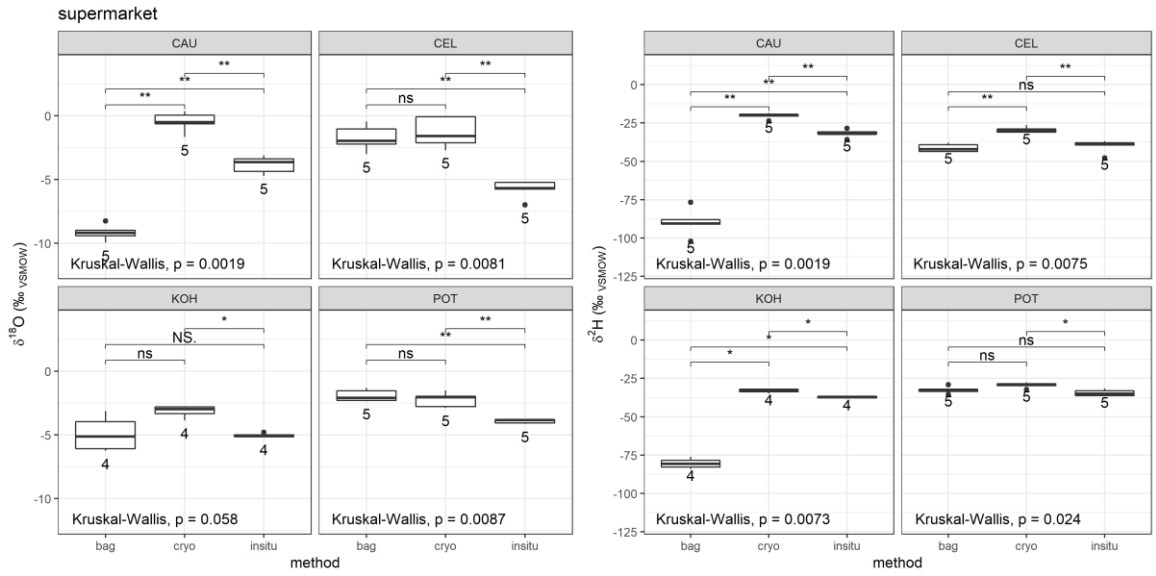

Figure A. 5: Boxplots of isotope data from all measured supermarket vegetable samples plotted by the different methods and kind of vegetable (left: $\delta^{18}O$ and right: $\delta^{2}H$). The number indicates the number of observations (n) and the lines and associated symbols indicate the results of the Kruskal-Wallis test. The respective comparisons are indicated by the p-value ('ns': p > a; '*': p ≤ 0.05; '**': p ≤ 0.05; '***': p ≤ 0.01).

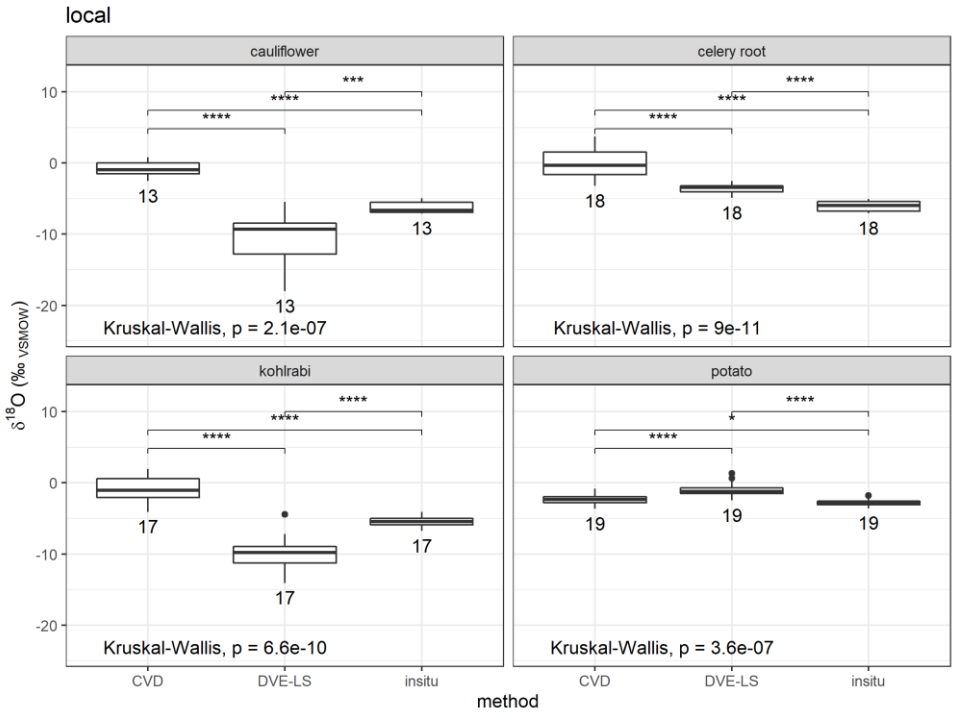

Figure A. 6: Boxplots of all measured local vegetable samples, plotted by the different methods and type of vegetable for $\delta^{18}O$ values. The number indicates the number of observations (n) and the lines and associated symbols indicate the results of the Kruskal-Wallis test. The respective comparisons are indicated by the p-value ('ns': p > a; '*': p ≤ 0.05; '**': p ≤ 0.05; '***': p ≤ 0.01).

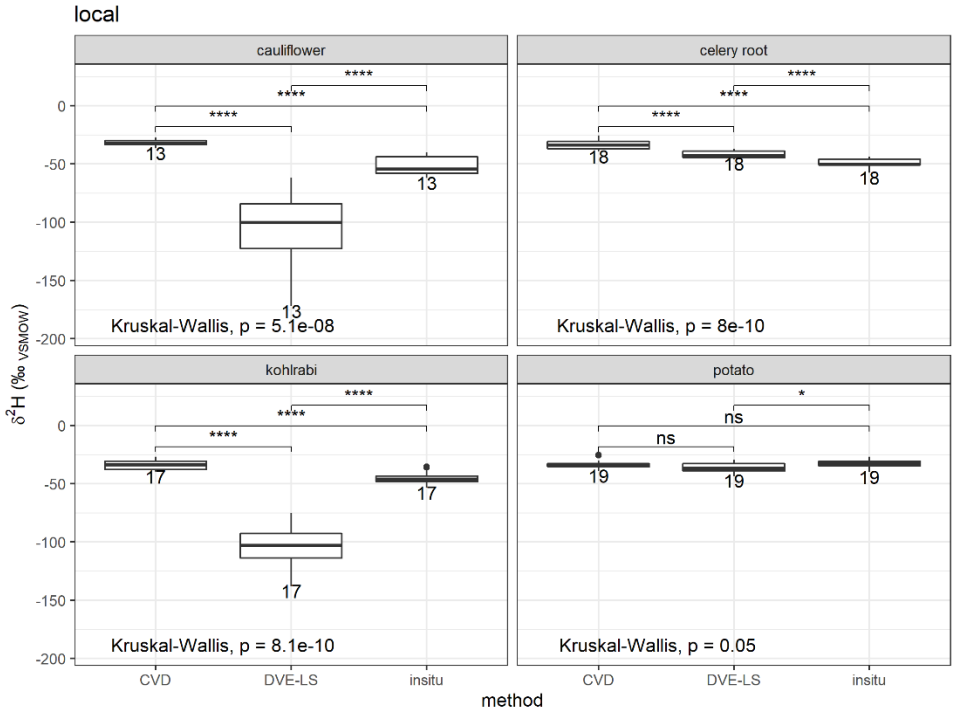

Figure A. 7: Boxplots of δ^2H values from all measured local vegetable samples, plotted by the different methods and type of vegetable. The number indicates the number of observations (*n*) and the lines and associated symbols indicate the results of the Kruskal-Wallis test. The respective comparisons are indicated by the p-value ('ns': p > a; '*': p ≤ 0.05; '**': p ≤ 0.05; '***': p ≤ 0.01).

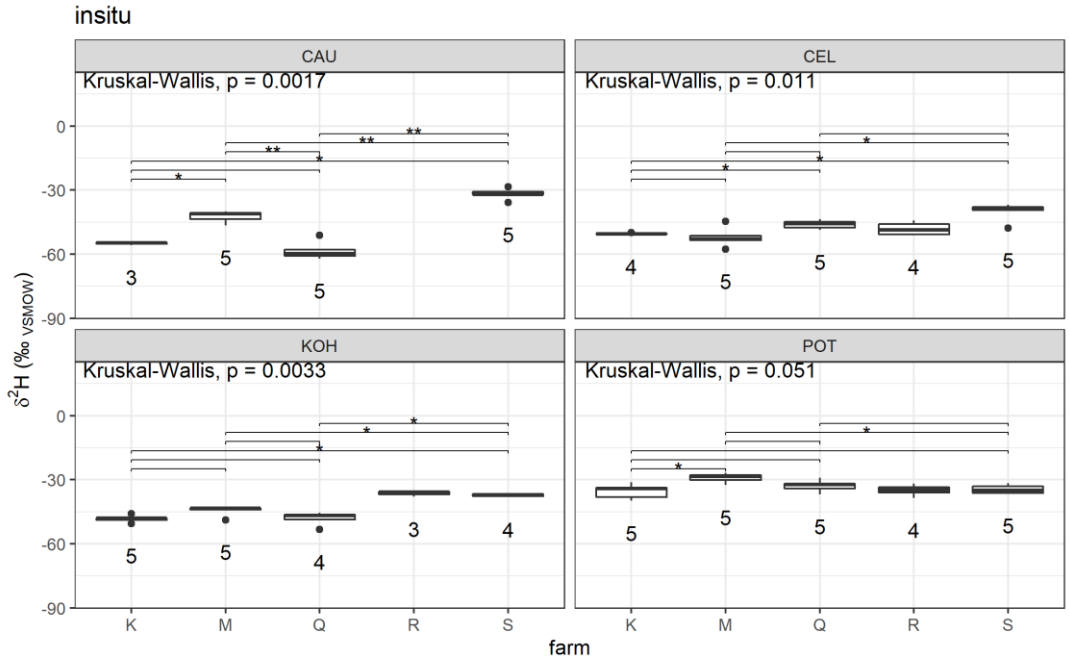

Figure A. 8: Boxplots of all vegetable samples of each farm and supermarket (δ^2H) for the *in situ* method, plotted by the different kinds of vegetables. The number indicates the number of observations (n) and the lines and associated symbols indicate the results of the individual Kruskal-Wallis test. The respective comparisons are indicated by the p-value ('ns': p > a; '*': p ≤ 0.05; '**': p ≤ 0.05; '***': p ≤ 0.01). In addition, the total result of the Kruskal- Wallis test for each vegetable variety (δ2H) is given.

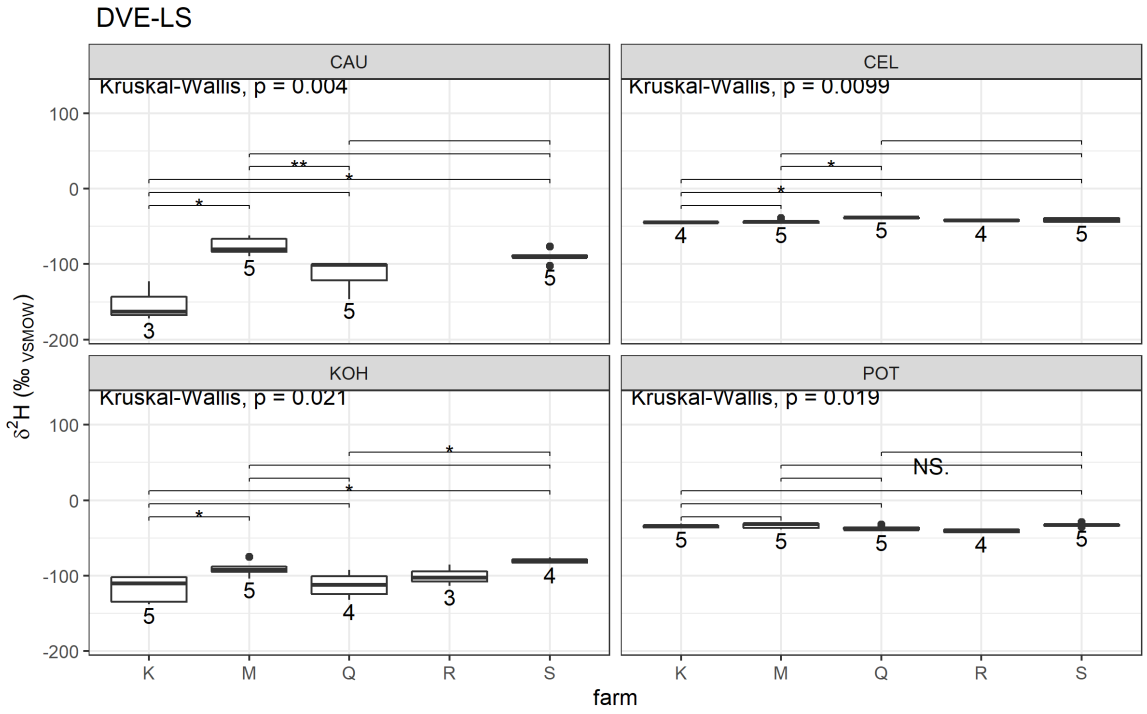

Figure A. 9: Boxplots of all vegetable samples from each farm and supermarket (δ^2H) for the DVE-LS method, plotted by the different kinds of vegetables. The number indicates the number of observations (*n*) and the lines and associated symbols indicate the results of the individual Kruskal-Wallis test. The respective comparisons are indicated by the p-value ('ns': p > a; '*': p ≤ 0.05; '**': p ≤ 0.05; '***': p ≤ 0.01). In addition, the total result of the Kruskal- Wallis test for each vegetable's variety (δ^2H) was given.

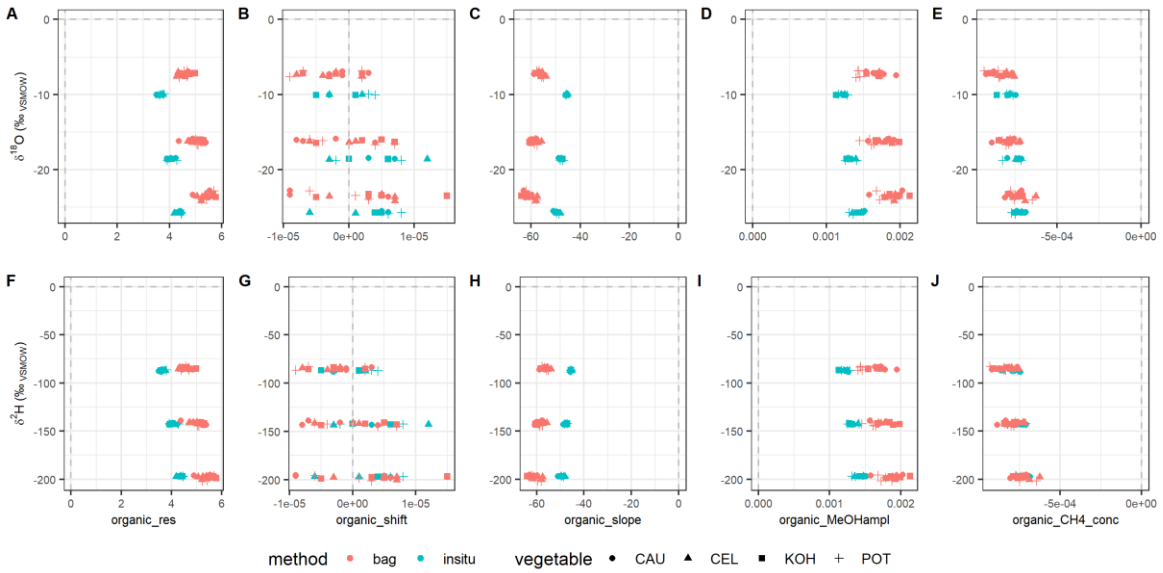

Figure A. 10: Selected spectral parameters, which were measured with the CRDS (L2120-*i*, Picarro) in the standards by the *in situ* and DVE-LS method. *A* to *E* plot these parameters against δ^{18}O and *F* to *J* against δ^2H. Dashed lines indicate the zero positions on each axis.

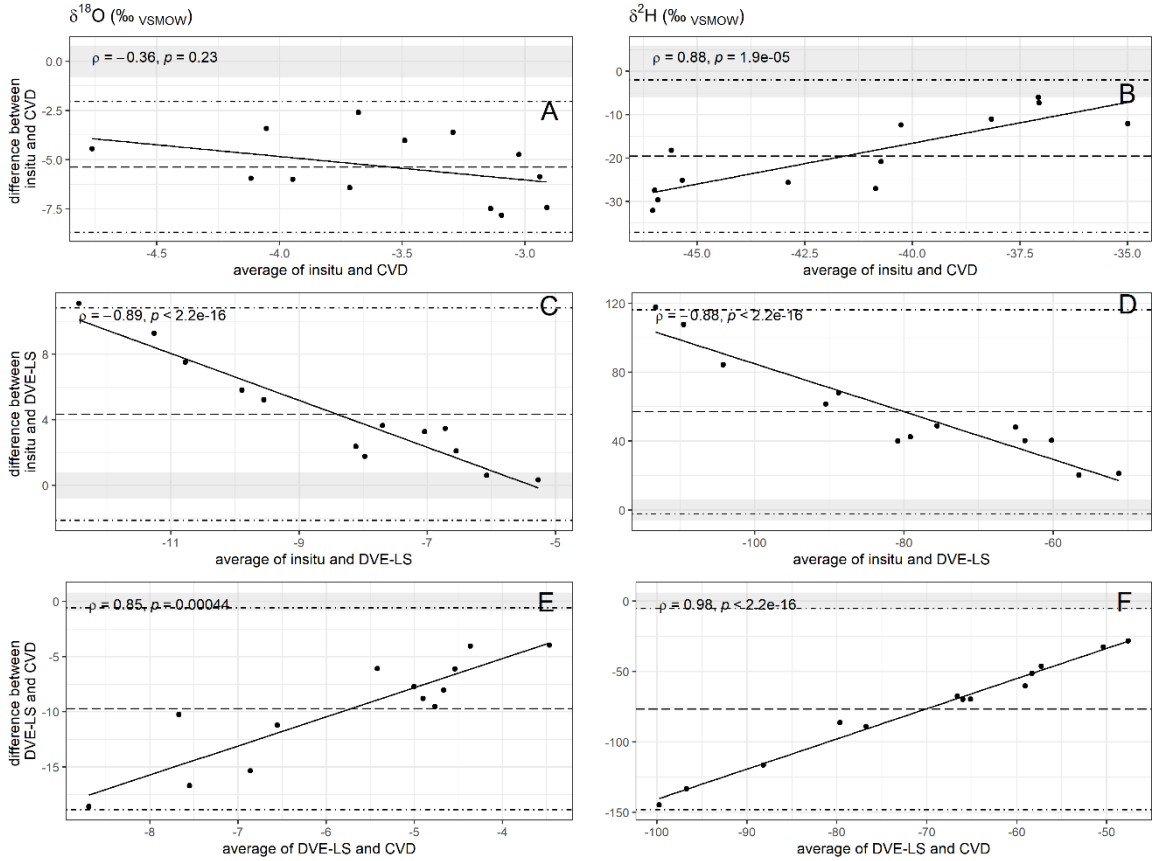

Figure A. 11: Bland- Altman plots of the CAU data. A and B plot the difference between the *in situ* and CVD for $\delta^{18}O$ and $\delta^{2}H$ in [‰], respectively. The other plots show the difference between the *in situ* and CVD (C and D) and between the DVE-LS and CVD (E and F) for $\delta^{18}O$ and $\delta^{2}H$, respectively. The dashed line indicates the bias, and the two dotted lines indicate the upper and lower 95% limits of agreement (LOA) (=bias ±1.96 ×SD) of the respective data. In addition, the regression line and the significance level p and spearman's ρ are given. The gray area indicates the maximum accepted bias of the data. All calibrated values are given in per mil (‰ VSMOW).

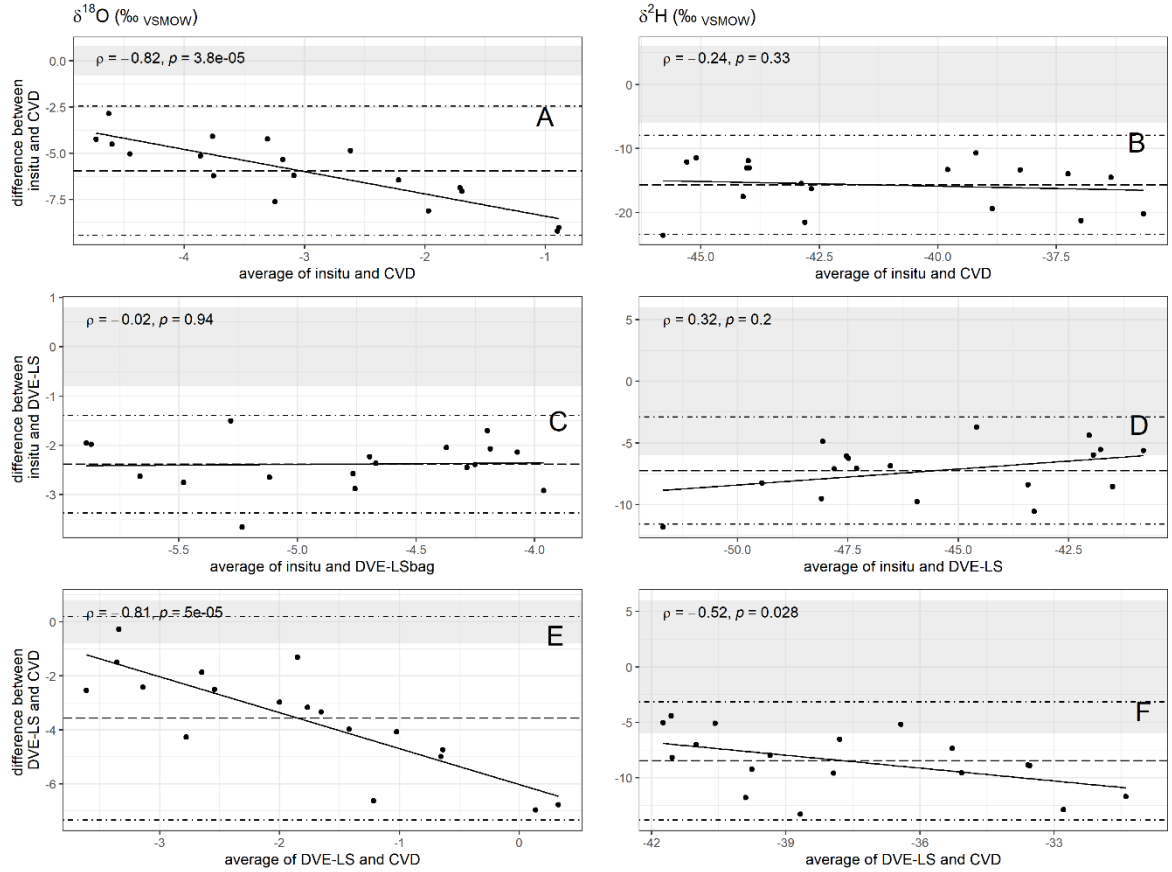

Figure A. 12: Bland- Altman plots of the CEL data. A and B plot the difference between the *in situ* and CVD for $\delta^{18}O$ and $\delta^{2}H$ [‰], respectively. The other plots show the difference between the *in situ* and CVD (cryo) (C and D) and between the DVE-LS (bag) and CVD (E and F) for $\delta^{18}O$ and $\delta^{2}H$, respectively. The dashed line indicated the bias, and the two dotted lines indicate the upper and lower 95% limits of agreement (LOA) (=bias ±1.96 ×SD) of the respective data. In addition, the regression line and the significance level p and spearman's ρ are given. The gray area indicates the maximum accepted bias of the data. All calibrated values are given in mil (‰ VSMOW).

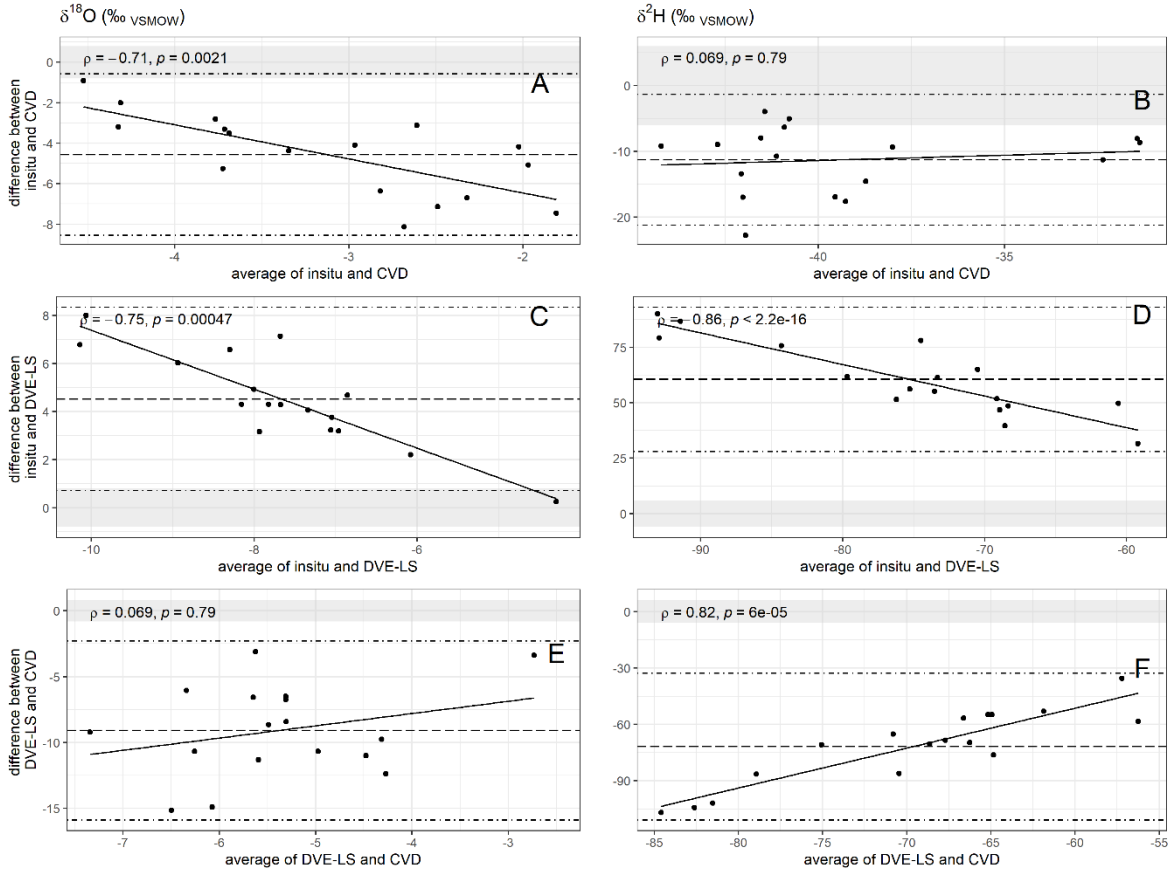

Figure A. 13: Bland- Altman plots of the KOH data. A and B plot the difference between the *in situ* and CVD method for $\delta^{18}O$ and $\delta^{2}H$ [‰], respectively. The other plots show the difference between the *in situ* and CVD method (C and D) and between the DVE-LS and CVD method (E and F) for $\delta^{18}O$ and $\delta^{2}H$, respectively. The dotted line indicated the bias, and the two dashed lines indicate the upper and lower 95% limits of agreement (LOA) (=bias ±1.96 ×SD) of the respective data. In addition, the regression line and the significance level p and spearman's ρ are given. The gray area indicates the maximum accepted bias of the data. All values are given in ‰ VSMOW.

Table A. 1: Mean, the standard deviations (SD) and the minimum (Min) and maximum (Max) values of the isotopically and volume weighted precipitation for the different growth phases of the vegetables for the $\delta^{18}O$ and δ2H values. All values are given in ‰VSMOW.

vegetable	$\delta^{18}O$	$\delta^{2}H$	SD $\delta^{18}O$	SD $\delta^{2}H$	Min $\delta^{18}O$	Max $\delta^{18}O$	Min $\delta^{2}H$	Max $\delta^{2}H$
CAU	-7.46	-49.33	2.89	23.45	-12.09	-1.90	-90.62	-0.26
CEL	-6.27	-41.88	2.92	20.44	-12.09	-0.53	-90.62	-4.00
KOH	-6.69	-44.43	3.05	22.65	-12.09	-1.23	-90.62	-0.26
POT	-5.32	-35.27	2.66	18.14	-9.47	0.40	-68.07	-1.08

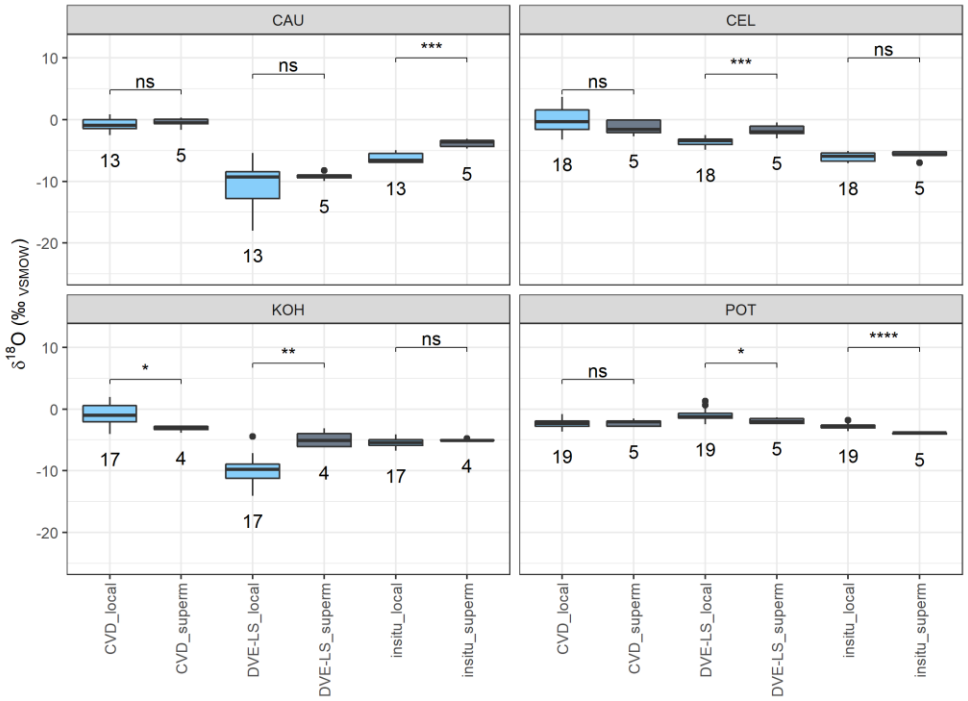

Figure A. 14: Scatter ranges of local and imported ('superm') samples divided by vegetable varieties and methods (CVD, DVE-LS and in situ) for δ^{18}O values.

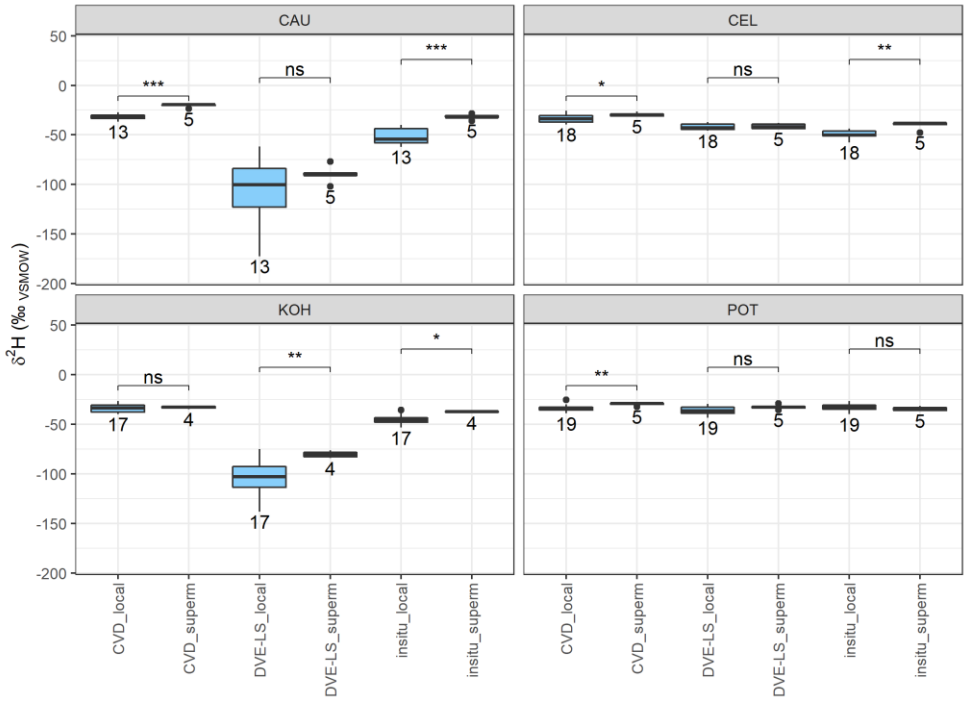

Figure A. 15: Scatter ranges of local and imported ('superm') samples divided by vegetable varieties and methods (CVD, DVE-LS and in situ) for δ^{2}H values.

Table A. 2: Results of the GLM for the $\delta^{18}O$ and $\delta^{2}H$ values of CEL (*in situ* and DVE-LS method) for the dependent variables ($\delta^{18}O$ and $\delta^{2}H$) and the parameter analyzed in Figure 10, reduced if dependent and not significant. '_p' indicates which parameters were shifted to the positive range.

	$\delta^{18}O$_p (*in situ*)		**$\delta^{2}H$_p (*in situ*)**		**$\delta^{18}O$_p (DVE-LS)**		**$\delta^{2}H$_p (DVE-LS)**	
Coeffcient	*Estimates*	*P-Value*	*Estimates*	*P-Value*	*Estimates*	*P-Value*	*Estimates*	*P-Value*
(Intercept)	-0.11	**0.038**	-0.51	0.113	18.11	**<0.001**	114.87	**<0.001**
organic_CH4_conc_p	24.35	0.152	6.28	0.163			4931.43	0.071
organic_slope_p	0.00	0.141	0.00	0.216				
organic_shift_p	245.84	0.089	11.68	0.241				
organic_MeOHampl			0.34	0.082	-2684.29	**0.002**		
organic_base			0.00	0.110				
Observations	19		19		20		20	
R^2 Nagelkerke	0.535		0.418		0.461		0.725	

Table A. 3: Results of the GLM for the $\delta^{18}O$ and $\delta^{2}H$ values of KOH (*in situ* and DVE-LS) for the dependent variables ($\delta^{18}O$ and $\delta^{2}H$) and the parameter analyzed in Figure 10, reduced if dependent and not significant. '_p' indicates which parameter were shifted to the positive range.

	$\delta^{18}O$_p (*in situ*)		**$\delta^{2}H$_p (*in situ*)**		**$\delta^{18}O$_p (DVE-LS)**		**$\delta^{2}H$_p (DVE-LS)**	
Coeffcient	Estimates	P-Value	Estimates	P-Value	Estimates	P-Value	Estimates	P-Value
(Intercept)	-0.07	0.157	-0.00	0.344	-343.90	0.273	158.60	**<0.001**
organic_CH4_conc_p	31.33	**0.008**	2.49	**0.005**	3287.79	0.390		
organic_MeOHampl	3.49	0.206	0.22	0.273	-675.78	**<0.001**	-5631.03	**<0.001**
organic_shift_p					-3982.79	0.095	-23142.95	0.105
organic_base					0.36	0.247		
organic_res							-2.69	**<0.001**
Observations	20		20		19		19	
R2 Nagelkerke	0.380		0.403		1.000		1.000	

Table A. 4: Results of the GLM for the $\delta^{18}O$ and $\delta^{2}H$ values of POT (*in situ* and DVE-LS) for the dependent variables ($\delta^{18}O$ and $\delta^{2}H$) and the parameter analyzed in Figure 10, reduced if dependent and not significant. '_p' indicates which parameter were shifted to the positive range.

	$\delta^{18}O$_p (*in situ*)		**$\delta^{2}H$_p (*in situ*)**		**$\delta^{18}O$_p (DVE-LS)**		**$\delta^{2}H$_p (DVE-LS)**	
Coeffcient	Estimates	P-Value	Estimates	P-Value	Estimates	P-Value	Estimates	P-Value
(Intercept)	-0.14	0.228	0.01	**<0.001**	580.71	0.069	124.44	**<0.001**
organic_CH4_conc_p	32.38	0.215			-15694.6	**0.008**		
organic_MeOHampl	2.32	0.223	0.48	**0.002**				
organic_slope_p	0.00	0.516			0.30	**0.027**	0.19	**0.004**
organic_res	0.01	0.189						
organic_shift_p	-143.54	0.086						
organic_base					-0.55	0.080		
Observations	20		20		20		20	
R2 Nagelkerke	0.468		0.436		0.799		0.998	

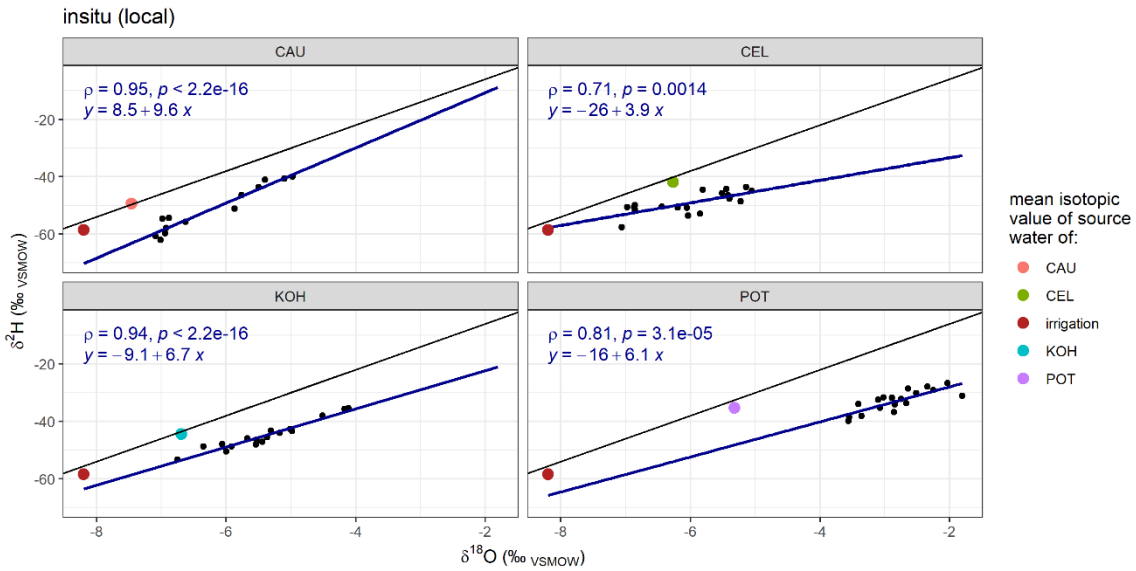

Figure A. 16: Dual isotope plot of data analyzed with the *in situ* method. Additionally, with regression lines, the formula, the correlation coefficient (spearman's ρ), and the significance level (p) for each local vegetable. The colored dots indicate the isotopic composition of the irrigation water, as well as the mean isotopic value of the precipitation of the respective growth phase of the vegetables.

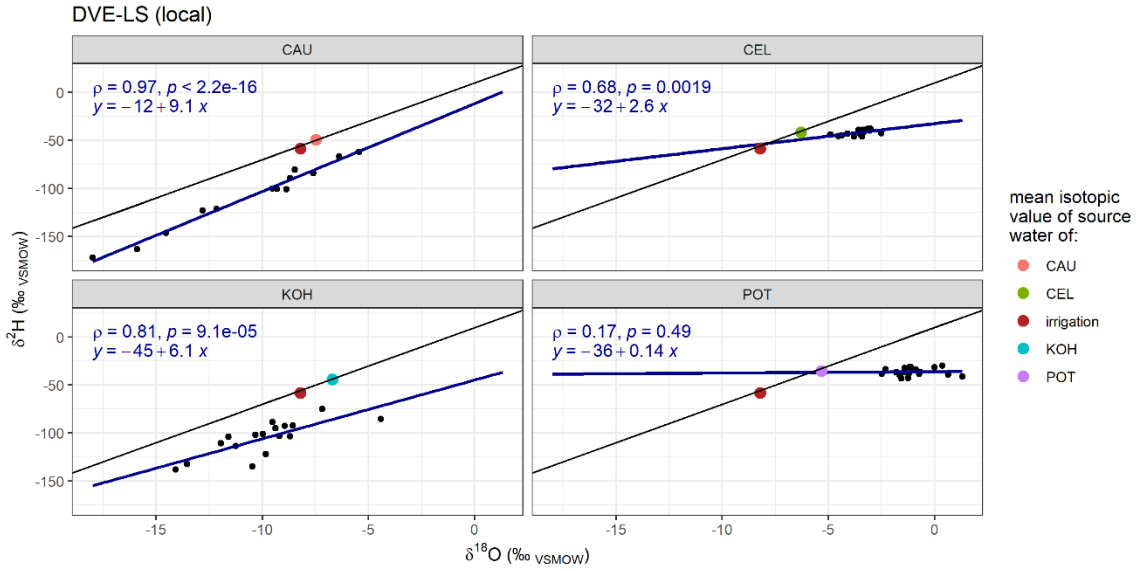

Figure A. 17: Dual isotope plot of data analyzed with the DVE-LS method. Additionally, with regression lines, the formula, the correlation coefficient (spearman's ρ), and the significance level (p) for each local vegetable. The colored dots indicate the isotopic composition of the irrigation water, as well as the mean isotopic value of the precipitation of the respective growth phase of the vegetables.

Table A. 5: Mean values ($\delta^{18}O$ and $\delta^{2}H$) for each vegetable per farm and method (CVD, DVE-LS and *in situ*) with standard deviations. The *n* indicates the number of samples.

			in situ		DVE-LS		CVD	
vegetable	farm	*n*	$\delta^{18}O$	$\delta^{2}H$	$\delta^{18}O$	$\delta^{2}H$	$\delta^{18}O$	$\delta^{2}H$
CAU			-6.83 ±	-54.93 ±	-15.56 ±	-152.8 ±	-0.38 ±	-31.29 ±
	K	3	0.18	0.69	2.61	26.33	1.88	4.71
			-5.35 ±	-42.37 ±	-7.31 ±	-76.39 ±	-1.67 ±	-32.65 ±
	M	5	0.32	2.66	1.38	11.65	0.72	2.14
			-6.77 ±	-58.32 ±	-10.88 ±	-113.79 ±	-0.36 ±	-31.28 ±
	Q	5	0.51	4.28	2.42	20.33	0.79	1.21
			-3.85 ±	-31.78 ±	-9.17 ±	-89.68 ±	-0.49 ±	-20.35 ±
	S	5	0.67	2.66	0.62	9.02	0.77	1.96
CEL			-6.79 ±	-50.41 ±	-4.29 ±	-44.4 ±	-1.62 ±	-37.04 ±
	K	4	0.24	0.3	0.47	1.03	0.84	1.29
			-6.32 ±	-51.98 ±	-3.98 ±	-43.54 ±	-0.38 ±	-34.9 ±
	M	5	0.59	4.75	0.68	2.7	1.78	2.69
			-5.26 ±	-46.1 ± 2	-3.18 ±	-38.28 ±	2.14 ±	-28.35 ±
	Q	5	0.19		0.16	0.8	1.61	2.43
			-5.78 ±	-48.07 ±	-3.09 ±	-41.85 ±	-0.84 ±	-34.33 ±
	R	4	0.4	3.3	0.43	1.74	1.81	3.79
			-5.78 ±	-40.07 ±	-1.74 ±	-41.33 ±	-1.32 ±	-29.37 ±
	S	5	0.73	4.36	1	2.65	1.19	1.96
KOH			-5.84 ±	-48.27 ±	-11.36 ±	-117.27 ±	0.33 ±	-33.23 ±
	K	5	0.22	1.63	1.69	17.91	1.8	3.74
			-5.36 ±	-44.44 ±	-9.32 ±	-90.98 ±	-2.35 ±	-36.83 ±
	M	5	0.57	2.47	1.58	10.6	1.37	2.46
			-5.77 ±	-48.13 ±	-10.15 ±	-112.59 ±	-0.94 ±	-35.52 ±
	Q	4	0.65	3.53	2.33	18.09	1.6	3.47
			-4.26 ±	-36.39 ±	-8.29 ±	-100.66 ±	-0.14 ±	-27.05 ±
	R	3	0.22	1.4	3.5	14.17	0.83	0.35
			-5.03 ±	-37.18 ±	-4.91 ±	-80.44 ±	-3.15 ±	-33.02 ±
	S	4	0.15	0.83	1.49	3.58	0.5	1.35
POT			-2.85 ±	-35.37 ±	-1.48 ±	-34.32 ±	-1.97 ±	-35.69 ±
	K	5	0.69	3.59	0.57	2.22	0.95	2.86
			-2.53 ±	-29.15 ±	-0.93 ±	-33.5 ±	-2.27 ±	-30.94 ±
	M	5	0.4	2.26	1.14	3.83	0.9	3.41
			-2.75 ±	-32.79 ±	-0.17 ±	-37.43 ±	-2.18 ±	-32.51 ±
	Q	5	0.29	2.87	1.11	3.42	0.43	1.94
			-3.23 ±	-34.89 ±	-1.42 ±	-40.8 ±	-3.03 ±	-35.97 ±
	R	4	0.3	2.79	0.22	2.51	0.55	2.23
			-3.93 ±	-34.42 ±	-1.92 ±	-32.6 ±	-2.24 ±	-29.46 ±
	S	5	0.17	2.08	0.47	2.32	0.57	1.79

Table A. 6: Mean, minimum (min), maximum (max) and standard deviation (SD) of the supermarket vegetables for each $\delta^{18}O$ and $\delta^{2}H$ determined with all three methods for each vegetable (veg).

Supermarket_ veg_method	Mean $\delta^{18}O$	Mean $\delta^{2}H$	min $\delta^{18}O$	max $\delta^{18}O$	SD $\delta^{18}O$	min $\delta^{2}H$	max $\delta^{2}H$	SD $\delta^{2}H$
S_CAU_CVD	-0,5	-20,4	-0,5	-0,5	-0,5	-20,4	-20,4	-20,4
S_CAU_DVE	-9,2	-89,7	-9,2	-9,2	-9,2	-89,7	-89,7	-89,7
S_CAU_insitu	-3,8	-31,8	-3,8	-3,8	-3,8	-31,8	-31,8	-31,8
S_CEL_CVD	-1,3	-29,4	-1,3	-1,3	-1,3	-29,4	-29,4	-29,4
S_CEL_DVE	-1,7	-41,3	-1,7	-1,7	-1,7	-41,3	-41,3	-41,3
S_CEL_insitu	-5,8	-40,1	-5,8	-5,8	-5,8	-40,1	-40,1	-40,1
S_KOH_CVD	-3,2	-33	-3,2	-3,2	-3,2	-33	-33	-33
S_KOH_DVE	-4,9	-80,4	-4,9	-4,9	-4,9	-80,4	-80,4	-80,4
S_KOH_insitu	-5	-37,2	-5	-5	-5	-37,2	-37,2	-37,2
S_POT_CVD	-2,2	-29,5	-2,2	-2,2	-2,2	-29,5	-29,5	-29,5
S_POT_DVE	-1,9	-32,6	-1,9	-1,9	-1,9	-32,6	-32,6	-32,6
S_POT_insitu	-3,9	-34,4	-3,9	-3,9	-3,9	-34,4	-34,4	-34,4

Ehrenwörtliche Erklärung

Hiermit erkläre ich, dass die Arbeit selbständig und nur unter Verwendung der angegebenen Hilfsmittel angefertigt wurde.

Freiburg i. Br., 15. Mai 2021 _____

Lena Wengeler